Åbo Akademi

Roger Bollström

Paper for printed electronics and functionality

Doctoral Thesis

Laboratory of Paper Coating and Converting
Department of Chemical Engineering
Center for Functional Materials

2013

Roger Christian Bollström

Born 1982 in Sjundeå, Finland

Obtained his M.Sc. (Tech) degree at the Faculty of Technology at Åbo Akademi University in 2007. Joined the Laboratory of Paper Coating and Converting in 2006.

Paper for printed electronics and functionality

Roger Bollström

Laboratory of Paper Coating and Converting
Center for Functional Materials
Department of Chemical Engineering
Åbo Akademi University
Åbo, Finland, 2013

Supervisor

Professor Martti Toivakka
Laboratory of Paper Coating and Converting
Åbo Akademi University, Turku, Finland

Reviewers

Professor Patrick Gane
Professor of Printing Technology, Aalto University, Espoo, Finland
Vice President, Research and Development, Omya International AG, Oftringen, Switzerland

Professor Bruce Lyne
Division of Surface and Corrosion Science
Royal Institute of Technology, Stockholm, Sweden

Opponent

Professor Patrick Gane
Professor of Printing Technology, Aalto University, Espoo, Finland
Vice President, Research and Development, Omya International AG, Oftringen, Switzerland

Juvenes print – Suomen Yliopistopaino Oy

ISBN 978-952-12-2934-3

Preface

This work was carried out in the Laboratory of Paper Coating and Converting and within the Center for Functional Materials. The work has been funded by the Academy of Finland through the National Center of Excellence program.

I want to thank my supervisor Professor Martti Toivakka for giving me the opportunity to work in this interesting field of "Paper Electronics". You have given me lot of responsibility but on the same time always been available, giving advice and support throughout the work.

Working in the Center for Functional Materials, and more specifically in the Functional Printing Laboratory, made my work very interdisciplinary. Among the various collaborators I wish to thank Anni Määttänen, Daniel Tobjörk, Fredrik Pettersson, Peter Dolietis, Roger Nyqvist, Petri Ihalainen, Jarkko J Saarinen, Tapio Mäkelä and Jani Kniivilä as well as Professor Ronald Österbacka and Professor Jouko Peltonen. I also want to thank Mikko Tuominen from Tampere University of Technology and Jukka Räty from University of Oulu. Furthermore I appreciate the cooperation carried out with Tommi Remonen, Sari Viljanen, Carl-Johan Wikman, Professor Johan Bobacka, and Professor Carl-Eric Wilén in order to manufacture and demonstrate various functional devices on paper. Many thanks also to Mikael Ek and Pauliina Saloranta for carrying out numerous measurements at the laboratory as well as to Björn Friberg for building of all kinds of parts and equipment needed in the work.

My work has been carried out in close collaboration with several industrial partners. I want to thank Imerys Minerals Ltd. and especially Adjunct Professor Janet Preston for all the help and advice you have given me through the years. I also greatly appreciate the work carried out at Styron Europe GmbH in Samstagern and the support and advice provided by Adjunct professor Pekka Salminen. Furthermore I would also like to thank Gilbert Gugler at Ilford Imaging for the work done and Seppo Sivén at Specialty Minerals Nordic Oy for his support regarding materials supply and advice.

The content of the work also led to a patenting process, and I want to acknowledge the support and help given by Olle Lagerroos from Research Affairs at Åbo Akademi University.

And many thanks to the entire staff at the Laboratory of Paper Coating and Converting; it has been a pleasure to work with all of you!

Last but not least, I want to express my gratitude to my parents for all their support.

List of Publications

List of included publications

I. R. Bollström, A. Määttänen, D. Tobjörk, P. Ihalainen, N. Kaihovirta, R. Österbacka, J. Peltonen, M. Toivakka, A multilayer coated fiber-based substrate suitable for printed functionality, Organic Electronics 10 1020–1023, 2009
II. R. Bollström, M. Tuominen, A. Määttänen, J. Peltonen, M. Toivakka, Top layer coatability on barrier coatings, Progress in Organic Coatings 73 26-32, 2012
III. R. Bollström, J.J. Saarinen, J. Räty, M. Toivakka, Measuring solvent barrier properties of paper, Measurement Science and Technology 23 015601, 2012
IV. R. Bollström, R. Nyqvist, J. Preston, P. Salminen, M. Toivakka, Barrier properties created by dispersion coating, Tappi Journal 12 (4) 45-51, 2013
V. R. Bollström, D. Tobjörk, P. Dolietis, P. Salminen, J. Preston, R. Österbacka, M. Toivakka, Printability of functional inks on multilayer curtain coated paper, Chemical Engineering and Processing 68 13-20, 2013
VI. R. Bollström, F. Pettersson, P. Dolietis, J. Preston, R. Österbacka, M. Toivakka, Impact of humidity on functionality of on-paper printed electronics, Nanotechnology, (In Press)

List of supporting publications

Peer-reviewed scientific publications

1. R. Bollström, D. Tobjörk, P. Dolietis, T. Remonen, C-J Wikman, S. Viljanen, J. Sarfraz, P. Salminen, M. Linden, C-E. Wilen, J. Bobacka, R. Österbacka and M. Toivakka, Roll-to-roll printed electronics on paper, Proceedings of Tappi PaperCon, New Orleans, 627-639, ISBN:978-1-59510-215-7, 2012
2. R. Bollström, A. Määttänen, P. Ihalainen, J. Peltonen, M. Toivakka, Influence of UVC treatment on sheetfed offset print quality, Advances in Printing and Media Technology 37,127-134, ISBN: 978-3-9812704-2-6, Montreal, 2010
3. R. Bollström, M. Tuominen, A. Määttänen, J. Peltonen, M. Toivakka, Top layer coatability on barrier coatings, Proceedings of Tappi PaperCon, Cincinnati, 511-521, 2011

4. R. Bollström, M. Toivakka, Paper substrate for printed functionality, Advances in pulp and paper research 15, 945-966, ISBN: 978-0-9926163-0-4, Cambridge, 2013
5. D. Valtakari, R. Bollström, M. Tuominen, H. Teisala, M. Aromaa, M. Toivakka, J. Kuusipalo, J. M. Mäkelä, J. Uozumi, J. J. Saarinen, Flexographic printing of PEDOT:PSS on coated papers for printed functionality, Journal of Print Media and Technology Research 2 (1) 7-14, 2013
6. J. Preston, R. Bollström, K. Nylander, M. Toivakka, J. Peltonen, A new test method to measure dynamic contact in a printing nip for rotogravure papers, Advances in Printing and Media Technology 35, 147-153, ISBN: 978-3-9812704-0-2, Valencia, 2008
7. J. Saari, R. Bollström, K. Mueller, M. Toivakka, Ink formulation with the new Multi-Phase Ink Model, Advances in Printing and Media Technology 36, 223-230, ISBN: 978-3-9812704-1-0, Stockholm, 2009
8. A. Määttänen, P. Ihalainen, R. Bollström, M. Toivakka, J. Peltonen, Wetting and print quality study of an inkjet-printed poly(3-hexylthiophene) on pigment coated papers, Colloids Surf. A: Physicochem. Eng. Aspects 367 76–84, 2010
9. A. Määttänen, P. Ihalainen, R. Bollström, S. Wang, M. Toivakka, J. Peltonen, Enhanced Surface Wetting of Pigment Coated Paper by UVC Irradiation, Industrial & Engineering Chemistry Research 4922 11351-11356, 2010
10. M. Pykönen, K. Johansson, R. Bollström, P. Fardim, M. Toivakka, Influence of Surface Chemical Composition on UV-Varnish Absorption into Permeable Pigment-Coated Paper, Industrial & Engineering Chemistry 49 2169-2175, 2010
11. J. Peltonen, A. Määttänen, R. Bollström, M. Toivakka, M. Stepien, J. Saarinen, P. Ihalainen, U. Mattinen, J. Bobacka, Printed electrodes on tailored paper enable extended functionalization of paper, Advances in Printing and Media Technology 37,335-339, ISBN: 978-3-9812704-2-6, Montreal, 2010
12. D. Tobjörk, H. Aarnio, P. Pulkkinen R. Bollström, A. Määttänen, P. Ihalainen, T. Mäkelä, J. Peltonen, M. Toivakka, H. Tenhu, R. Österbacka, IR-sintering of ink-jet printed metal-nanoparticles on paper, Thin Solid Films, 520(7), 2949–2955, 2012
13. J.J. Saarinen, P. Ihalainen, A. Määttänen, R. Bollström, J. Peltonen, Printed sensor and electric field assisted wetting on a natural fibre based substrate, Nordic Pulp and Paper Research Journal, 25, 133-141, 2011
14. P. Ihalainen, A. Määttänen, U. Mattinen, M. Stepien, R. Bollström, M. Toivakka, J. Bobacka, J. Peltonen, Electrodeposition of PEDOT-Cl film on a fully printed Ag/polyaniline electrode, Thin Solid Films, 2172-2175, 2011
15. S. Thiemann, S. Sachnov, F. Pettersson, R. Bollström, R. Österbacka, P. Wasserscheid, J, Zaumseil, Cellulose-based Ionogels for Paper Electronics, Advanced Functional Materials (In Press)

Non-reviewed scientific publications

16. R. Bollström, A. Määttänen, D. Tobjörk, P. Ihalainen, N. Kaihovirta, R. Österbacka, J. Peltonen, M. Toivakka, A recyclable paper substrate suitable for printed functionality, Proceedings of NEXT, Shanghai, 87-94, 2009
17. R. Bollström, D. Tobjörk, A. Määttänen, P. Ihalainen, J. Peltonen, R. Österbacka, M. Toivakka, Towards Paper Electronics – Printing Transistors on Paper in a Roll-To-Roll Process, Proceedings of the NIP 27 and Digital Fabrication, Minneapolis, 636-639, 2011
18. R. Bollström, D. Tobjörk, P. Dolietis, M. Ahtinen, P. Salminen, J. Preston, R. Österbacka, M. Toivakka, Printed electronics enabled by multilayer curtain coating, Proceedings of PTS, Munich, 235-243, 2011
19. R. Bollström, M. Toivakka, D. Tobjörk, P. Salminen, Eletrônica Impressa em Papel Através de Aplicação por Cortina Multicamadas, Proceedings of ABTCP, Sao Paulo, 2011
20. R. Bollström, D. Tobjörk, P. Dolietis, A. Määttänen, P. Ihalainen, P. Salminen, J. Preston, J. Peltonen, R. Österbacka, M. Toivakka, Printability of functional inks on multilayer curtain coated paper, Proceedings of European Coating Symposium, Turku, 66-69, 2011
21. R. Bollström, R. Nyqvist, J. Preston, P. Salminen, M. Toivakka, Optimizing barrier properties of dispersion coating, Proceedings of Tappi PLACE, Seattle, 2012
22. R. Bollström, J.J. Saarinen, J. Räty, M. Toivakka, Measuring solvent barrier properties of paper, Proceedings of Tappi PLACE, Bregenz, 16, 2011
23. D. Tobjörk, R. Bollström, P. Dolietis, A. Määttänen, P. Ihalainen, T. Mäkelä, J. Peltonen, M. Toivakka, R. Österbacka, Printed low-voltage organic transistors on plastic and paper, Proceedings of European Coating Symposium , 62-65, Turku, 2011
24. D. Valtakari, R. Bollström, M. Toivakka, M. Tuominen, H. Teisala, J. Kuusipalo, J. Uozumi, J.J. Saarinen, Conductive surfaces on coated papers by flexographical printing, Proceedings of TAPPI Advanced Fundamentals Symposium. Atlanta, GA: TAPPI Press, 2012
25. A. Määttänen, R. Bollström, D. Tobjörk, P. Ihalainen, M. Toivakka, J. Peltonen. Multilayer-coated fiber based substrate for printed functional devices, Proceedings of European Coating Symposium, Karlsruhe, 2009
26. J.J. Saarinen, R. Bollström, A. Määttänen, P. Ihalainen, J. Peltonen, M. Toivakka, Printed functionality on a multilayer coated paper, Proceedings of Japanese Society of Printing Science and Technology, 2010
27. M. Pykönen, R. Bollström, M. Toivakka, P. Fardim, K. Johansson, G. Ström, Influence of Plasma Coating on Fluid Absorption into Pigment-Coated Paper, TAPPI Advanced Coating Fundamentals Symposium, 2010

28. J. J. Saarinen, P. Ihalainen, R. Bollström, A. Määttänen, J. Peltonen, Electrowetting on a paper substrate, TAPPI International Conference on Nanotechnology for the Forest Products Industry, Edmonton, 2009
29. D. Tobjörk, N. Kaihovirta, R. Bollström, A. Määttänen, T. Mäkelä, P. Ihalainen, J. Peltonen, M. Toivakka, R. Österbacka, Printed low-voltage organic transistors on paper substrates. European Conference on Molecular Electronics (ECME), Copenhagen, 2009
30. P. Ihalainen, A. Määttänen, U. Mattinen, M. Stepien, J. Saarinen, R. Bollström, M. Toivakka, J. Bobacka, J. Peltonen, Electrochemical applications in paper substrate, the 9th ELKIN conference, Turku, 2010
31. J.J. Saarinen, P. Ihalainen, A. Määttänen, R. Bollström, J. Peltonen, Printed sensor and liquid actuation on natural fiber based substrate, Tech Connect World Conference and Expo, Proceedings 2 527-530, 2010
32. I. Reinhold, W. Voit, M. Thielen, M. Müller, M. Müller, S. Farnsworth, I. Rawson, R. Bollström, W. Zapka, Inkjet Printing of Electrical Connections in Electronic Packaging, Proceedings of the NIP 27 and Digital Fabrication 445-451, Minneapolis, 2011
33. R. Bollström, R. Nyqvist, J. Preston, P. Salminen, M. Toivakka, Optimizing barrier properties of dispersion coating, Proceedings of Tappi PLACE, Seattle, 2012
34. S. Thiemann, F. Pettersson, S. Sachnov, P. Wasserscheid, R. Bollström, R. Österbacka, J. Zaumseil, Microcellulose-based Ionogels for Low-Voltage ZnO Circuits on Paper, 9Th international thin film conference (ITC) , Tokyo (Poster), 2013

Immaterial property rights

R. Bollström, A. Määttänen, P. Ihalainen, M. Toivakka J. Peltonen, Method for creating a substrate for printed or coated functionality, substrate, functional device and its use

- PCT/FI2010/050056
- WO 2010/086511
- EP 10704581.7
- US 13/147,424
- China 201080006446.5

Contributions

I: The author planned the work, designed the multilayer coating structure, the recipes and carried out the coatings. AFM surface analysis and roughness measurements were done by Anni Määttänen. The transistor was printed and measured by Daniel Tobjörk.

II: The work was planned by the author. The preparation of the coating colors, coating, and contact angle measurement were performed by Vesa Tertsunen as a bachelor thesis work, supervised by the author. The plasma and corona treatments were carried out by Mikko Tuominen.

III: The work was planned by the author. The testing of the trace color method was performed by Tommy Back as a bachelor thesis work, supervised by the author. Jukka Räty built the first prototype of the prism method setup.

IV: The work was planned by the author, in close cooperation with Janet Preston. The laboratory scale barrier coatings were carried out by Roger Nyqvist, as a master thesis work, supervised by the author. The ATR IR measurements were carried out at Imerys Minerals Ltd. by John Parsons. Marco Ahtinen and Gilbert Gugler performed the pilot scale curtain coating trials.

V: The work was planned by the author. The pilot scale curtain coating recipes were planned together with Pekka Salminen and the trial performed by Marco Ahtinen at Styron Europe Samstagern. Mikael Ek did the AFM measurements. Printing and analysis was carried out together with Daniel Tobjörk and Peter Dolietis.

VI: The author planned the work together with Martti Toivakka. The author designed the coating recipes and carried out the pilot scale curtain coating trial together with the personnel at Metso Paper Oyj, Järvenpää. The inkjet printing was done by Peter Dolietis. The transistor was designed and measured by Fredrik Pettersson. AFM analysis and roughness measurements were carried out by Anni Määttänen and assisted by Petri Ihalainen.

Abstract

Mass-produced paper electronics (large area organic printed electronics on paper-based substrates, "throw-away electronics") has the potential to introduce the use of flexible electronic applications in everyday life. While paper manufacturing and printing have a long history, they were not developed with electronic applications in mind. Modifications to paper substrates and printing processes are required in order to obtain working electronic devices. This should be done while maintaining the high throughput of conventional printing techniques and the low cost and recyclability of paper. An understanding of the interactions between the functional materials, the printing process and the substrate are required for successful manufacturing of advanced devices on paper.

Based on the understanding, a recyclable, multilayer-coated paper-based substrate that combines adequate barrier and printability properties for printed electronics and sensor applications was developed in this work. In this multilayer structure, a thin top-coating consisting of mineral pigments is coated on top of a dispersion-coated barrier layer. The top-coating provides well-controlled sorption properties through controlled thickness and porosity, thus enabling optimizing the printability of functional materials. The penetration of ink solvents and functional materials stops at the barrier layer, which not only improves the performance of the functional material but also eliminates potential fiber swelling and de-bonding that can occur when the solvents are allowed to penetrate into the base paper. The multi-layer coated paper under consideration in the current work consists of a pre-coating and a smoothing layer on which the barrier layer is deposited. Coated fine paper may also be used directly as basepaper, ensuring a smooth base for the barrier layer. The top layer is thin and smooth consisting of mineral pigments such as kaolin, precipitated calcium carbonate, silica or blends of these. All the materials in the coating structure have been chosen in order to maintain the recyclability and sustainability of the substrate. The substrate can be coated in steps, sequentially layer by layer, which requires detailed understanding and tuning of the wetting properties and topography of the barrier layer versus the surface tension of the top-coating. A cost competitive method for industrial scale production is the curtain coating technique allowing extremely thin top-coatings to be applied simultaneously with a closed and sealed barrier layer.

The understanding of the interactions between functional materials formulated and applied on paper as inks, makes it possible to create a paper-based substrate that can be used to manufacture printed electronics-based devices and sensors on paper. The multitude of functional materials and their complex interactions make it challenging to draw general conclusions in this topic area. Inevitably, the results become partially specific to the device chosen and the materials needed in its manufacturing. Based on the results, it is clear that for inks based on dissolved or small size functional materials, a barrier layer is beneficial and ensures the functionality of the printed material in a device. The required active barrier life time depends on the solvents or analytes used

and their volatility. High aspect ratio mineral pigments, which create tortuous pathways and physical barriers within the barrier layer limit the penetration of solvents used in functional inks. The surface pore volume and pore size can be optimized for a given printing process and ink through a choice of pigment type and coating layer thickness. However, when manufacturing multilayer functional devices, such as transistors, which consist of several printed layers, compromises have to be made. E.g., while a thick and porous top-coating is preferable for printing of source and drain electrodes with a silver particle ink, a thinner and less absorbing surface is required to form a functional semiconducting layer.

With the multilayer coating structure concept developed in this work, it was possible to make the paper substrate suitable for printed functionality. The possibility of printing functional devices, such as transistors, sensors and pixels in a roll-to-roll process on paper is demonstrated which may enable introducing paper for use in disposable "one-time use" or "throwaway" electronics and sensors, such as lab-on-strip devices for various analyses, consumer packages equipped with product quality sensors or remote tracking devices.

Keywords: paper electronics, multilayer curtain coating, mineral pigments, barrier properties, tortuosity, printing, functional inks, transistor, sensor

Svensk Sammanfattning

Massproduktion av papperselektronik, bestående av till exempel tryckt organisk elektronik på papperssubstrat, kommer att möjliggöra nya flexibla elektroniska produkter för vardaglig användning. Även om papperstillverkning och tryckning har en lång historia, har de inte utvecklats med tanke på elektroniska produkter. Både papperssubstratet och tryckmetoderna bör därigenom modifieras för att fungerande elektronik skall kunna tillverkas. Detta bör göras så att den höga produktionshastigheten från de konventionella tryckmetoderna bibehålls, likaså återanvändningen av pappret. Noggrann förståelse om hur de funktionella materialen, tryckmetoderna och substratet interagerar är ett krav för lyckad produktion av avancerade elektroniska anordningar på papper.

Baserat på denna förestålse utvecklades i detta arbete ett multiskiktbestruket papperssubstrat där goda barriäregenskaper kombineras med tryckbarhet vilket möjliggör tryckning av elektronik och sensorer. I denna multiskiktsstruktur har ett tunt toppskikt bestående av mineralpigment bestrukets ovanpå ett dispersionsbestruket barriärskikt. Toppskiktet möjliggör väl-kontrollerbar färgsättning av de funktionella tryckfärgerna genom kontrollerad tjocklek och porositet. Penetration av lösningsmedel från tryckfärgerna genom substratet förhindras av barriärskiktet, vilket både förbättrar funktionaliteten av det funktionella materialet men också hindrar eventuell fibersvällning som kunde ske om lösningsmedlen skulle gå in i baspappret. Multiskiktstrukturen i fråga består av en förbestrykning och ett utjämnande skikt, ovanpå vilka barriärskiktet har applicerats. Bestruket finpapper ger också en slät grund för barriärskiktet och kan därigenom likväl användas direkt som baspapper. Toppskiktet är tunt och slätt och består av mineralpigment, som till exempel kaolin, utfälld kalciumkarbonat, kisel eller en blandning av dessa. Alla material i bestrykningsstrukturen har valts med tanke på att en återvinning av substratet skall vara möjlig. Substratet kan bestrykas stegvis, alla skikt separat ovanpå varandra, men kräver noggrann kännedom och optimering av vätningen och topografin hos barriärskiktet gentemot ytspänningen i toppskiktsdispersionen. En kostnadseffektiv metod för produktion i industriell skala är ridåbestrykning som möjliggör bestrykningen av ett extremt tunt toppskikt ovanpå barriärskiktet i samma kör.

Med kunskap om hur funktionella material applicerade som tryckfärger på papper interagerar, möjliggörs tillverkning av pappersbaserade substrat som kan utnyttjas som underlag för tryckta elektronikbaserade anordningar och sensorer. Mångfalden av funktionella material och deras komplexa interaktioner gör det dock svårt att dra generella slutsatser inom detta område. Resultaten blir delvis specifika för anordningen i fråga, samt beroende av materialen som används. Baserat på resultatet är det klart att för tryckfärger baserade på lösligt material eller material bestående av mycket små partiklar krävs ett barriärskikt för att bibehålla detta material på ytan. Den krävda livslängden på barriärskiktet beror av lösningsmedel eller analysvätskorna och deras flyktighet. Mineralpigment av hög formfaktor resulterar i hög tortuositet och bildar en

fysisk barriär som hindrar eller begränsar penetration av lösningsmedel från de funktionella tryckfärgerna. Ytporositeten i form av porstorlek och porvolym kan optimeras för en särskild tryckprocess genom val av pigmenttyp och skikttjocklek. Dock, vid produktion av funktionella anordningar bestående av flera tryckta lager måste vanligen kompromisser göras. Ett tjockt toppskikt är till exempel ändamålsenligt för tryckning av elektroder, bestående av silverpartiklar, medan en mindre absorberande yta krävs för att åstadkomma ett fungerande halvledarskikt.

Konceptet för multiskiktsbestrykningsstruktur som utvecklades i detta arbete möjliggjorde tryckning av funktionalitet på papper. Möjligheten att trycka funktionella anordningar som transistorer, sensorer och pixlar på papper i en rulle till rulle process demonstreras, vilket kan öppna upp nya möjligheter för användning av papper i så kallad ”engångselektronik”, som t.ex. ”lab-on-strip” för integrerad analys av olika vätskor, i konsumentförpackningar med sensorer för analys av produktkvalitet eller fjärravläsning och kontroll via RFID (radio frequency identification device).

Nyckelord: papperselektronik, multiskiktsridåbestrykning, mineral pigment, barriäregenskaper, tortuositet, tryckning, funktionella tryckfärger, transistor, sensor

Nomenclature

AFM	atomic force microscope
CPVC	critical pigment volume concentration
DCB	dichlorobenzene
DIM	diiodomethane
EA	ethylene acrylic
EG	ethylene glycol
FET	field effect transistor
FIB	focused ion beam
GCC	ground calcium carbonate
HIFET	hygroscopic insulator field effect transistor
IGT	Institut für Graphische Technik
LED	light emitting diode
MEK	methyl ethyl ketone
MLC	multilayer coated
MLCC	multilayer curtain coated
NTP	normal temperature and pressure
OFET	organic field effect transistor
P3HT	poly(3-hexylthiophene)
PANI	polyaniline
PBTTT	poly(2,5-bis(3-tetradecyllthiophen-2-yl)thieno[3,2-b] thiophene)
PCC	precipitated calcium carbonate
PEDOT:PSS	poly(3,4-ethylene dioxythiophene) with poly(styrene sulfonate)
PET	polyethylene terephthalate
PM-acetate	1-methoxy-2-propanol acetate
PPS	Parker Print Surf
PVC	pigment volume concentration
PVP	poly(4-vinylphenol)
PQT	poly(3,3’’’-didodecyl quaterthiophene)
RFID	radio frequency identification
RH	relative humidity
RMS	root mean square
SA	styrene acrylic
SB	styrene butadiene
SEM	scanning electron microscope
SF	shape factor
TLC	thin layer chromatography
UV	ultra violet
WVTR	water vapor transmission rate

Table of Contents

1. Introduction and objectives

Paper and board are versatile materials with numerous end-use applications. Coated paper and board grades are typically used for magazines, brochures and packages, where control of surface properties is important. Paper coating with aqueous mineral pigment dispersion improves its compatibility with various converting and finishing operations, such as printing. The coating improves smoothness, surface strength, optical and absorption properties. Rising costs, limited market growth and expansion of electronic media have led the paper industry to search for new innovative and value-added fiber-based products, such as functional packages and biologically active papers for sensor or medical applications.

Mass-produced *paper electronics* (on paper printed electronics) has the potential to introduce the use of flexible electronic applications in everyday life. While paper manufacturing and printing have a long history, they were not developed with electronic applications in mind. Modifications to paper substrates and printing processes are required in order to obtain working electronic devices. This should be done while maintaining the high throughput of conventional printing techniques and the low cost and recyclability of paper. An understanding of the interactions between the functional materials, the printing process and the substrate are required for successful manufacturing of advanced devices on paper.

Much research has been and is being done to develop value-added functionalities on paper or paper-like substrates. Especially printed sensors and displays are capturing much attention (*1*,*2*). Low-cost and recyclable paper substrates have been considered for various printed functional applications outside of the conventional graphical arts industry *(1-4)*. Electronic devices such as transistors, capacitors, RFID antennas and batteries have been fabricated on paper or paper-like substrates by using functional inks containing conducting and semiconducting materials, such as silver, organic polymers as well as carbon nanotubes *(5-9)*. Organic photodiodes and photovoltaic cells, electronic paper displays, foldable thermochromic displays and high-performance organic thin film transistor arrays on paper have also been demonstrated *(10-14)*. Recently also sensors for analysis of ionic concentration, analysis of modified atmosphere conditions, as well as sensors for use in diagnostics applications, have been manufactured by printing on paper *(15-19)*.

In the present work, requirements for using paper as substrate for different functional applications are investigated. For such applications to come into everyday use, devices with reasonable electrical performance and practically negligible production cost are required. The low cost can be achieved with manufacturing techniques such as printing or coating, which enable large scale production in a roll-to-roll process. Printing of functional materials requires detailed knowledge of the ink-substrate interactions and in case of devices consisting of several printed layers, compromises might be necessary. One of the most important advantages for paper, in addition to the low cost, is the

biodegradability and recyclability which should be kept in mind and maintained by choice of only biodegradable, recyclable or at least disposable coating materials. Improving barrier properties by for example extrusion coating or lamination reduces the recyclability of the end-product. The biodegradability or recyclability is important considering the targeted end-use applications, which could be "one-time-use electronics" or "throw-away electronics," i.e. products such as lab-on-strip devices for various analyses, consumer packages equipped with sensors for product quality analysis or remote tracking, such as radio frequency identification devices (RFID).

In traditional graphical printing, the print results are evaluated according to their visual and optical properties, where images are built up by printing of non-connected dots. In functional printing the functionality is often measured as for example conductivity, which may only be achieved by connected features. Additionally, the functional material, whether it is metal particles, organic conductive polymers or semi-conductive polymers, is not originally designed with printing in focus, which means the solutions or dispersions made of these seldom have suitable printing properties.

The objective of this work was to understand what are the requirements set for paper when it is used as substrate for printed functional devices. Influence of critical paper surface properties, such as roughness, porosity and wettability, and their impact on printability of various functional materials was in focus. An understanding of the compatibility between functional inks, printing and coating methods, and substrate properties is essential for successful manufacturing of complex, multilayer devices on paper. Barrier properties of the paper were also investigated, in order to enable device fabrication and to ensure satisfactory performance of the devices in the end-use of application. Considering the requirements set by functional materials and their processing, a multilayer-coated, paper-based substrate concept suitable for printed electronics and functionality was developed. Fabrication of several functional devices, such as transistors and sensors, on paper was demonstrated.

2. Paper electronics

2.1. Paper

Paper is a versatile substance made from naturally occurring plant fibers mainly containing cellulose, hemicellulose and lignin. Originally fibers were derived from cloth rags and grass but are today predominantly sourced from wood. The water suspension of fibers, which is called pulp, is made by separating the wood into its constituent fibers in a mechanical, thermomechanical, or chemical process. A paper that is made of mechanical pulp is referred to as a wood-containing, while a paper made entirely from chemical pulp is called wood-free. In chemical pulp the cellulose fibers have been separated by use of chemicals, in a process called cooking, which results in long fibers and enables removal of amorphous lignin. The pulp is then refined and cleaned before being pumped onto a moving screen on a paper machine. As the pulp travels along the screen the excess water is drained away and a paper sheet made from interlocking cellulose fibers is formed (Figure 1 A and B, left side) (*20*,*21*). In order to improve the optical properties such as light scattering, whiteness and opacity as well as for ensuring printability, mineral fillers such as calcium carbonate and kaolin that fill the pores of the fiber matrix are often introduced already in the pulp. Once the paper has been dried and pressed, depending upon its end use, it may be finished with mineral pigment coatings or other additives to ensure uniform smoothness and thickness (Figure 1 A and B, right side). High-quality papers with smooth surfaces and improved optical properties are produced by applying additional coating layers of pigments and by calendering (*22*). The white background of paper is beneficial for contrast when text or images are printed. To improve the optical properties, in addition to bleaching the pulp and using mineral fillers and coatings, fluorescent whitening agents are often added in order to make the surface appear whiter and brighter. The fluorescent materials absorb UV light and re-emit it in the blue part of the visible spectrum, which compensates for the otherwise yellowish color of paper (*23*). In addition to being used as the printing substrate in newspapers, magazines and office papers, paper and board are used in several specialized products. Most common are packages, which can be divided into primary packages (direct contact with the product, e.g. milk carton), secondary packages (collates primary packages, e.g. portion packs) and tertiary packages (collates secondary packages, e.g. roller cages). A new, however not yet well defined, expression is “smart packaging” representing packages with novel features going beyond traditional product protection, graphics and barcodes. Terms such as “active”, “intelligent” and “diagnostic” have been used to promote the functionality the package may bring to the user. RFID-enabled packages and packages equipped with different sensors for streamlining logistics and transport conditions are common on tertiary packages but recently the interest for bringing them towards the consumer, i.e. including them on the primary packages, has also risen. Paper and board are also common construction materials, comprising the surfaces in plasterboard as well as in wallpapers. Besides these application areas, a wide variety of specialty papers are used, for example different

tissue grades, filter papers, sandpaper, label and release papers, blueprint and thermal printing papers as well as photo papers and security papers (*24*).

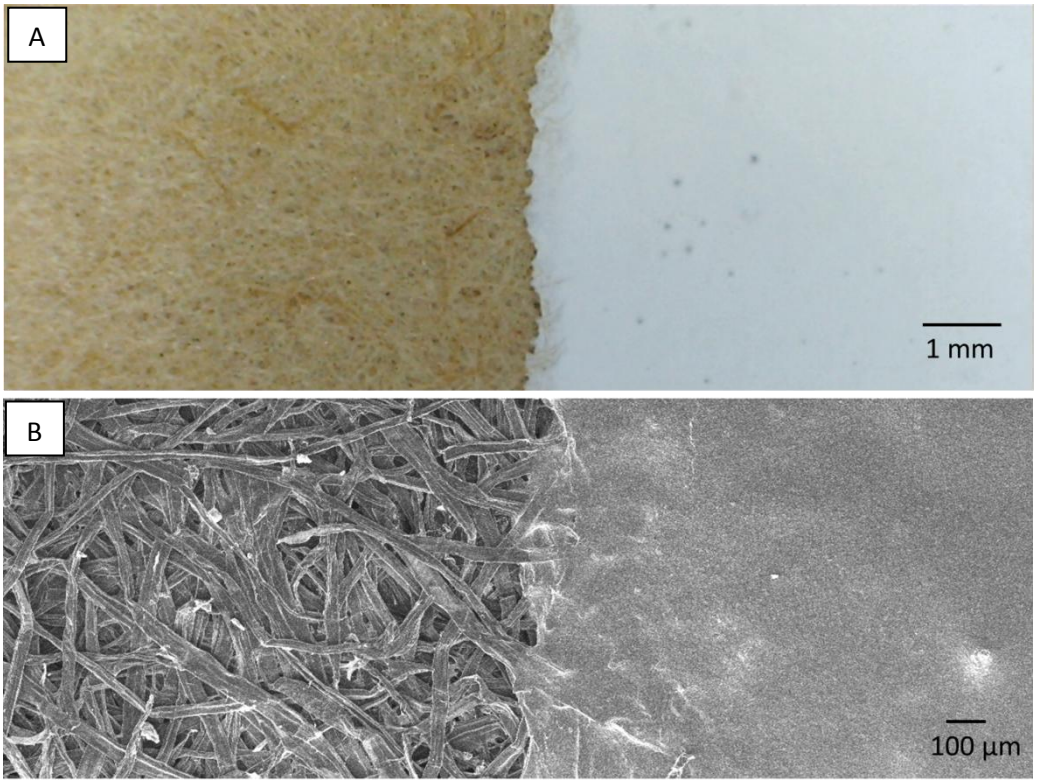

Figure 1. Optical microscopy (A) and scanning electron microscopy (B) image of coated and uncoated paper surface. To the left in the images the fiber network can be seen and to the right the surface as pigment coated.

2.2. Paper as carrier of functionality

The idea of incorporating advanced functionality to paper beyond its traditional areas of use, is not new. E.g., already in 1968 at Westinghouse, first attempts were made to manufacture transistors on paper (*25*). A stenciling method for depositing inorganic thin-film transistors on paper substrates on a roll inside a vacuum chamber was used. However, the approach for making flexible electronics on paper did not become a commercial reality at that time. One reason may have been the required vacuum, which prevented the manufacturing process from being truly low-cost. Paper has also been used as an insulating material for over a century in cables and capacitors. While paper nowadays has been replaced by thinner insulating plastic materials in many applications, oil impregnated paper is still used in high voltage and high-power applications (*26*).

Recently there have been many advances in the field of paper electronics. However, many examples of paper electronics involve the use of paper substrates covered with plastic films, lamination of a plastic film, having electronic components between paper or board sheets that are glued together, or attaching electronic components such as silicon chips onto paper substrates. Actually, the term or field "paper electronics" can be divided into three categories. The very paper itself can be electronic or electrical. Secondly, traditional silicon-based electronics can be placed onto paper as is done in talking gift cards and RFID tags; however an increasing part (wires and antenna) of them is being printed to save cost. Thirdly, electrics, or parts of it can firmly be buried in paper or operated by being on both sides of a paper sheet, like batteries or capacitors.

The paper itself has been made conductive by addition of conducting materials such as carbon and metalized fibers to the pulp. Conductivity up to 0.3S/cm was achieved by addition of 20 weight % of silver plated carbon fibers in the paper (*27*). For electromagnetic shielding applications paper has also been dispersion coated with graphite (*28*). However, the addition of large amounts of conductive fillers into the paper both darkens and weakens the paper. Various types of paper-polymer composite materials have been created by polymerizing polypyrrole and polyaniline into cellulose substrates *(29-34)*. As high as 20S/cm conductivity has been obtained when covering cellulose fibers with a blend of poly(3,4-ethylene dioxythiophene) with poly(styrene sulfonate) (PEDOT:PSS) and carbon nanotubes *(35-37)*.

Manufacturing electronic devices, such as organic transistors that usually require molecularly smooth interfaces, directly onto paper substrates is challenging. Nevertheless, there have been many promising reports of electronic devices and sensors fabricated directly onto paper, and for some of the applications the porous paper surface is even advantageous. Perhaps the most advanced device fabricated directly onto unmodified newspaper is the photovoltaic cell demonstrated by Barr et al. (*14*). Manufacturing of that photovoltaic cell however required an oxidative chemical vapor deposition technique, which is a limiting factor regarding large scale manufacturing. The porous and wetting structure of the fiber network in filter and chromatography papers has been widely utilized for sensor and diagnostics applications, where liquid transport is required *(38-43)*. Having the cellulose paper structure as an active material in for example, sensor applications, expressions like "electroactive paper" or "smart paper" have been used to capture the incorporation of this activity.

Manufacturing techniques utilizing solution processing can be used to produce inexpensive products in large scale. These techniques, e.g. printing and coating, require substrates which retain the used functional materials on their surfaces. A surface can be made impermeable to liquids and solvents by laminating or extrusion coating with polyethylene, polypropylene or polyethylene terephthalate. Polymer-covered paper substrates have been used, for example for electrochemical displays (*12*). Another alternative is pigment coating, which was used by Trnovec et al. (*4*). By coating the paper with a dispersion consisting of $CaCO_3$ blended with latex, PVA and starch a surface roughness of down to 0.26μm was achieved after calendering, enabling gravure

printing of transistors. That pigment coated paper improves printability compared to uncoated paper is a clear fact. Additionally, covering the fiber structure with mineral pigments improves heat resistance and stability *(44-46)*, thereby enabling use of high temperature infrared sintering (*47*), which is advantageous when using metal particle based inks in roll-to-roll processes (Section 2.3.). Surface roughness has been considered an important factor regarding functionality of conductive prints (*48*), and recently a detailed study was conducted by Ihalainen at al. (*49*) pointing out the importance of the low roughness at the shorter length scales. Although pigment coating improved the smoothness compared to uncoated paper as well as limited considerably absorbency or penetration of inks into the fiber structure, nevertheless, the remaining absorbency was still the main factor limiting the performance of the printed transistors as reported by Trnovec et al. Both the conductive and semiconductive materials were to a large extent absorbed by the coating structure (*4*). Similar problems with absorbency of functional inks on various commercial coated paper grades have been reported by Denneulin (*50*), Zhou (*51*) and Mäkelä (*52*). Compared to plastic substrates paper generally resulted in much poorer surface conductivities of printed or coated conductors; for example 100 times higher resistivity for PEDOT:PSS on commercial coated paper compared to plastic was reported by Denneulin (*50*). In addition to problems with absorbency, issues related to surface charge and pH have been speculated to influence the conductivity of the organic conductors. Recently various types of nanocellulose based coatings have also been suggested for creation of smooth surfaces for printed functionality (*53*,*54*). It should be pointed out that the expression "paper electronics" is not to be confused with "electronic paper" or "e-paper", which refer to paper-like electronic displays, that are in fact not fabricated on paper *(1*,*55)*.

2.3. Functional materials

To fabricate electronics basically three types of materials are required, divided according to their electrical properties as conductors, semiconductors and insulators or dielectrics. In addition to these, materials with properties such as electrochromism, luminescence or sensing properties are needed for certain devices. The functional materials may be either organic or inorganic, the former being preferred due to its flexibility and lower cost, however regarding conductivity, the inorganic material is better. Composite materials have also been made by mixing inorganic metallic nanoparticles with organic conducting polymers. Common printable metals are silver, gold and copper, which as nanoparticles in a thin layer result in high conductivity ($<5x10^5$S/cm) and a smooth surface but require sintering and might suffer from oxidation. The same metals are also common as larger micron sized flakey particles, used in flexographic, screen or pad printing inks. Sintering, or removal of surrounding stabilizing polymers from the metal particle surface is required for obtaining conductivity, but the required energy (temperature) is very ink specific. The micron sized particles result in rougher printed layers compared to the nanoparticles. Common

organic conductive materials are PEDOT:PSS and polyaniline (PANI), which may be considered semitransparent as thin layers and are very flexible. The conductivity is however relatively low ($<10^3$S/cm). Recently carbon nanotubes have gained increasing interest and conductivities of $< 10^{3-4}$ S/cm have been reported, however they are still quite expensive. As printable semiconductors, different types of polythiophenes are common. Regioregular poly(3-hexylthiophene) (P3HT) has high mobility but is prone to oxygen doping, which in transistor use will lead to high off-currents. Poly(3,3'''-didodecyl quaterthiophene) (PQT) and poly(2,5-bis(3-tetradecylthiophen-2-yl)thieno[3,2-b] thiophene) (PBTTT) have higher ionization potential and thereby also better air stability, however the reachable conductivity is slightly lower compared to P3HT (*56*,*57*). Insulating or dielectric materials are also required in electronic devices, not only as active components as in the transistor or capacitor but also for preventing short circuits of crossing conductive wires. Most polymers are good insulators as well as soluble in organic solvents enabling printability. Poly(4-vinylphenol) (PVP), poly(methyl methacrylate), polypropylene, polyethylene terephthalate, polyimide, polyvinyl alcohol, and polystyrene are examples of insulating polymers. In organic field effect transistors (OFET) the dielectric - semiconductor interface is of extra importance because most of the charge transport in the semiconductor takes place within a few nanometers from this interface (*58*).

2.4. Paper electronics "State of the art"

Printed electronics, including functional materials research and development, has been a target of intensive research in the academic world for soon twenty years. Related research is going on in several universities, Massachusetts Institute of Technology, Harvard University, Chemnitz University of Technology, University of Toronto, Western Michigan University, Mid Sweden University, Uppsala Universitet, KTH Royal Institute of Technology, Monash University and Swansea University, just to mention a few. Recently also the use of paper as substrate has been brought in focus, not only for printed electronics but especially for sensors and diagnostics applications. For example, the Whitesides Research Group at Harvard University has demonstrated several diagnostics concepts on paper (*59*). In addition to journal publications several academic theses have also been published in the field, for example PhD Theses by Tapio Mäkelä (*60*), Daniel Tobjörk (*61*), Peter Angelo (*62*), Ana Lopez Cabezas (*63*) and Aamir Razag (*64*) as well as the Licentiate Thesis by Thomas Öhlund (*65*). Several research institutes are active in the field, for example the Technical Research Centre of Finland (VTT), Fraunhofer Institut, Holst Centre, Welsh Centre for Printing and Coating (WCPC) and Acreo, cooperating both with universities and industry. The printed electronics sector is now beginning to move into the marketplace after years of development work in laboratories and pilot printing facilities. However, many obstacles still have to be overcome, not only in improving the technologies but also in achieving competitive costs. Electronics and electrics on or in paper and board products such as

packages, is being used for security, safety, crime prevention, brand enhancement and anti-counterfeiting. Cost, weight and bulk are a problem, so conventional electronics in paper products is being replaced with printed electronics. According to IDTechEx analysis in the report, "Brand Enhancement by Electronics in Packaging 2012-2022", the global demand for electronic smart packaging devices is currently at a tipping point and will grow rapidly from $0.03 billion in 2012 to $1.7 billion in 2022. The electronic packaging market will remain primarily in consumer packaged goods reaching 35 billion units that have electronic functionality in 2022 (*66*). StoraEnso has brought to the market intelligent medicine packages, registering whether or when pills have been taken and via a GSM device included in the package, transferring the information to the medical personnel (*67*). Raflatac, starting as part of UPM, produces a wide variety of RFID tags and applications for streamlining logistics as well as for security purposes (*68*). A recent concept presented by Fulton Innovation is the Nestlé's Cheerios cereal box, using inorganic electroluminescent displays on the packaging combined with wireless power supply via inductive coupling (*69*). Bar codes, and 2D codes such as the QR Code and the UpCode™ are widely used, as so called hybrid media, meaning the printed code gives access to further information, either available in the code or as a web link. Reading the code however requires a reader, which most often is a mobile phone with a camera. Printechnologics GmbH, has recently presented a technique where the code is printed with conductive ink and may be read with a multi-touch screen, available on most smart phones today (*70*). An alternative will probably in the future also be the Near Field Communication (NFC) technology, that can be used to interrogate RFID labels on or in packaging, posters etc. (*71*).

2.5. Electronic devices and components

Electronic components can be categorized either as passive or active. The simplest components such as conducting wires, resistors, inductors, and antennas are considered passive, while transistors, diodes, batteries, and solar cells are considered active components. The transistor is perhaps the most important building block in electronics, but in comparison to the passive components much more complicated to fabricate. Most electronics also require some kind of power source which may be a battery or a solar cell or if energy is transferred via induction, an antenna. For a standalone electronic device, a combination of an input and output device, a logic device including memory and a power source may be needed. Functional devices, such as sensors, may also work completely without electricity, for example by change in color as in pH-sensitive Litmus paper. A short explanation of active electronic components and sensors demonstrated on paper substrates is briefly given below.

2.5.1. Energy sources

Capacitor

A capacitor is made up of two electrodes separated by an electrolyte (Figure 2A). Cellulose papers filled with a liquid electrolyte have been used as a separating membrane between the electrodes. In a capacitor the electrostatic charge is stored through the formation of an electric double layer at the interface between the electrolyte and the electrodes. Figure 2B shows a capacitor constructed from two electrodes separated by a dielectric, in which the energy is stored by the mechanism of charge polarization *(72-74)*.

Battery

The structure of a battery is similar to the capacitor structure, but in contrary to the capacitor the electric charge is stored as chemical energy through the electrochemical redox reaction in the electrode materials (Figure 2B). The most common thin-film flexible batteries are based on Li-ion, Li-polymer, Zn-MnO_2, or Zn-C. Batteries based on Zn-C/MnO_2 are already fabricated commercially (Enfucell Oy, Power Paper and Blue Spark Technologies) on paper by screen printing and lamination *(75-77)*. A drawback with the metals in the batteries has been the difficulties regarding recycling. A solution to this may be the all-polymer battery structure developed at Johns Hopkins University (*78*).

Solar cell

An alternative energy source for a battery or capacitor is the solar (photovoltaic) cell. While the performance is higher in inorganic solar cells, organic bulk heterojunction solar cells are considered to be most suitable for applications where low cost and flexibility are important (*79,80*). The schematic principle of an organic solar cell is demonstrated in Figure 2D, where the donor and acceptor stand for the key semiconductive materials enabling release of electrons when exposed to light. Photovoltaic cells have been fabricated on glass and plastic substrates as well as on lacquered paper (*13*) and recently also the Barr et al. demonstration of photovoltaic cells manufactured onto an ordinary newspaper by oxidative chemical vapor deposition (*14*).

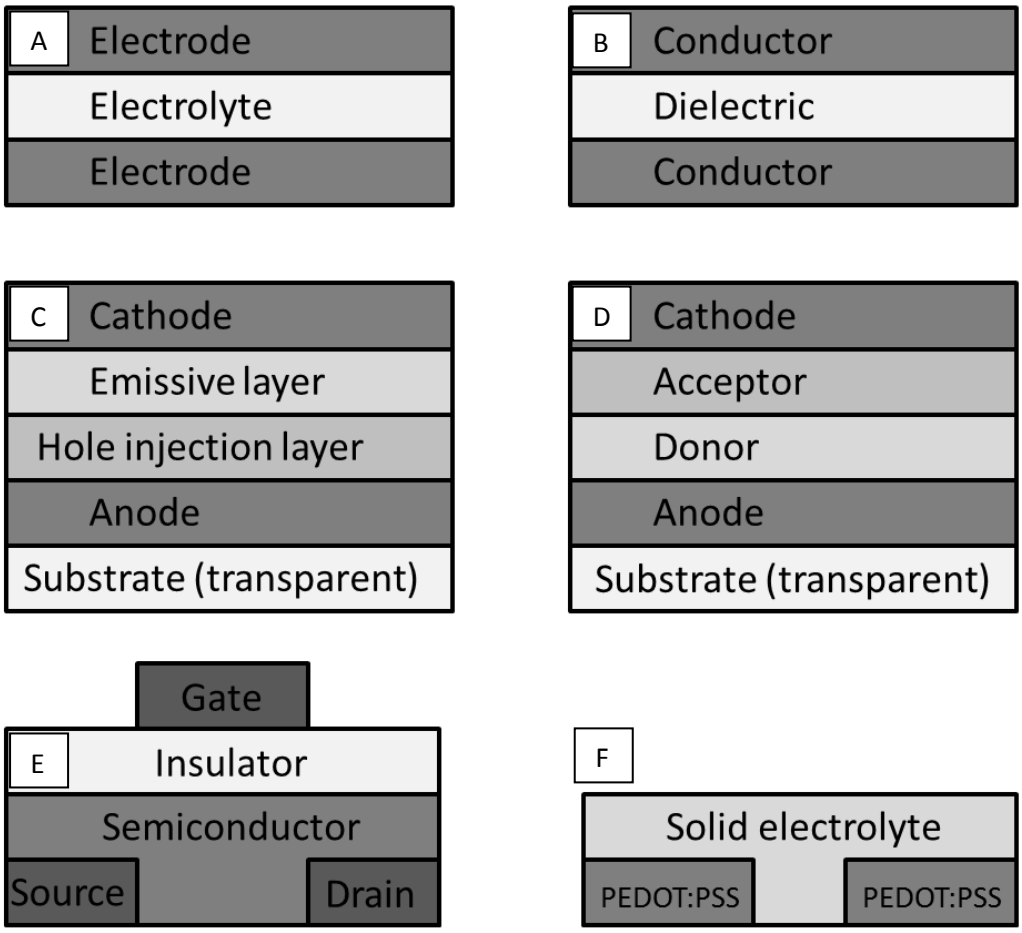

Figure 2. Schematics of common functional devices. A: electrolytic capacitor, B: dielectric capacitor or battery, C: OLED, D: Solar cell, E: Transistor, F: Electrochromic pixel.

2.5.2. Logic devices

The field effect transistor (FET) is a key component in most electronic logics. Transistors are used for driving elements in displays and as logic gates in digital electronic circuits. A FET consists of source and drain electrodes, a semiconductor, an insulator and a gate electrode and may exist in different geometries (Figure 2E). In a FET, the drain-to-source current flows via a conducting channel that connects the source region to the drain region. The conductivity is adjusted by the electric field that is produced when a voltage is applied between the gate and source. The current flowing between the drain and source is thereby controlled by the voltage applied between the

gate and source *(61,81-84)*. Several types of transistors have been fabricated with different printing methods on paper (*4,85,86*) or by using the paper as an active (dielectric) component (*87*). Memory devices are needed for storage of digital information and required in applications such as RFID tags. There are several ways of creating a memory device, but they are generally all based on a capacitor (on/off depending on charge), a resistor (on/off, may be destroyed once, to off stage, by applying high voltage), or a transistor (on/off depending on applied gate voltage. A transistor based memory requires continuous power, whereas a capacitor based one stores the information as long as the charge is maintained, i.e. both types can be considered volatile memory devices. The resistor based type does not need power to retain the information and is thereby non-volatile. Scott and Bozano (*88*) as well as Ling et al. (*89*) reviewed different types of memory devices, but there have been only few approaches directed toward printing memories onto paper. However, XaarJet AB has demonstrated inkjet manufactured 100-bit memory arrays consisting of ferroelectric cells on polyethylene terephthalate (PET) film *(90)*.

2.5.3. Output devices

Electrochromic low-resolution flexible displays can be made from low-cost materials using simple printing and lamination techniques. For example PEDOT:PSS organic conductive polymer can depending on its redox state show either blue color or transparency. An electrochromic (electrochemical) display was fabricated by Andersson et al. on PE-coated paper *(12,91)*. An opaque electrolyte was placed between two conducting polymer (PEDOT:PSS) layers (Figure 2F). A different type of simple display demonstrated on paper is a thermochromic display, consisting of patterned conducting wires on one side and a coated or printed thermochromic ink on the other side of the paper. When current is applied to the wires, resistive heating causes the dye in the thermochromic ink to turn transparent (*92*). A resolution of down to 200μm has been claimed for this device. In addition to the electrochromic and thermochromic displays, luminescent flexible displays can be made of organic light emitting diodes (OLED) (Figure 2C), light-emitting electrochemical cells, or phosphor-based electroluminescent devices *(93-96)*. However, the requirements on the drive transistors, sealing, and expensive fabrication processes of luminescent displays make the use of low-cost paper as substrate questionable.

2.5.4. Sensors

In addition to the electronic components there are various types of sensors, which in their simplest form reversibly or irreversibly detect some kind of stimulus, such as gas, pH, temperature, light, or biological compounds. The sensor signal may be read electrically, but there are also simple colorimetric indicators. Examples of sensors are

glucose sensors, ion-selective electrodes, hydrogen sulfide sensors and oxygen sensors. Among the most important properties of a sensor are the specificity, sensitivity, cross-sensitivity, and stability.

3. Fabrication of functional devices

A wide variety of methods exist for application of functional materials onto a substrate. The suitability of a given method is determined, together with the substrate properties, by the physico-chemical properties of the material to be deposited, the possible need for patterning, and the thickness and resolution requirements. Generally, slow methods used in highly controlled clean room conditions allow for high accuracy, whereas methods used in fast roll-to-roll processes enable low cost production, but provide less control over the fabrication accuracy. Below, printing and coating techniques that can be used for material deposition on paper are presented, with the focus on roll-to-roll processing techniques.

3.1. Batch processing methods

Photolithography is a commonly used process in microfabrication to pattern parts of a thin film on a substrate. It is a typical example of a subtractive method; first a uniform film is applied where after the pattern is created by engraving or etching. Etching may be carried out chemically or by use of a mask and UV light. Nano imprinting or stamp fabrication (*97*) are also used to mechanically pattern for example semiconductor films. For applying film, various coating methods, for example spin-coating may be used, but also deposition under vacuum is common. Photolithography allows for high resolution, down to nanometer scale, as for example in production of integrated circuits, but is relatively slow, requires cleanroom conditions and is not roll-to-roll applicable. Material may also be deposited by evaporation or vapor deposition and patterned via a mask. The limiting factor regarding resolution is in this case the accuracy for the mask production. Application and patterning via evaporation or vapor combined with a mask is an additive method, meaning the pattern is created onto the substrate directly to its final pattern. Evaporation requires vacuum and cleanroom conditions, which limits the roll-to-roll applicability. Pad printing is a simple batch printing technique, where the ink is transferred from an inked gravure plate or ink filled fabric to the substrate via a silicone rubber stamp. Inkjet printing is a common and widely used batch printing method, the most common method for printing documents at home, which has also gained a growing interest for printing functional materials. Inkjet has many advantages; it uses low viscosity inks, has low ink consumption, low cost and it is simple to change the digital print pattern.

3.2. Roll-to-roll processing methods

3.2.1. Coating methods

Different variants of roll-to-roll coating techniques for coating or sizing of paper have been used since the early 20th century. The first versions were brush and roll coaters. In roll coating the coating color is applied in a nip between rollers (Figure 3A). The principle of the premetered size press is similar as in roll coating, but addition of a premetering blade or rod on the application roller allows for control of the applied amount. The smoothness development is however somewhat limited with both methods due to film splitting occurring in the coating nip. This may be overcome by first applying an excess amount of coating color on the paper where afterwards the excess amount is metered by a blade (Figure 3B), an airknife (Figure 3C) or a rod. Blade coating is one of the most common coating methods for paper today. Recently, pre-metered contactless coating methods have gained increasing interest. While spray coating (Figure 3D) has not enjoyed much success, due to the poor coverage and smoothness it provides, curtain coating (Figure 3F) is today being used not only for specialty papers, such as thermal and photo papers, but also in traditional pigment coating. This is especially the case with board coating, in which high coat weights are used and good optical coverage is needed. An advantage of curtain coating is the possibility to apply several coating layers simultaneously in one pass. As paper coating is a high volume production process, the speed of the coating method is essential. When producing specialized coatings and thereby higher value products, a slower coating speed may be acceptable. Coating methods such as reverse gravure (Figure 3E) or slide bead coating allow for wide tunability of the coating color but have limited production speed. In addition to the wet coating methods, recently even gas phase deposition methods, such as plasma coating, chemical vapor deposition and atomic layer deposition, have been operated as roll-to-roll processes (*98,99*). However, the low pressure operation required by these techniques makes them complex and expensive.

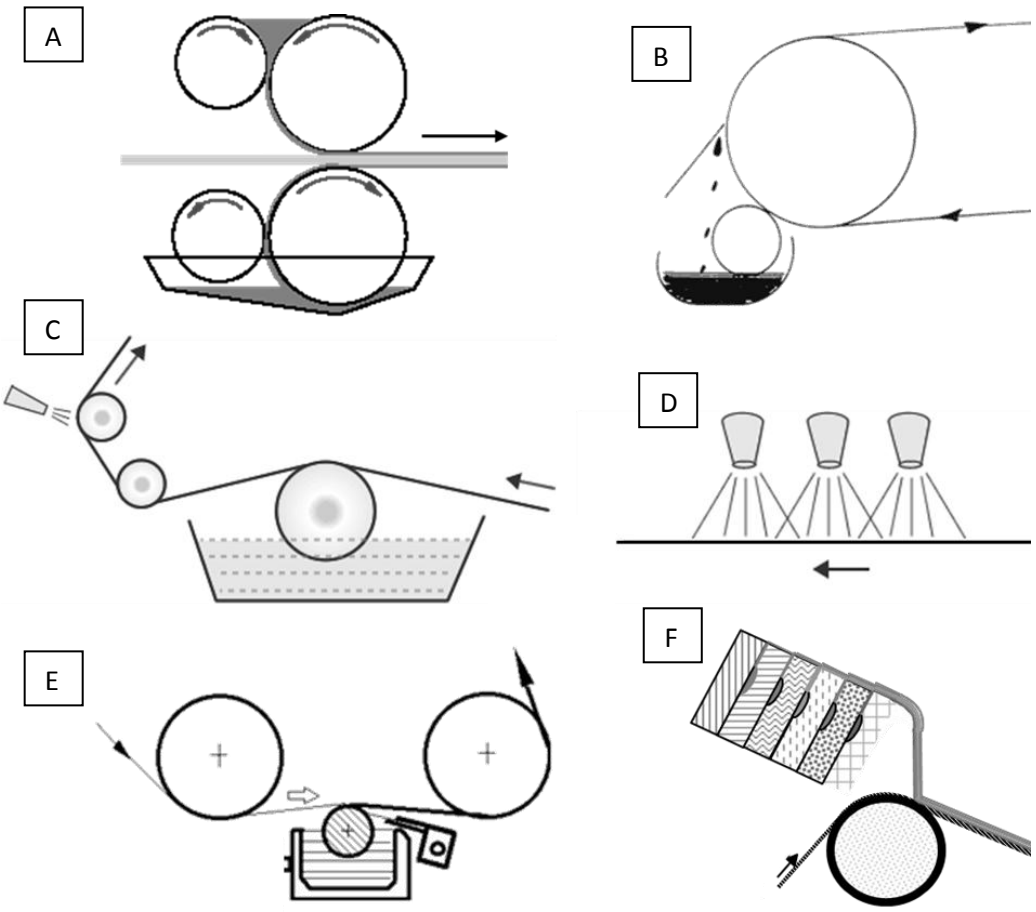

Figure 3. Schematic principle of coating methods. A: Roll coating (double sided). B: Blade coating. C: Air knife coating. D: Spray coating. E: Reverse gravure coating. F: Curtain coating with slide die.

3.2.2. Printing methods

Printing can be defined as patterned coating, i.e. material is only applied on desired areas. The most common rotary printing methods are offset lithography, rotogravure, flexography and screen printing. In a rotary printing method the same pattern is rotating on a cylinder from where it is either directly (rotogravure, flexography, screen) or indirectly (offset) transferred to the substrate. Printing methods such as inkjet and

electrophotography may also be used in a roll-to-roll process and the printed pattern may be continuously changed. A common term in graphical printing is “print quality” which may have various definitions, but is usually related to a visual impression of the reproduced text or image. When printing electronics, the term print quality should, in addition to, or perhaps even instead of, the optical impression, measure the functionality, for example obtained conductivity. It should also be noted that in all traditional printing methods the image is built up from a raster of discrete dots. For achieving conductivity, it is essential that these dots are connected, i.e. overlapping or merged. Continuous lines, or image areas, may however be created in an offset plate or engraved in a rotogravure cylinder.

Table 1. General parameters and requirements for the common printing methods (*100*).

Printing method	**Offset**	**Rotogravure**	**Flexography**	**Letterpress**	**Inkjet**	**Screen**
Transfer method	rollers	rollers	rollers	plate	thermal, piezo, continuous	ink pressed through holes in screen
Pressure applied	1MPa	3MPa	0.3MPa	10MPa		
Drop size	-	-	-	-	1–100pl	-
Ink viscosity	40–100Pa·s	0.05–0.2Pa·s	0.05–0.5Pa·s	50–150Pa·s	1–20mPa·s	1–50Pa·s
Thickness of ink layer on substrate	0.5–1.5µm	0.8–8µm	0.8–2.5µm	0.5–1.5µm	<0.5µm	<12µm
Comments	high print quality	excellent image reproduction	high quality	slow drying	special paper required	versatile method, low quality
Cost-effective run length (copies)	>5,000 (sheet-fed) >30,000 (web-fed)	>500,000			<350	

Offset lithography

Offset lithography (Figure 4C and Table 1) printing is the most common printing technique today. The print pattern is based on local differences in surface energy, created by photolithography. In normal offset, the nonprinting areas of the printing plate are first wetted with a water-based fountain solution, whereby the oil based ink transfers only to the image areas. In waterless offset presses, no dampening solution is used. Instead the plate's nonimage areas consist of a layer of silicone rubber that repels the ink. The temperature of the inks must however be exactly controlled to maintain the correct viscosity since the plate surface is designed to repel inks only of a specific viscosity. In comparison with normal offset, waterless offset allows for higher screen ruling and better image definition, however the silicon rubber plates are more expensive as well as more vulnerable compared to normal plates. Additionally the requirement for heated roller increases the printing costs (*101*). The offset inks are tacky and have high viscosities (40-100Pas). High print resolution can be achieved with offset technique, but

the presence of water and the restrictions on the viscoelastic properties of the ink limit the use of offset for printing electronics. Waterless offset has, however, been used for printing PEDOT:PSS (*4*).

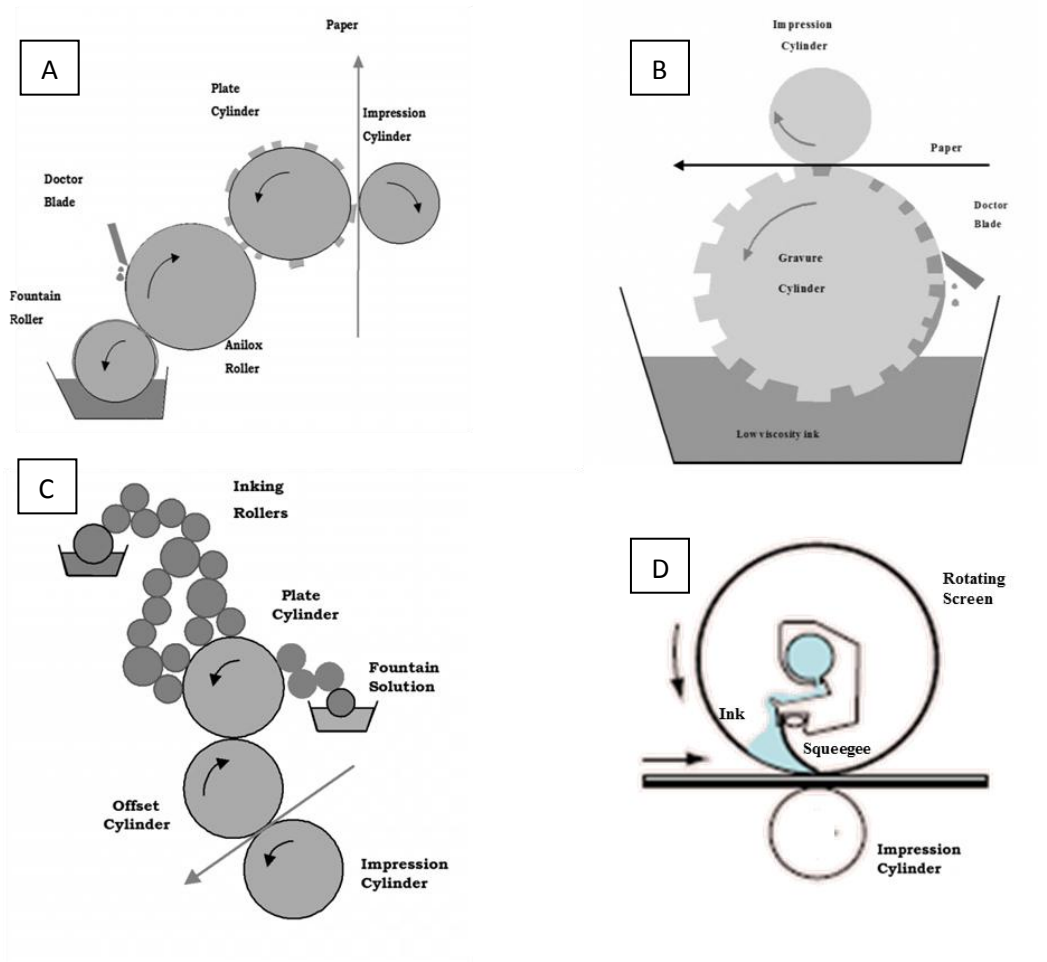

Figure 4. Schematic principle of the printing methods. A: Flexography, B: Rotogravure, C: Offset, D: Rotary screen. The schematic figures are reproduced with slight modification from "Handbook of Print Media" (*100*).

Rotogravure

Rotogravure printing (Figure 4B and Table 1) is a high volume printing process. The print pattern is engraved into a ceramic or metallic cylinder by laser, chemical etching, or mechanically as separate cells or intaglio trenches and high print resolution (~20µm) can be achieved. The rotogravure rolls have a long lifetime, but are expensive to

produce, which makes rotogravure a technique mainly suitable for large print volumes. Low viscosity (50-200mPas) solvent based inks are used. Continuous print patterns can be created by using a small enough cell spacing compared to the cell width, if the ink viscosity and surface tension are also low enough to allow the printed dots to merge. The ink transfer may be further enhanced by use of electrostatic assist. Rotogravure has been widely used for fully or partly fabricating functional devices such as wires (*52,102*), antennas (*103*), organic solar cells (*104*) and OLEDs (*105*).

Flexography

Flexography (Figure 4A and Table 1) originates from the letterpress technique and is today one of the main methods for printing of packages. In flexographic printing the pattern to be printed is raised on a flexible plate that is attached to a cylinder. The raised surfaces of the printing roll are inked when in contact with an ink-covered anilox cylinder that consists of homogeneously distributed, laser or mechanically engraved cells. The ink amount is adjusted by the cell volume of the anilox, and the viscosity of the flexographic inks is usually in the range of 50 - 500mPas. A lower viscosity and surface tension as well as low nip pressure enhance the possibility to achieve continuous print patterns, even though the anilox roll consists of engraved discrete dots. The print resolution in flexographic printing is lower than in rotogravure printing, mainly due to limitations in plate manufacturing, but also due to distortion of the pattern on the flexible plate during printing. Another common defect is observed when a flexographic plate is pressed against the substrate thereby causing excessive squeezing of the ink, which results in undesired halo-like shapes around the edges of the printed pattern. Flexographic printing has been used for printing conductive inks, for example electrodes in sensor applications, and for fabrication of RFID antennas and transistors (*48,106,107*).

Screen printing

Screen printing has lower requirements for substrate and ink when compared to the other traditional printing techniques. The surface does not have to be printed under pressure and it does not necessarily even have to be planar. The most common form of screen printing is the batch method, used for printing of clothes, signs and irregularly formed items such as balloons. Rotary screen (Figure 4D and Table 1) is used for printing of for example textiles and wallpapers. In screen printing the ink is dragged across the surface of a screen and squeezed through the open pores of the patterned mesh onto the substrate. Print resolution and print thickness depend on the density of the mesh and the ink properties. A rather high ink viscosity of 1000 - 50000mPas is required and a print resolution of ca 100µm as well as wet layer thicknesses up to 100µm can be printed. The possibility of printing thick layers has been an advantage for functional

printing and screen printing has successfully been used for manufacturing for example antennas (*108*), photovoltaic cells (*79*) and even pyrotechnics (*109*).

Inkjet

Inkjet printing has gained increasing interest for graphical printing, both as a standalone and as an afterwards added method in hybrid printers. The advantages of inkjet versus the conventional rotary printing methods are continuously changeable print pattern and low material consumption (Table 1). Although inkjet is roll-to-roll compatible it has limitations regarding printing speed as well as high requirements regarding printing ink quality, since the small nozzles are sensitive to impurities. The requirement of low viscosity inks which contain large amounts of ink vehicle/solvents set further limitations to the printing speed by prolonging the drying time. Narrow structures as small as 1μm have been printed by inkjet, when using extremely small nozzles (*110*), however in practice today structures down to 20-30μm are reality. Inkjet has been used for printing a variety of functional materials and is today a common method for fabricating functional devices *(111-113)*.

4. Materials and methods

The materials and methods used in this work are outlined in this chapter. All product trademarks are listed in the attached publications.

4.1. Substrates

As reference substrates were used commercially available coated fine paper (StoraEnso Lumipress 115g/m^2), inkjet photo paper (Canon Photo Paper Plus Glossy II, 260g/m^2) and a standard 80g/m^2 copy paper (Image Volume). Mylar A (DuPont Teijin Films) flexible plastic was also used as reference substrate. For the coating structure introduced in this work, the base web substrate may be any coatable substrate and further studies regarding the base substrate were therefore not made. The requirement was suitable strength for roll-to-roll coating and printing. Pre-coated base paper (90-107g/m^2) fulfilled that requirement and was therefore chosen as basepaper. The precoated basepaper was blade coated with a ca. 10g/m^2 kaolin layer (smoothing layer) to increase the surface smoothness. Commercially available coated fine paper (StoraEnso Lumipress 115g/m^2) was also used as basepaper as such. When using readily coated smooth basepaper there is no need for coating a smoothing layer.

4.2. Coating materials

4.2.1. Mineral pigments

The main component in a coating layer is the pigment. Characteristics like pigment particle size distribution and particle shape affect the properties of the final paper, such as the optical and the structural properties but also printability. Mined minerals tend to have broad particle size distribution whereas synthesized mineral particles can be controlled in size and shape. Influence of pigment size and shape on coating microstructure and furthermore its relationship to printability has been widely studied and reported *(114-117)*. For coater runnability, platy pigment particles usually increase the water retention (resist dewatering of the coating color) due to high tortuosity caused by the particle orientation perpendicular to the liquid flow direction. Isotropic particles, such as ground calcium carbonate, create structures with higher permeability allowing the water to penetrate them more easily.

Kaolin

Kaolin has been used both as filler and as coating pigment for over a century. Kaolin consists of two atomic layers, an octahedrally co-ordinated aluminium oxide layer and a tetrahedrally co-ordinated silica layer. The layers are bound to each other by oxygen atoms. The particle shape and size differ depending on where the pigment originates from. Several different shape factor (1 - 100:1) kaolins were used, all supplied by Imerys Minerals Ltd. The trademarks of the pigments are listed in the attached publications [Publication II- VI].

GCC

Ground calcium carbonate has been an important coating and filler pigment for half a century. The calcite mineral occurs in various rock forms: chalk, limestone and marble. The grinding is done through either wet or dry processing and the product is today usually delivered in slurry form because of a smaller storage volume and because of the feasibility to be pumped. GCC was used as precoating pigment, coated in industrial scale by the basepaper manufacturer.

PCC

Precipitated calcium carbonate is produced via a synthesis, by a reaction between calcium hydroxide and carbon dioxide. The physical properties for PCC are the same as for GCC but the particle shape and particle size distribution differ. There are two different mineralogical forms of PCC, calcite and aragonite. Calcite assumes hexagonal or rhombohedral structures while aragonite assumes orthorhombic, needle-like structures. The particle size distribution can for PCC be made very narrow, which creates a highly porous coating structure. Narrow PSD aragonite PCC (Opacarb 3000, Specialty Minerals Nordic Oy) was used as top-coating pigment [Publication II and V].

Talc

Talc is a common platy mineral composed of hydrated magnesium silicate. Talc is the softest mineral in the world. It is formed either through regional or contact metamorphosis of carbonate sediments or through hydrothermal alteration of magnesium-rich magmatic rocks. Talc (Mondo Minerals B.V., C10B, delivered as dispersion) was used in barrier layer coatings [Publication II].

Mica

Ground mica is used in the paint industry as a pigment extender to reduce chalking, to prevent shrinking as well as to increase resistance of the paint film to water penetration. Mica has not been a common pigment for paper coating, but was included due to its extremely high aspect ratio (>200:1) as a reference in barrier coatings [Publication IV].

Silica

The chemical compound silicon dioxide, also known as silica, is an oxide of silicon with the chemical formula SiO_2. Silica is a porous pigment, i.e. the pigment itself contains nanoscale pores. In a coating layer this feature results in a bimodal porosity. Due to its porosity and large pore volume silica is commonly used in inkjet papers. Different particle size silica pigments were used for top-coatings. Large particle size (Syloid C807, Grace GmbH, DE) was used in Publication V.

4.2.2. Latex

Latex is a colloidal dispersion of spherical polymer particles in water. The particles do not float or sink due to gravity and in one liter there are approximately $3 * 10^{15}$ particles with a surface area of 20,000m². Styrene is a common backbone polymer, but also ethylene and propylene are used. Styrene-butadiene latex as supplied by Styron Europe GmbH or BASF was used as binder in top-coatings. Styrene-acrylic and ethylene-acrylic latexes were also used for barrier coatings. The trademarks are listed in the attached publications.

4.2.3. Starch

Starch can be anionic or cationic and it functions as a binder or barrier. It has been used for bringing stiffness and posture to the paper and lowering the surface porosity. In this work starch was used as an alternative binder in barrier coatings. Chemigate Raisamyl® 01151 surface sizing and coating starch, supplied as powder and prepared according to instructions by supplier, was used as a reference binder in barrier coatings.

4.2.4. Additives

Different additives are required during coating color preparation and coating, such as dispersing agents, surfactants and rheology modifiers. Sodium polyacrylate dispersing agent was added according to instructions by supplier when dispersing kaolin, GCC and

mica. The other pigments were delivered as slurries and ready to use. Coating color rheology was adjusted by carboxymethyl cellulose (CMC) or synthetic thickener. Surface tension of coating color was adjusted by either replacement of water with iso-propanol [Publication II] or addition of surfactants [Publication VI].

4.3. Paper coating methods

A mini pilot scale blade coater (Rotary Koater, RK Print-Coat Instruments Ltd., UK) was used for applying both the precoating and the second "precoating" (smoothing layer) as well as for applying of barrier coatings. A laboratory scale table top rod coater (K Control Coater, RK Print-Coat Instruments Ltd., UK) was used for applying top-coatings. A Minilabo, (Yasui Seiki, JP) as well as a custom built reverse gravure coater, were used for applying barrier coatings and top-coatings. The same equipment was also used for functional coatings, described in section 4.6 and Figure 5C. Two pilot scale slide curtain coating trials were performed, the first trial at Styron Europe GmbH in Samstagern Switzerland and the second one at Metso Paper Oyj in Järvenpää, Finland. Both the barrier layer and the top-coating layer were applied simultaneously [Publications IV, V and VI]. The slide bead coating method is very similar to the curtain coating technique, with the difference that in the slide bead coating method, the coating color falls in a narrow gap (zero length curtain) onto the running web. Pilot scale slide bead coating trials were carried out at Ilford Imaging GmbH in Marly, Switzerland [Publication IV].

4.4. Surface treatment

Corona and plasma treatment

Corona treatment is a surface modification technique that uses low temperature discharge plasma to impart changes in surface properties, usually increasing the surface energy by oxidization. The corona plasma is generated by the application of high voltage to sharp electrode tips which forms plasma at the ends of the sharp tips. Both corona and plasma treatments use high voltage electrodes, which charge the surrounding gas molecules and ionize them. Both treatments were performed on a pilot scale in a roll-to-roll process (Vetaphone, Corona Plus) at normal atmosphere (air). In the corona treatment, the plasma state occurs between two electrodes, one of which is a grounded metal roll under the substrate. The atmospheric plasma is generated using a dielectric barrier discharge, which eliminates the backside treatment of the substrate [Publication II].

Ultra violet (UV-C) radiation treatment

Low-pressure mercury lamps with radiation mainly composed of two wavelengths, 185 and 254nm, can be used for increasing surface wettability of polymer and rubber films. The UV radiation at 185nm generates ozone from oxygen in air. The germicidal wavelength of 254nm has conventionally been used for cleaning and removing organic material. In publication II, UV-C surface treatment was performed using a germicidal, ozone-free UV-C lamp (maximum wavelength=254nm) supplied by Heraeus. The irradiation intensity was varied between 30 and 70mW/cm^2.

4.5. Functional inks

Nanoparticle silver ink

A commercial silver-nanoparticle ink (SunTronic Silver, U5603, Sun Chemicals Corp.) consisting of ca. 30–50nm large dispersed silver nanoparticles (20 wt-%) in the solvents ethanol and ethylene glycol with a viscosity of 10–15mPas and a surface tension of 27–31mN/m was used in Publications I, V and VI.

Micron-size particle silver ink

For flexographic printing a commercial silver flake based ink (125-06, Creative Materials Corp.) was used after required dilution with 1-methoxy-2-propanol acetate (PM-acetate) [Publication V].

Micron-size particle carbon ink

Flexographic printing in Publication V was carried out with a micron-size particle based carbon ink (Creative Materials Corp., 110-04). The ink was diluted with methyl ethyl ketone (MEK).

Conductive polymer inks

Conductive polymer ink, poly(3,4-ethylene dioxythiophene) with poly(styrene sulfonate) (PEDOT:PSS) was used both for inkjet and flexographic printing. Heraeus Clevios PH 500, which is water based, was used for ink-jet printing in the roll-to-roll process after adding 0.1 vol-% surfactant (Triton X-100) just before printing. For flexographic printing relatively viscous PEDOT:PSS ink was used; both Baytron P (increased viscosity by roto-evaporation to a concentration of about 1.7 wt-%) and Heraeus Clevios P HC V4 as delivered [Publications I and V].

Organic semiconductor ink

Regioregular poly(3-hexylthiophene) (P3HT) (Plexcore OS-1100, Plextronics Inc.) was used as semiconductor material. Depending on the application method and need of evaporation time different solvents or solvent mixtures were used as described in [Publication I, V and VI].

Organic dielectric ink

Non-cross-linked poly(4-vinylphenol) (PVP) (P25ED, DuPont Electronic Polymers) with a molecular weight of 25,000 was used as the hygroscopic electronic insulating material when fabricating hygroscopic insulator field effect transistors. Iso-propanol or ethyl acetate were used as solvents and solids contents between 10 and 20% were used. In order to strengthen the PVP film, kaolin particles (up to 10 wt-%) were added to form a composite structure [Publication I and V].

4.6. Functional printing and coating

Flexographic printing was carried out using a custom-built roll-to-roll mini pilot scale printer (web width 10-12cm) (Figure 5A) with Commercial ASAHI DSH® (Shore A 69°) photopolymer plates. The ceramic anilox cylinder (Cheshire Engraving Cervices Ltd., UK) used with the silver ink had a cell angle of 60° with 120 lines/cm and a cell volume of 12cm^3/m^2, while the one used with the carbon ink and the PEDOT:PSS had a cell angle of 60° with 70 lines/cm and a cell volume of 30cm^3/m^2. The printing speed was 10m/min and eight 500W infrared sintering units (HQE 500, Ceramicx, IRL) (700°C) were mounted online (Figure 5D). Flexography register control was carried out manually with step motors [Publication V].

Inkjet printing in batch processing was carried out with a drop-on-demand Dimatix Materials inkjet printer (DMP-2831, Dimatix-Fujifilm Inc., US). All inks were filtered through 0.45μm filters before filling the 1.5 ml-cartridge (DMC-11610) consisting of 16 piezoelectric nozzles. The batch printed silver was sintered for 10 to 30 seconds at a light intensity of around 2W/cm^2 with an offline infrared heater (2kW) (IRT systems, Hedson Technologies AB). In roll-to-roll processing the inkjet printhead (Xaar 128/80, Xaarjet Ab, SE), consisting of 128 nozzles with a nominal drop volume of 80pl, was operated by an Imaje 4400 controller and software, and fed by a custom-built ink-feed setup (Figure 5B). Alignment of inkjet printing was controlled with the help of an optical sensor that was coupled to the inkjet control unit [Publication V and VI].

Two different reverse gravure coaters were used, namely a commercially available MiniLabo (Yasui Seiki Co., Japan) and a custom built one. The latter was included

inline in the custom-built mini pilot scale printer (Figure 5C). The maximum web speed of the Mini-Labo test coater was 1.6m/min and the maximum gravure roll speed 48 rpm (surface speed: 3m/min) while in the custom built reverse gravure coating head the maximum roll speed is ca. 200 rpm, which allows for web speeds of up to 10m/min. The gravure rolls were the same in both coaters, 20mm in diameter, and the grooves/inch were chosen according to required application amount.

A custom built spray coater consisting of four airbrushes was used for applying of semiconductor material as well as copper chloride. The coating thickness was controlled by varying the web speed, spraying distance, spraying pressure and ink/air ratio. Drying was enhanced by a hotplate behind the substrate [Publication V].

A Chemat Technology KW-4A spincoater was used for coating semiconductor (P3HT) and insulator (PVP) material [Publication I and VI].

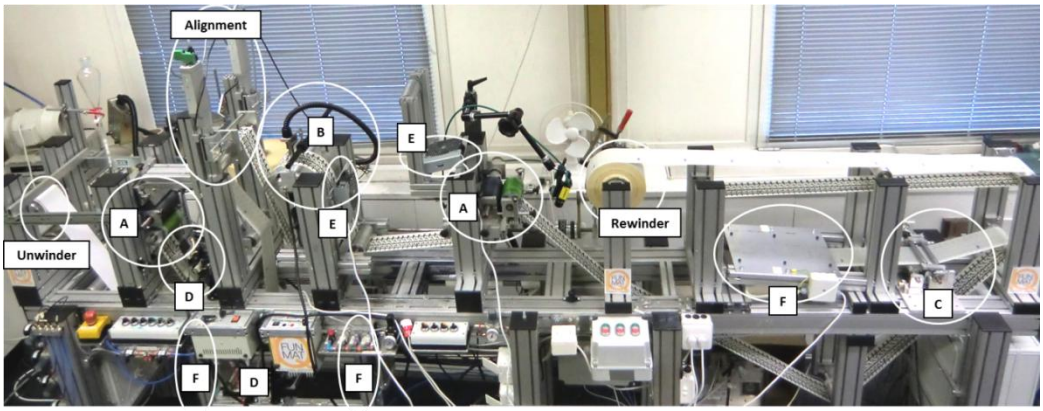

Figure 5. The custom-built roll-to-roll hybrid printer with exchangeable units. A: Flexography, B: Inkjet, C: Reverse gravure, D: Infrared sintering, E: Fan driers, F: Oven driers. Spray coating unit not installed in the setup above due to space limitations.

4.7. Characterization methods

Substrate characterization

An FEI FIB201 gallium focused ion beam instrument was used for sectioning and high-resolution imaging of paper cross sections. A JEOL JSM-6335F field emission scanning electron microscope (SEM) was used for surface imaging and cross-section imaging of resin embedded substrates. The PPS surface roughness was measured with a ME 90 Parker Print-Surf (PPS), Messmer Instruments Ltd. roughness meter. An NTEGRA Prima (NT-MDT) atomic force microscopy (AFM) was also used to analyze the surface topography. Topographical imaging was carried out in semi-contact mode. All the AFM

images (1024 x 1024 pixels) were measured at ambient conditions (RH = 24 ± 3%, and RT = 24 ± 1°C). Scanning Probe Image Processor (SPIP, Image Metrology, DEN) software was used for the roughness analysis of the images. The pigment particle shape factor was determined through the conductivity based measurement method described in Webb et al. (*118*).

The liquid-solid surface contact angles were measured at ambient conditions (RH = 22 ± 3%, T = 22 ± 2°C) using a CAM 200 contact angle goniometer (KSV Instruments Ltd). For calculating the surface energy, the apparent contact angles of the probe liquids, i.e., water, ethylene glycol (EG), and diiodomethane (DIM), were measured. The calculations were performed using the theory proposed by Owens and Wendt (*119*), Kaelbe (*120*) and Fowkes (*121*), subdividing the surface energy into polar and dispersive parts. No roughness corrections were made.

The surface porosity was analyzed according to the IGT W24 print penetration test (Dutch standard NEN 1836) with an AC2 (IGT Testing Systems Ltd., Netherlands) tabletop printability tester. A Pascal 140/440 (Thermo Fisher Scientific Inc., GER) mercury porosimeter was used for analyzing the porosity of coating tablets. A DeWetPres (DT Paper Science, FI) tablet press was used for pressure filtration of the coating colors to form the tablets for the mercury porosimetry measurements.

An Elrepho 070 (Lorentzen&Wettre, SE) spectrophotometer was used for the whiteness, brightness and opacity measurements. A Zehntner ZLR 1050 gloss meter was used for the gloss measurements. An Epson Perfection V750 Pro scanner (6400 dpi) was used for scanning the images for image analysis.

A Weiss Umwelttechnik SB111/300 humidity chamber (RH=90%, T=23°C) and an MBraun UNIlab glovebox (H_2O:1.4ppm, O_2:11.6ppm) were used for modified atmosphere simulation.

Electrical characterization

A Keithley 2100 multimeter (four-probe setup) was used for resistance measurements and an Agilent 4142B instrument operated with a custom written LaBView program was used for measuring the transistor characteristics.

Characterization of barrier properties

Water Vapor Transmission Rate (WVTR) was measured according to the ASTM standard (E 96/E96M-10), which monitors the water penetration as a function of time at chosen temperature and humidity (*122*). In the current work a temperature of 23°C and a relative humidity (RH) of 85% was used. Barrier properties against solvents and acidic

liquids were measured with the prism method described in detail in Publication III. The method monitors penetration of a liquid through a substrate as function of time through observation of changes in effective refractive index on a prism surface placed under the sample. Publication III and Results section 5.2.1. describe and compare barrier measurement techniques.

5. Results and discussion

This chapter contains a summary of the main results and findings from the attached publications. In section 5.1. the structure of the developed multilayer coating construct is explained as well as requirements and possibilities regarding manufacturing. Section 5.2. describes barrier properties, introducing novel measurement methods for short term barrier properties of paper substrates. Barrier properties created by dispersion coating and the influence of coating structure is discussed. Section 5.3. focuses on the top-coating and the impact of surface structure on printability of functional inks. In section 5.4. the influence of humidity on dimensional stability and its impact on functionality is discussed. Section 5.5. demonstrates proof-of-concept devices manufactured by printing or coating on the multilayer coated substrate.

5.1. Paper for printed electronics

It is not possible to define a single paper concept that could be considered a "the paper for printed electronics." The suitability of the paper depends on the functional materials deposited on it to fabricate the targeted device. However, there are some general properties, which either are a prerequisite for the functioning of a printed device, or which improve the performance of it. These include surface smoothness, barrier properties to maintain the functional materials on the paper surface as well as print definition.

5.1.1. Multilayer coating structure

Based on the requirements listed above (section 5.1.), initial testing of a few concepts, as well as by comparison to commercially available paper and polymer substrates, led to a multilayer coated paper substrate being developed. In this multilayer structure, shown in Figure 6, a thin top-coating consisting of mineral pigments is coated on top of a dispersion-coated barrier layer. The top-coating provides well-controlled sorption properties through controlled thickness and porosity, thus enabling an optimization of the printability of functional materials (section 5.3.). The penetration of ink solvents and functional materials stops at the barrier layer, which not only improves the performance of the functional material but also eliminates potential fiber swelling and de-bonding that can occur if the solvents are allowed to penetrate into the base paper (section 5.2.). The multi-layer coated paper under consideration in the current work consists of a pre-coating and a smoothing layer under the barrier layer. Coated fine paper may also be used directly as basepaper, as long as a smooth base for the barrier layer is ensured. The top coating layer is thin and smooth (coat weight 0.5–10g/m², layer thickness 0.5–5µm, RMS surface roughness 55-75nm) consisting of mineral pigments such as kaolin,

calcium carbonate, silica or blends of these. All the materials in the coating structure were chosen in order to maintain the recyclability and sustainability of the substrate.

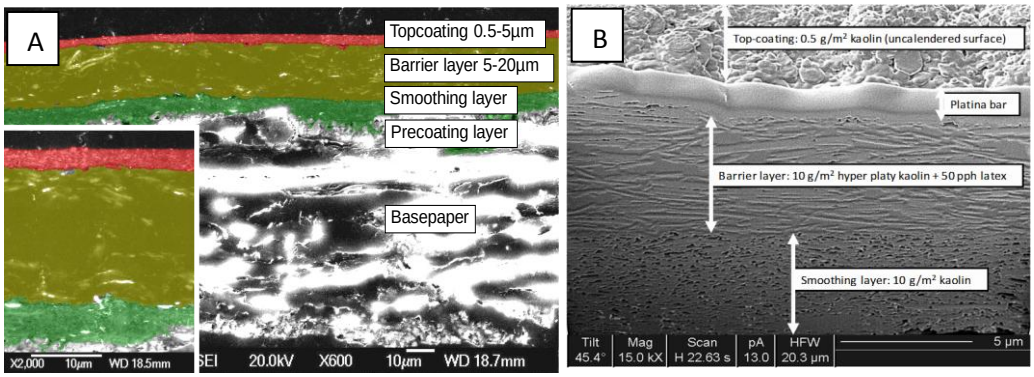

Figure 6. A: Cross-section SEM image showing the layer structure of the paper substrate: top-coating, barrier layer, smoothing layer, pre-coating and basepaper. B: Focused ion beam etched cross-section image.

5.1.2. Multilayer structure manufacturing

The multilayer substrate developed in this work can be produced by coating each layer sequentially, by laying down all the coating layers simultaneously, or by combining these approaches. Sequential coating was used in laboratory scale, since most multilayer coating methods require minimum process speeds of approximately 300m/min, which is impractical for small scale studies. Simultaneous multilayer coating was carried out in minipilot and pilot scale. In the sequential approach, the coating of the thin top-coating on top of the closed and often relatively hydrophobic barrier layer requires detailed understanding and tuning of the wetting properties and topography of the barrier layer in relation to the surface tension of the top-coating formulation [Publication II]. Incompatibility of the barrier and the top-coating material may cause insufficient wetting of the barrier layer by the top-coating dispersion during coating, which can lead to an uneven top-coating thickness or uncoated spots. The top-coating coatability was studied by creating barrier layers with as distinct as possible surface properties (surface energy, hydrophilicity and roughness) while maintaining adequate barrier properties. Furthermore, different post treatment methods were used to modify the surface energy and wettability. Plasma and corona treatments were used at two power levels and ultra violet (UV-C) radiation was also tested. The full experimental plan, including the detailed recipes, is listed in Tables 1-3 in Publication II. In addition to the modifications of the barrier layer also the surface tension of the top-coating dispersion was adjusted to three different levels (49.4, 43.3 and 35.2mN/m) by partially replacing water with iso-propanol. The reverse gravure coating technique was used for coating of the top-coating because it enabled the coating of thin (0.5-10g/m²) top-coating layers onto the barrier

layer. The laboratory scale blade coating technique was not able to generate uniform coating layers, since the coating did not adhere to the barrier layer and was scraped off.

The coatability, or wetting of the barrier layer by the top-coating, was visually evaluated on a scale from 1 to 4. Figure 7 shows examples of the coating layer quality. The scale grades indicate the following characteristics: grade 1, no wetting; grade 2, inadequate wetting resulting in areas being uncoated; grade 3, small defects, i.e., at the minimum limit to required wetting; and grade 4, proper wetting and adequate coatability. From a research point of view, the grade 3 is the most interesting one, indicating that the wetting is only slightly inadequate. From a manufacturing point of view, only the grade 4 is acceptable and results in a defect-free coated layer.

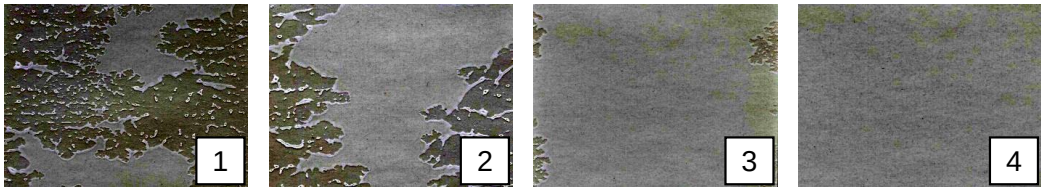

Figure 7. The coatability was visually evaluated on a scale of 1-4. The image contrast has been increased to show the differences better between the barrier and the top-coating layers.

The water contact angle of the barrier layer was found to be the most important factor for predicting the coatability. On the barrier layers with water contact angles less than 100°, it was possible to coat with all the studied top coat pigment dispersions. In a water contact angle range from 100° to 110°, there is a variation in the coatability, and the effect of the reduced surface tension in the top coat dispersion can be observed. When the water contact angle on the barrier layer reaches 110°, the coating of the top coat in an aqueous suspension becomes impossible (Figure 8). Beyond this point, the cohesive forces in the coating color are stronger than the adhesive forces to the barrier layer. A lower surface tension clearly improved coatability, especially in the water contact angle range from 100° to 110° on the barrier layer. A reduction of 10 to 15mN/m in surface tension could counteract ca. 5 to 10° higher water contact angle on the barrier layer.

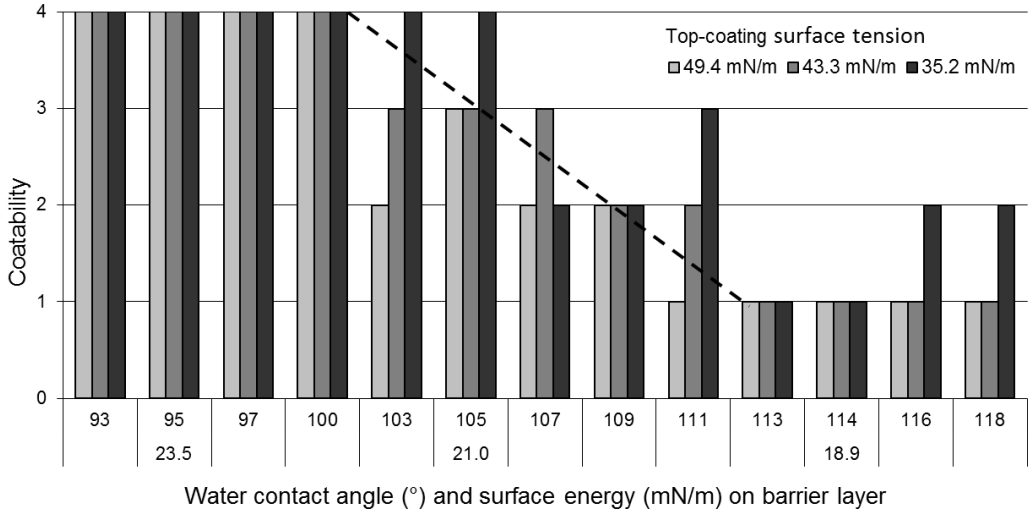

Figure 8. Top-coating coatability against contact angle for water on the barrier layer. Three different surface tensions in the top-coating dispersion were used: 49.4mN/m, 43.3mN/m and 35.2mN/m. The surface free energy of the barrier layer was measured at three points: 95°, 105° and 114° water contact angle.

Although there is only negligible nip pressure in the reverse gravure coating method, the coating process can still be considered forced wetting because the web is pressed against the gravure roller by the web tension. This means that the coating color is forced to contact angles smaller than would be the case without external pressure. Because the coating color is a dispersion consisting of pigments in water at a relatively high viscosity of 500mPas, viscous resistance plays a role in the wetting behavior. The dispersion does not have time to return to the contact angle set by the chemistry alone before the water is removed by evaporation. The evaporation increases the viscosity rapidly, and the pigments are immobilized where they have been deposited by the gravure roller. The surface roughness of the barrier layer appeared to have only a minor impact on the coatability.

A cost competitive method for industrial scale production of the multilayer coated paper is the curtain coating technique, which enables coating of all the layers in one pass [Publication V and VI]. While in curtain coating both the top-coating and the barrier layer are coated simultaneously, wet on wet, there is no such relationship between surface tension and surface energy as described for the layer by layer coating. Curtain coating, however, sets high requirements for elongational viscosity and surface tension of the coating colors in order to ensure a stable curtain. Additionally, deaeration is required, since possible air bubbles will cause holes in the coated layers. In practice, successful coating of thin top-coating layers also requires very low solids contents (down to 5%), addition of synthetic thickeners and surfactants as well as a stable barrier-layer curtain to support it. A variety of coating recipes and parameters are described in

Publications V and VI. Curtain coating coatability was not explored in the present work since it is difficult to carry out such an investigation in small scale. The practical difficulties here arise from the minimum coating speed requirement of ca. 300 m/min, and the relatively large coating color amounts needed for deaeration.

5.2. Barrier properties

In functional printing and coating, conductive, semi-conductive and insulating materials are usually dissolved in organic solvents such as dichlorobenzene or toluene. Although these liquids are brought into a direct contact with the substrate, the solvents evaporate quite rapidly, suggesting that short term barrier properties might suffice. On the other hand, in throw-away sensor applications, for example for medical use, acidic or basic analytes may be used, the sensoring process might last for several minutes and long term barrier properties are needed *(123-128)*. In the multilayer coating structure the barrier layer both controls the absorption of the inks during device fabrication and ensures the end-use function. A simple example of a sorption test for a semiconductor ink, regioregular poly(3-hexylthiophene) (P3HT) dissolved in ortho-dichlorobenzene (DCB), is shown in Figure 9. The amount of ink applied was the same for each sample, 5 µl, and the scanned area was 25 × 25mm^2 except for the Mylar® A where an area of 35 × 35mm^2 was needed because of the excessive droplet spreading. A visible spot on the backside indicates poor barrier properties against the solvent and the functional ink. To be able to study in detail the effective barrier life time, novel barrier measurement methods were developed.

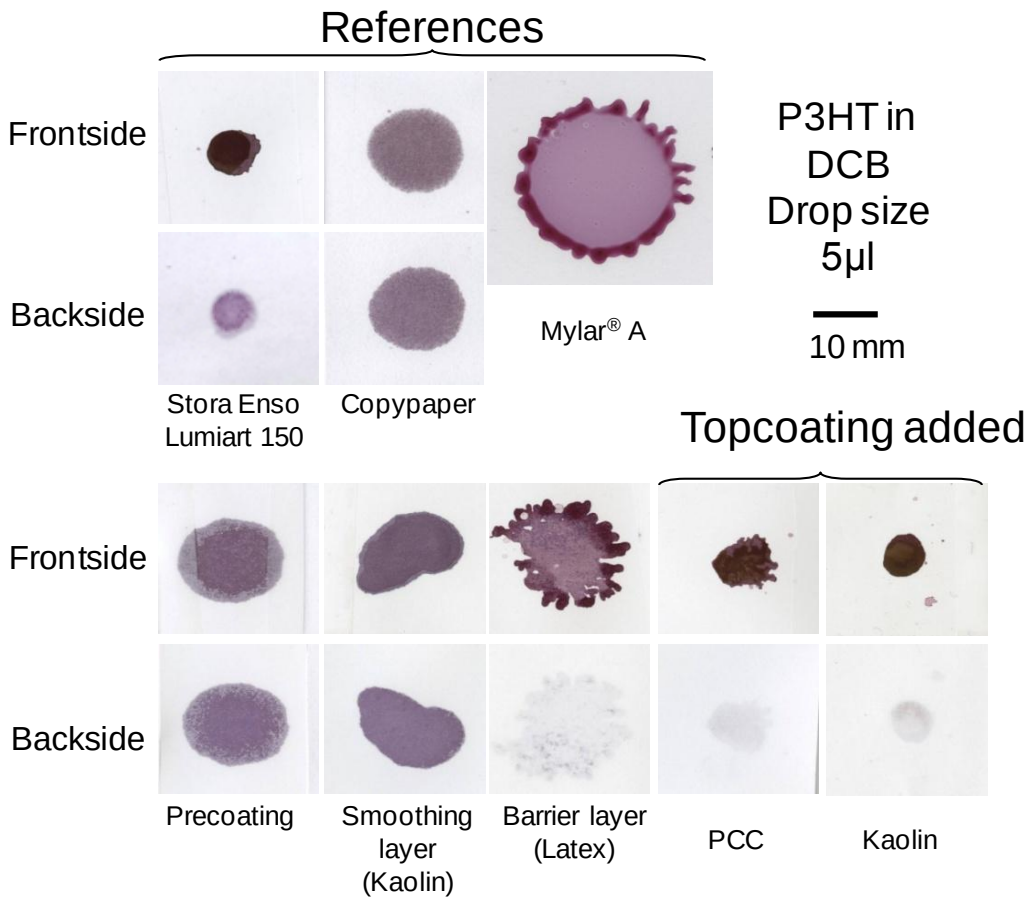

Figure 9. A simple barrier test, application of semiconductor ink dissolved in DCB onto different substrates and scanning of the spots from the front and backside of the substrate. A visible spot on the backside indicates solvent and functional ink penetration.

5.2.1. Barrier measurement methods

There are two common methods for measuring barrier properties of paper, one being the Cobb test "Standard Test Method for Water Absorptiveness of Nonbibulous Paper and Paperboard" (ASTM standard D3285-93(2005), which has been withdrawn in 2010, but exists as Tappi Test Method T 441 om-09 (*129*). The other method is the "Water Vapor Transmission Rate method" (WVTR) (ASTM standard (E 96/E96M-10) (*122*). The WVTR method monitors the water penetration by measuring gas phase penetration as a function of time at chosen temperature and humidity. Therefore, it is not suitable for measuring barrier properties against liquids applied directly onto a substrate. The packaging industry uses widely the standardized method (ASTM F119 - 82(2008)),

"Standard Test Method for Rate of Grease Penetration of Flexible Barrier Materials (Rapid Method)", for measuring barrier properties against grease (*130*). The principle of the method is to apply a certain type of grease on a substrate, apply a weight on the grease spot and a thin layer chromatography (TLC) plate below the substrate. In case of penetration, the TLC plate picks up a spot of grease. In the present work, three methods for measuring barrier properties against solvents, acids and bases were developed. The experimental setup for the methods is based on the method for measuring of grease barrier (*130*), meaning the solvent is directly applied onto the substrate. The first method utilizes a trace color dissolved in a solvent combined with optical analysis of the backside of the substrate. The second one monitors conductivity through the barrier layer as function of time when the liquid applied on top of the substrate penetrates it. The third one quantifies the penetration through the substrate as changes in effective refractive index on a prism placed on the backside of the substrate.

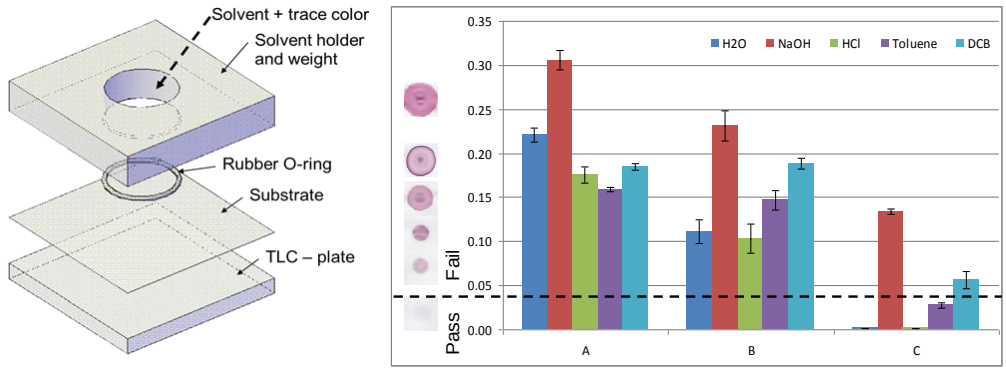

Figure 10. The schematic setup of the trace color based measurement system and example results for three substrates (A, B and C) tested with different solvents.

Trace color method

In the trace color method, a trace color (Amaranth red or Sudan red) is dissolved in the solvent to be studied and the solution is placed on the front side of the substrate as shown in Figure 10. Once the solvent has dried, both through evaporation and absorption into the substrate, the possible trace color spot on the backside and on the TLC plate placed below the substrate are studied. A visible colored spot on the backside of the substrate indicates a penetration whereas no visible spot usually indicates high barrier properties. In order to obtain more information of the penetration a possible spot on the TLC plate can be further analyzed. This gives a qualitative result of the barrier properties in form of passed / failed. A quantification of the amount of trace color that has penetrated through the substrate can be carried out by image analysis. A simple way to convert the penetration and spreading into a numerical value is to calculate the sum of the spot area in pixels × intensity of each pixel (grayscale 0-255, rescaled to 0-1), which

gives a dimensionless number related to the volume of penetrated liquid (Figure 10). The volume is thereby calculated as the average color density × number of pixels in the spot. With this method it is not possible to measure short time behavior, i.e. effective barrier lifetime, since the spots are studied after the solvent has dried and variations in applied solvent amount as well as evaporation time influence the result. In addition, the observed spot on the backside is influenced by the relative affinity of the trace color to the paper components and the carrier solvent, which makes the method inapplicable to some solvents.

Conductivity method

An alternative method for measuring the barrier properties to solvents is measuring conductivity through the substrate as a function of time. By replacing the TLC plate with a conductive aluminum plate connected to an electrode that is inserted in the liquid on the top side of the substrate, the conductivity through the substrate can be measured as a function of time. Dry substrate acts as an insulator, but since most solvents are at least slightly conductive, penetration of solvent through the substrate increases its conductivity. The testing procedure (Figure 11) is the same as for the method based on trace color, except for that now no trace color is needed but the solvent has to be conductive.

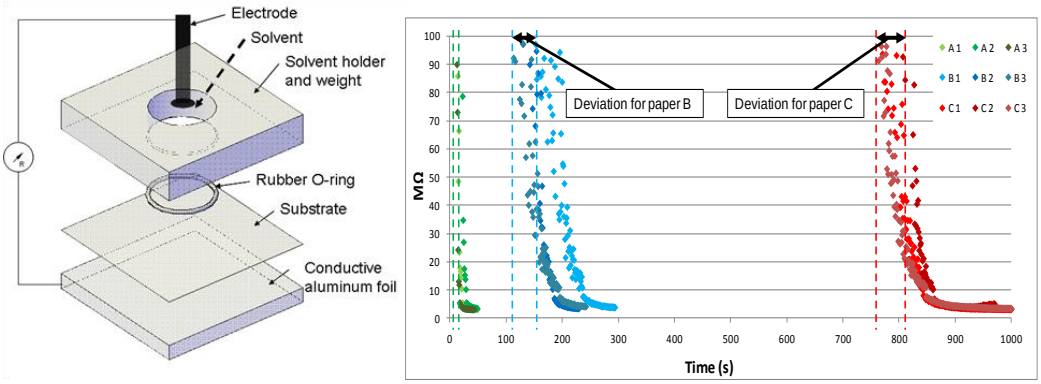

Figure 11. Schematic setup of the conductivity based measurement system and example results for three substrates (A,B and C) tested with NaOH as conductive solution/solvent.

Refractive index method

Light reflection provides a sensitive probe to monitor minute changes in the complex refractive index of the investigated sample *(131-135)*. In the prism method a glass prism is utilized to monitor reflection from the paper surface, with a green light emitting diode (LED) as the light source. Figure 12 shows the schematic diagram of the set-up and

measured image of the camera detector. Initially, the detector signal is a plain white spot as no liquid is in contact with the prism. The investigated liquid is applied as a pillar through the pinhole (diameter of 8mm) of the cylinder that is used as an external weight to improve the contact between the prism and paper. The liquid penetration through the barrier layer is immediately observed as a darker spot in the image due to the effective refractive index increase toward that of the value of the investigated liquid. This is also shown by the inserted images in Figure 12. In order to quantify the degree of penetration, image analysis can be used. The relative spot area is measured through pixel count and plotted against time.

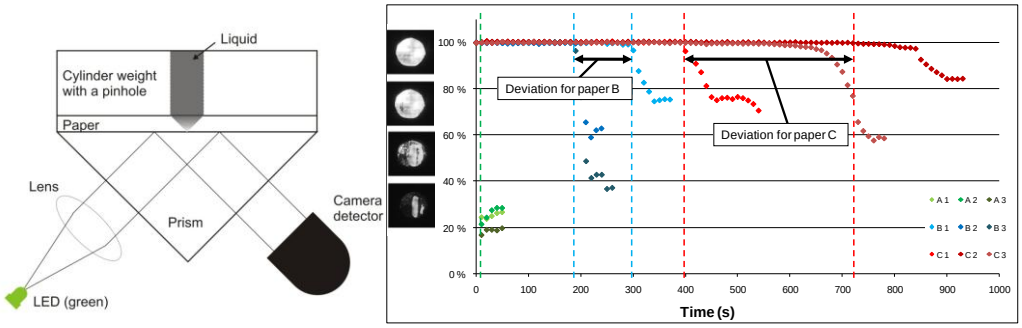

Figure 12. Schematic setup of the measurement system based on reflectometry. The paper surface is white until the solvent penetrates through the barrier layer. In the dark regions solvent has penetrated through the sample and is in contact with the prism. Pixel count was carried out for the images and the relative spot area is plotted against time, indicating the time when penetration occurs.

As a general conclusion, all three methods provide information about barrier properties. The trace color method is a qualitative method, giving a pass / fail indication. Since it is often sufficient to have short term barrier properties, due to rapid evaporation of solvents, a failed result in the trace color method may still be acceptable in regards to printability of a functional ink. A serious drawback of the trace color method is the affinity of the trace color to mineral pigments, which in certain cases could be observed as a penetration of solvent without penetration of trace color. With careful investigation the penetration could be detected as a barely visible solvent spot on the TLC plate, but it should be noted that a severe risk for not detecting it remains. The second method tests barrier lifetime, by measuring conductivity through the substrate as a function of time, but it can only be used for conductive solvents. The third method monitors changes in the effective refractive index at the prism-paper interface as a function of time. It proved to be the most applicable method, capable of analyzing any solvent. The prism method was utilized for determination of barrier properties against solvents and acids as a function of barrier layer formulation, described in section 5.2.2.

5.2.2. Barrier properties of dispersion coating

Dispersion coating has received attention as a production method for barrier coatings, since it has been considered to be more environmentally friendly regarding composting and recyclability in comparison to extrusion coating and lamination *(136-139)*. Traditional paper- and board-based products, such as those used in packaging, require high barrier properties against gases and liquids. If paper is to be used as a substrate in functional applications, the required barrier properties against solvents and acids need to be understood and developed, since the functional inks are commonly dissolved in organic solvents and acidic analyte carriers might be required in the end-use devices [section 5.5]. As part of the objective to create a paper-based substrate that can be used in printed electronics applications, an understanding regarding how a dispersion coated barrier layer optimally should be built up was needed. Improving the barrier properties of dispersion coated paper with mineral platelets, is based on the tortuous structure, introduced by the lengthened pathway (for the penetrant liquid) which arises from the high aspect ratio compared to particles of other shapes such as spheres or needles. It is generally agreed that the barrier properties depend on factors, besides the barrier polymer chemistry and the coated layer thickness, such as the pigment particle volume fraction, particle shape, particle aspect ratio and the orientation of the particles in the built up structure *(140-143)*.

Different size, shape and shape factor pigments were blended with different amounts of styrene-acrylate (SA), styrene-butadiene (SB) and ethylene-acrylate (EA) latex as well as starch. For barrier dispersions, a specific ratio between the pigment and the binder exists, acting as a threshold level, at which barrier properties change significantly. For barrier coating, it is of utmost importance to have knowledge of this critical pigment volume concentration (CPVC). The CPVC was determined by measuring light scattering as a function of drying time *(144-146)*. Latex and pigment particles have a higher refractive index compared to water and air. In the wet coating color the latex and pigment particles are surrounded by a water layer, resulting in interfaces causing high light scattering. When the coating color is dried, the water content and the coating layer thickness decrease, and interparticle void spaces become smaller, thereby reducing the light scattering. In case air voids (porosity) arises along with the disappearance of water, the light scattering starts to increase again as function of the increased number of air / pigment interfaces. A plateau value in light scattering indicates that all voids are filled with latex and the critical pigment volume concentration is yet not reached (Figure 13).

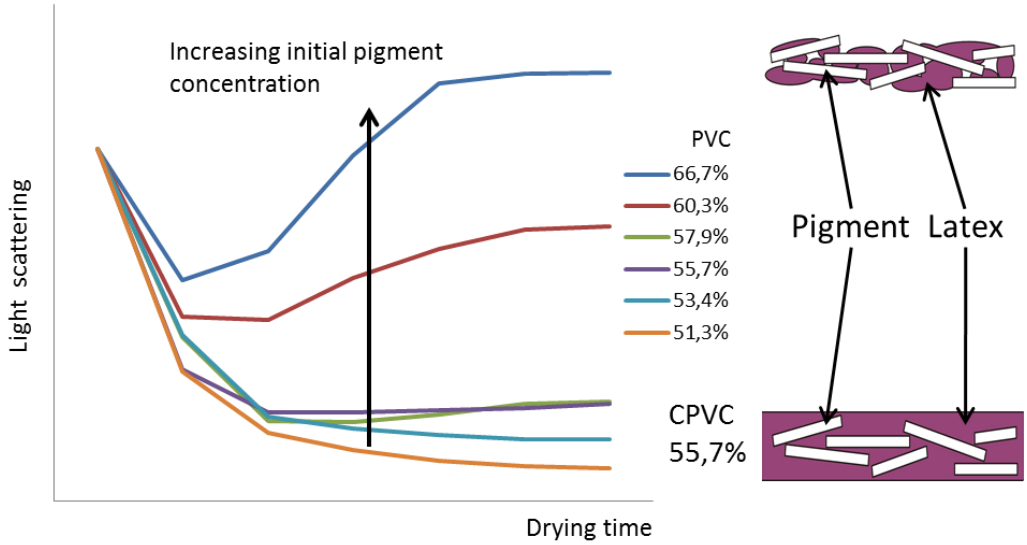

Figure 13. Principle for determining pigment volume concentration by measuring light scattering as a function of drying time. The schematic image shows the air voids (pores) at pigment volume concentrations above the critical pigment volume concentration.

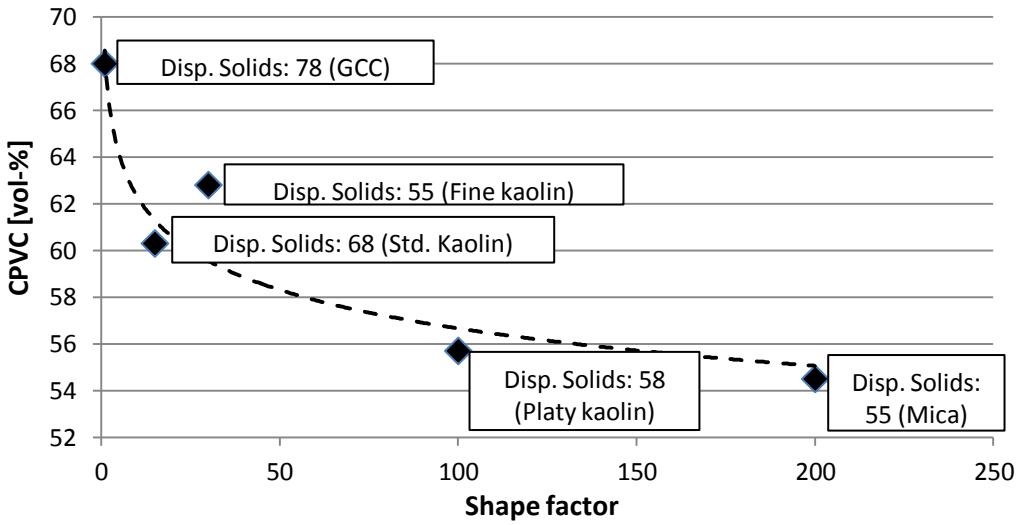

Figure 14. Critical pigment volume concentration as function of shape factor. The shape factor of Mica is in practice higher than 200. Low shape factor pigments, which have high CPVC, allow the use of high dispersing solids content.

Pigments with small particle size (in comparison to latex particle size, which was the same in all the studied blends) and low shape factor result in a high packing density and

a high CPVC, and therefore allow the use of a high dispersing solids content (Figure 14). Pigment particle size distribution also impacts the CPVC, since a broad distribution leads to a high pigment packing density. Figure 14 plots the measured CPVC values against shape factor. The shape factor of the mica is in practice higher than 200, but due to limitations of the measurement method (*118*), shape factors higher than 200 could not be reliably measured.

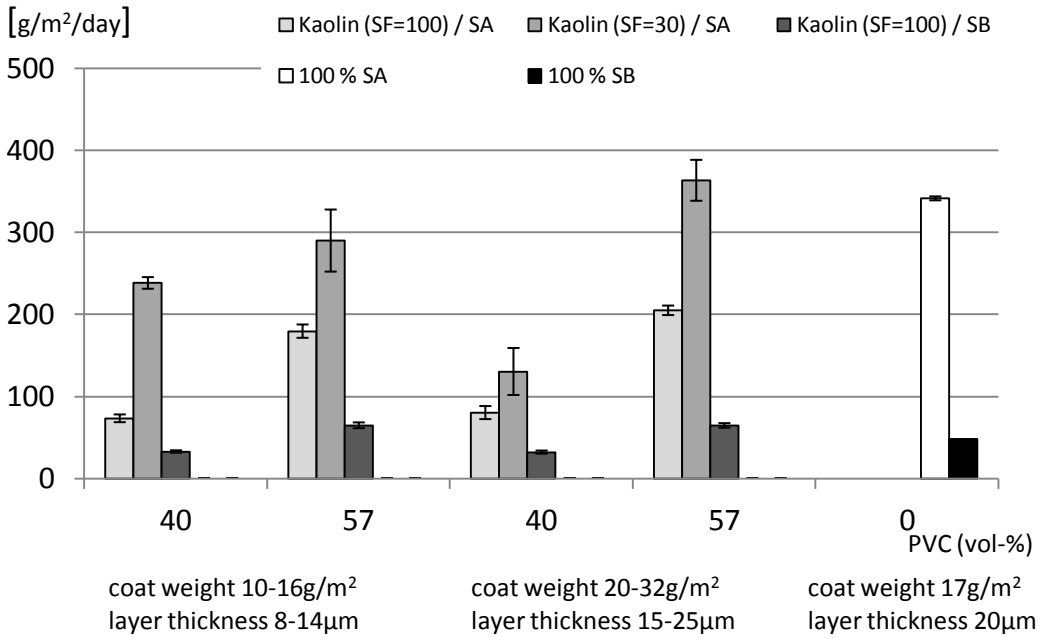

Figure 15. Normalized (15µm thickness) water vapor transmission (WVTR) at 23°C and 85% RH for kaolin with a shape factor SF=30 and SF=100 combined with different amounts of SA and SB latex.

Figure 15 shows the influence of high (SF=100) and low (SF=30) shape factor kaolin additions on barrier properties (WVTR, normalized to 15µm). In the case of low shape factor kaolin, the improvement in barrier properties is only minimal compared to pure SA latex. However, the addition of pigments reduces the blocking problem (undesired adhesion of the coating layer to the back of the adjacent paper in a roll), which occurred for the sticky surface of the pure SA latex and caused defects in rewinding, thereby deteriorating the barrier properties. Addition of high shape factor (SF=100) kaolin significantly reduces the penetration at both PVC levels when combined with SA latex. The standard deviation of the barrier properties measured from the coatings containing low shape factor kaolin were significantly larger compared to the practically negligible standard deviation of the barrier results obtained from the coatings filled with high shape factor kaolin. This may be a result of nonhomogenous or poor alignment of the low shape factor particles, as shown in figure 16B.

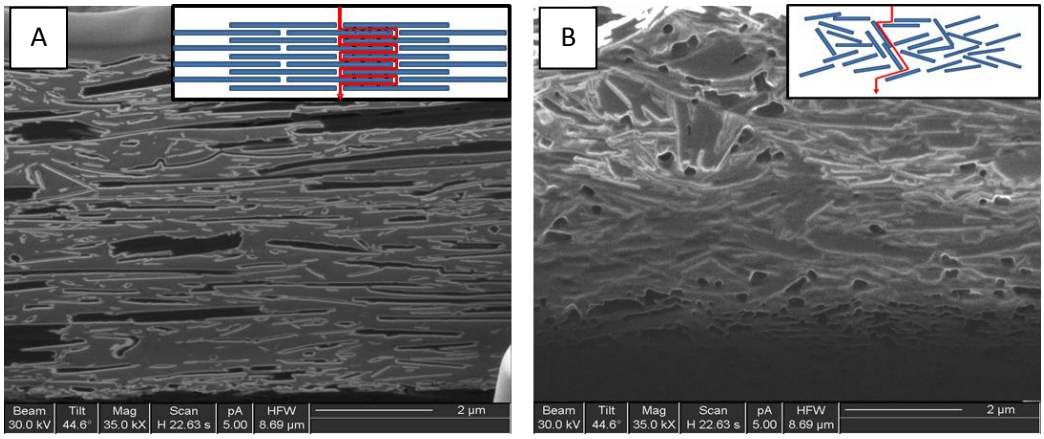

Figure 16. Focused ion beam images showing the alignment of the kaolin particle filled latex barrier layer. A: Highly aligned high shape factor (SF=100) kaolin. B: Less aligned low shape factor (SF=30) kaolin. The tortuosity of the structures is shown schematically in the inserted images.

Figure 17 shows the WVTR for three latexes with different chemistry, filled with the high shape factor (SF=100) kaolin. As a reference material to the latexes, starch was also tested as barrier polymer. However, the water soluble anionic starch dissolves resulting in very poor barrier properties against water vapor (note the discontinuous y-axis in Figure 17). Despite the dissolution of the starch, the thicker layer (25µm) clearly improves the barrier properties compared to the thinner one (10µm), which is explained by the longer migration pathway through the tortuous kaolin structure. Regarding the latexes, the most obvious difference can be seen for the styrene acrylate latex where the addition of kaolin clearly improves the barrier properties at the same layer thickness, whereas for the styrene butadiene latex the difference is smaller. While the highest barrier properties could be obtained by using pure ethylene acrylic latex, an addition of 44 vol-% kaolin did not significantly weaken the barrier properties against water vapor, which is an economic advantage in commercial applications. The WVTR barrier for the basepaper, including the porous precoating and smoothing layers, was 795g/m²/day.

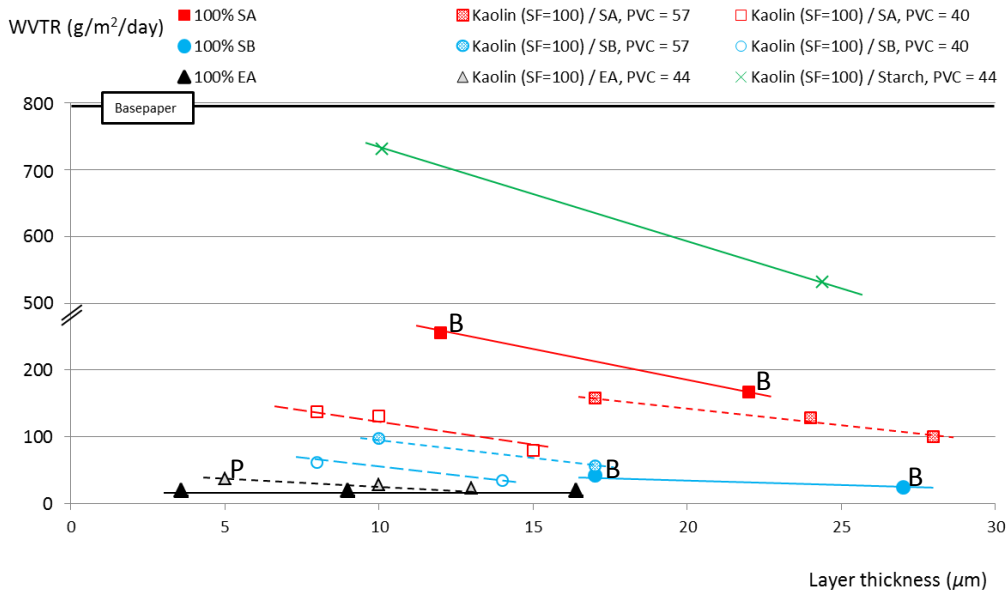

Figure 17. Barrier properties against water vapor (WVTR) at 23°C and 85% RH as function of barrier layer thickness. The values are average values of three parallel measurements, with a negligible standard deviation. (B = Tendency for blocking, P= Tendency for pinholes). Note the discontinuous y-axis.

In addition to barrier properties against water vapor, barrier properties against liquids directly applied onto surfaces of the substrates were measured. These measurements were made in order to mimic a coating or a printing operation, or an analysis procedure in a printed functional application. Organic solvents are common as ink vehicles [Section 5.5.1] and acids are used as analyte carriers in sensor applications [Section 5.5.5], both requiring barrier properties for varying times. Figure 18 plots the time it takes for ortho-dichlorobenzene (DCB) to penetrate the substrates. As can be seen for all the latexes, the addition of high shape factor kaolin clearly improves the barrier properties. This can be related to the increased tortuosity through the particle filled structure (Figure 16A). The organic solvent dissolves partially the latex but the inert high shape factor mineral particles create a long pathway for the solvent to migrate through. DCB, on the contrary to the water vapor, does not dissolve the starch, which as a polar molecule performs well as a barrier against the nonpolar DCB. Figure 18 only plots the short term barrier properties, but for the starch coatings the barrier measurements were extended to three days by addition of DCB to counteract the evaporation. No DCB penetrated the starch based barrier coatings during the three days, indicating the starch is completely insoluble in DCB. Differences in dissolving or degrading of the latexes can also be seen, the styrene-butadiene and styrene-acrylic latexes dissolving most rapidly while the ethylene-acrylic can withstand the organic solvent for longer.

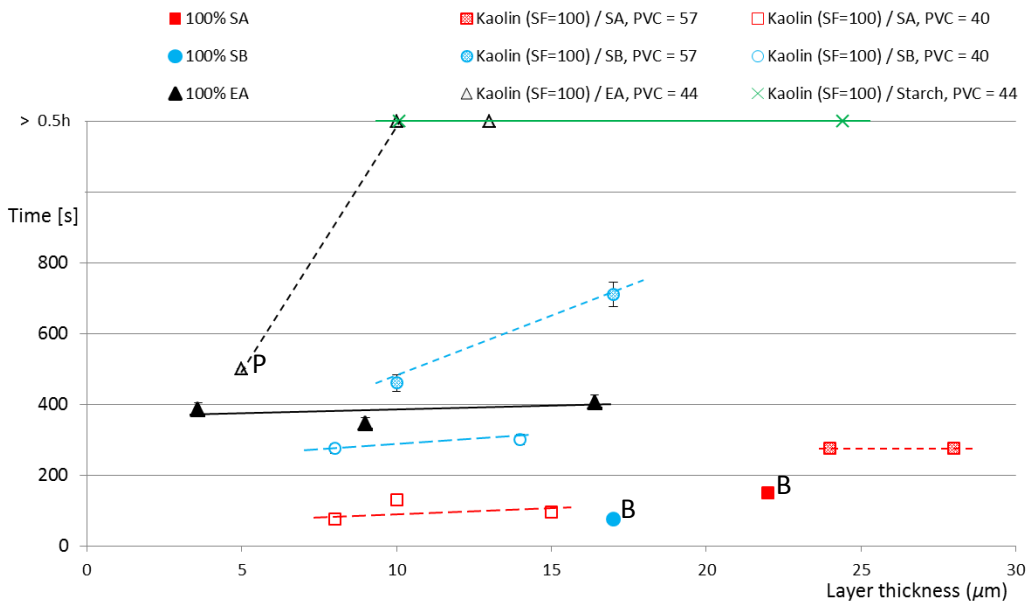

Figure 18. Barrier properties against ortho-dichlorobenzene. The figure shows the time in seconds for the liquid to penetrate the substrate. (B = Tendency for blocking, P = Tendency for pinholes).

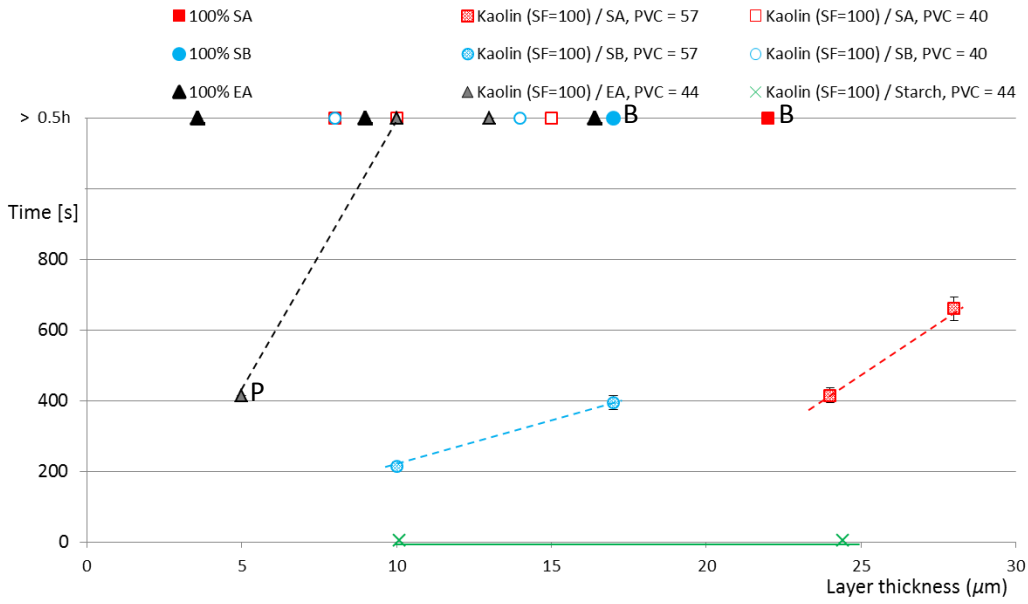

Figure 19. Barrier properties against 1 M hydrochloric acid. The figure shows the time in seconds for the liquid to penetrate the substrate. (B = Tendency for blocking, P = Tendency for pinholes).

In contrast to the barrier properties against DCB, the pure latexes, and the layers with low pigment volume concentration show the best barrier properties against 1M hydrochloric acid (Figure 19). This can be related to voids existing in the layers filled to 57% by volume of pigments, since the critical pigment volume concentration for the platy kaolin was found to be 55.7% (Figure 13 and 14). The lower amount of organic material on the surface of these layers can result in a more hydrophilic surface and more complete wetting [Publication II, Table 2]. In the case of the thin 5µm kaolin/ethylene acrylic latex layer, the penetration was caused by pinholes. The latexes are all inert against the hydrochloric acid showing no degradation or dissolving tendency contrary to the case for the organic solvent. The water soluble starch was dissolved immediately by the hydrochloric acid. Both the DCB and the hydrochloric acid penetrate the basepaper, including precoating and smoothing layer, in less than 5 seconds.

The binder, whether it is latex or starch can be considered the most important material for creating a sealed layer, but an addition of mineral pigments can both improve the barrier properties as well as ensure problem free runnability. Latexes, especially with low Tg, tend to cause blocking problems, which can be significantly reduced by use of mineral pigments in the barrier layer. The addition of high shape factor kaolin improved barrier properties by increasing tortuosity, i.e., the migration pathway of a liquid through the structure. The tortuosity created by the inert mineral pigments was shown to be extremely important against DCB, which can dissolve or degrade the latexes, as well as against water vapor which dissolved the starch. The addition level of mineral pigments should not exceed the critical pigment volume concentration, since any porosity will deteriorate the barrier properties.

5.3. Functional printability

The ability to print narrow and well defined lines or structures is important, especially when high resolution devices are produced. In addition to the high requirements regarding line definition, functional printing also sets further demands regarding the actual functionality of the printed material, which often is measured as electrical conductivity. Resistance is normally measured, which can be converted to conductivity. Since exact thicknesses and thereby volume resistivities are practically impossible to measure accurately on absorbing surfaces, surface resistivity (Ω/sq) was chosen as the main parameter for evaluating conductivity. In the multilayer coating structure it is the top-coating that determines the printability of the functional inks. Coating layer properties that can influence printability of functional inks are thickness, porosity, pore volume, surface energy and roughness. These can be adjusted by the choice of pigment, its shape, size and their distributions as well as by calendering [Publication V and VI].

5.3.1. Impact of porosity and pore size

Impact of the top layer porosity and pore size was investigated by printing conductive silver of micro- and nanoparticle size with flexography and inkjet. The ink designed for flexography consisted of micrometer-sized particles with a propylene glycol monomethyl ether acetate (PM acetate) as solvent, and the one designed for inkjet of nano-sized particles with ethylene glycol as solvent. As can be seen in the SEM image (Figure 20A), the nanoparticles of the silver ink penetrate into the pores of the silica coating rendering it nonconductive, but stay on the surface of both the kaolin and the kaolin/PCC blend top-coatings. The pore volume of the top-coating was measured by mercury porosimetry *(147-150)*. Since it is not possible to measure reliably the porosity of only the top-coating of a multilayer coated structure, pressure-filtrated tablets of the top-coating formulations were measured instead. With the knowledge of the porosity and the coat weight of the top-coating, the pore volume in the top-coating could then be estimated. The penetration of ink particles correlates with the top-coating dominant pore size, which for the kaolin and kaolin/PCC coatings was in the range of 13 to 80nm and ca 380nm for the silica coatings [Publication V, Table 2]. The large pore size of the silica pigment is a consequence of the relatively large particle size of the pigment used here. It should also be noted that the silica pigment itself is nano-porous resulting in a bimodal coating layer porosity. However, the modal value for the nano-scale porosity was ca. 10nm, which in comparison to the dominant coating layer pore size of ca. 380nm is almost negligible. The flexographic silver ink with micrometer-sized flaky particles remained on the surface on all the top-coatings, and is thereby less sensitive to pore size (Figure 20B). High porosity and total available pore volume in the top-coating allowed for fast ink vehicle uptake, which reduced the squeeze (ink spreading under printing nip pressure), thereby improving the flexographic printability of the micrometer-sized particle ink [Publication V, Table 3].

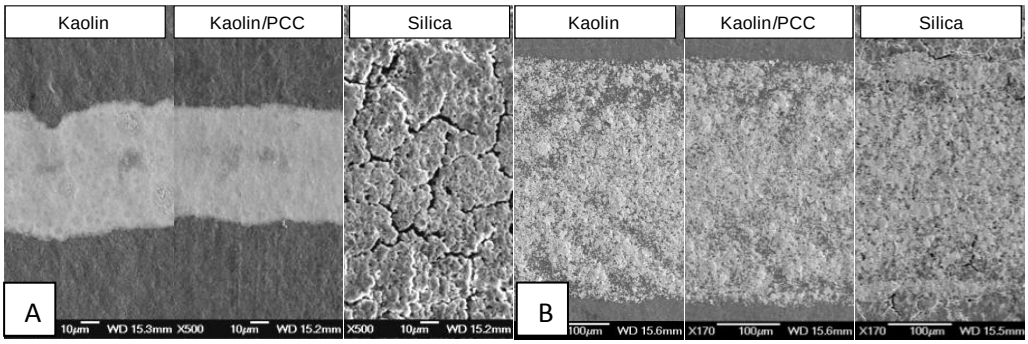

Figure 20. SEM images of silver particle inks printed with inkjet (A) and flexography (B) (3g/m^2 top-coating).

The difference in silver particle size and their relationship to the pore size of the top-coating is further visualized in the focused ion beam image (Figure 21). The conductive layer formation by the several micrometers in diameter flaky silver particles is insensitive to the pore size as well as any possible roughness variations, whereas the thin silver layer formed by the nanoparticles is very dependent on the pore size. In the case where fine kaolin is used in the top-coating, the pore size is small enough to keep the nanoparticles on the surface, enabling printing of an evenly thick (ca. 1µm) conductive layer.

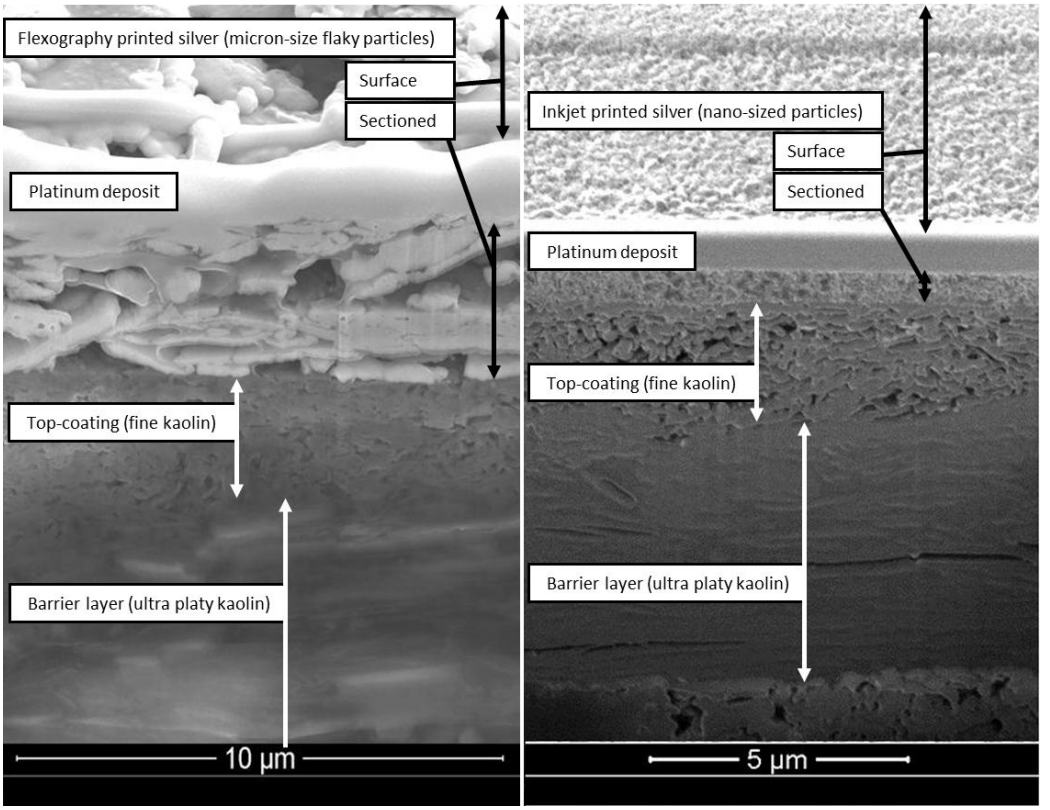

Figure 21. Focused ion beam cut and imaged cross-section of the coated paper substrate, showing flexography printed micrometer-sized silver (LEFT) and inkjet-printed nanoparticle silver (RIGHT) on the multilayer coating structure. The sectioned layers in the multilayer structure are, from the top: top-coating (5g/m^2 fine kaolin), the barrier layer (10g/m^2 platy kaolin) and the basepaper coating. The platinum deposit is required for the milling (ion beam cutting) through the coating structure.

In addition to studying the impact of top layer porosity and pore size on functionality of particle based inks, printability and functionality of fully dissolved organic

semiconductor was investigated. Semiconductor, regioregular poly(3-hexylthiophene) (P3HT) dissolved in a mixture (1:1:2) of xylene:chlorobenzene:ortho-dichlorobenzene, was printed with inkjet, both in a roll-to-roll process and as batch printing. The main difference between the roll-to-roll inkjet and the batch inkjet was the nominal drop volume, which in the roll-to-roll inkjet was 80 pl and in batch 10 pl. P3HT was printed at a solids content of 0.25 weight-%. The low solids content means a large amount of solvent is applied which has to evaporate or absorb into the coating structure. The solvent mixture vapor pressure was chosen to provide an evaporation rate, which is slow enough to eliminate clogging of the printing nozzles but fast enough to be printed in a roll-to-roll process. Too fast evaporation of the ink solvent leads to a viscosity increase and deposits in the inkjet nozzle, whereas too slow drying requires either slowing down of the roll-to-roll printing process or use of additional driers. However, excessive drying can potentially render the printed device inoperable, e.g. due to crack propagation or a too high temperature destroying the semiconductive polymer. Semiconductor ink was printed in both batch and roll-to-roll processes at three different amounts, giving equal theoretically uniform dry thicknesses of 20nm, 40nm and 80nm. This corresponds to applied P3HT-volumes of 2, 4 and 8nl/cm² and to total printed volumes of 800, 1600 and 3200nl/cm², respectively. These volumes were compared to the pore volumes in the top-coatings, which were in the range of 4 to 400nl/cm².

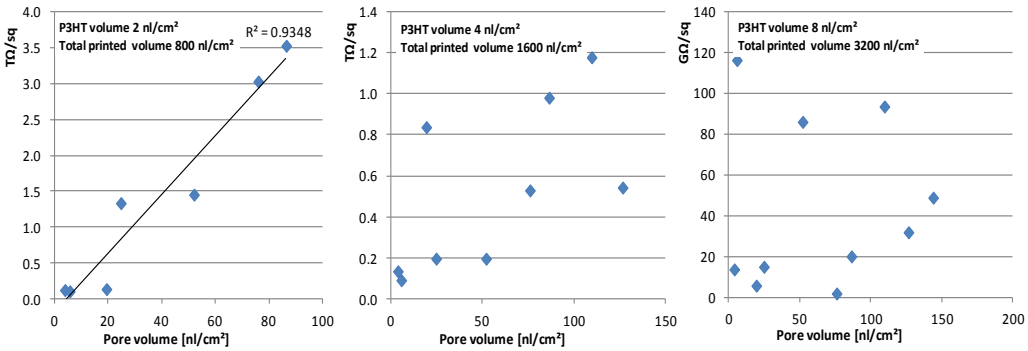

Figure 22. Surface resistivity as function of pore volume in the top-coating for 2nl/cm^2 (left), 4nl/cm^2 (middle) and 8nl/cm^2 (right) total (roll-to-roll) printed semiconductor amounts.

All printed amounts on all the surfaces gave a visibly purple color, with darker color intensity for the higher amounts. Visually evaluated the most even films were achieved for the thinnest printed amounts (2nl/cm²) whereas the larger printed amounts (4 and 8nl/cm²) resulted in slow and uneven drying. Especially the substrates with low pore volume, and thereby limited absorptivity, exhibited the coffee stain effect. Surface resistivity was measured for all the printed amounts and was correlated with the pore volume. As is shown in Figure 22, the relationship between the surface resistivity and the pore volume is almost linear for the small coating pore volumes (< 100nl/cm²) and the small amount of printed semiconductor (2nl/cm²), while the impact of pore volume

decreases as higher amounts of ink are applied. It is likely that for small printed ink volumes the semiconductor penetrates fully into the coating structure and surrounds the mineral particles, thereby creating a connected network. Once the pores are filled, with both semiconductor and evaporating solvent, the rest of the applied amount will be on the surface where the continued evaporation seemed to lead to an irregular film.

5.3.2. Impact of substrate roughness

Control of substrate surface roughness has in several studies been suggested to be one of the most important factors for successful functional printing. High surface roughness, especially on the shorter length scales, has in previous studies been found to decrease the conductivity *(49,151,152)*. The influence of roughness on functionality is however very dependent on the properties of the functional ink. As shown visually in Figure 21, the substrate role is of minor impact when printing with large micrometer-size based particle inks, but when printing thin layers with nanoparticle-sized inks the surface smoothness appears essential. In order to minimize the influence of surface chemistry, i.e. different surface energy, but highlight the impact of surface roughness, a multilayer coated substrate with a kaolin-based top-coating was, by calendering, adjusted to four different roughness levels (Figure 23). Nanoparticle silver ink was printed with inkjet (10pl drop volume with a drop spacing of 20μm) on these substrates. The lines were printed to widths based on 2, 4, 8, 16 and 32 drops, and the actual line widths measured by a high resolution scanner. The average line width (required for surface resistivity calculation, listed in Table 2, Publication VI) varies somewhat depending on ink spreading.

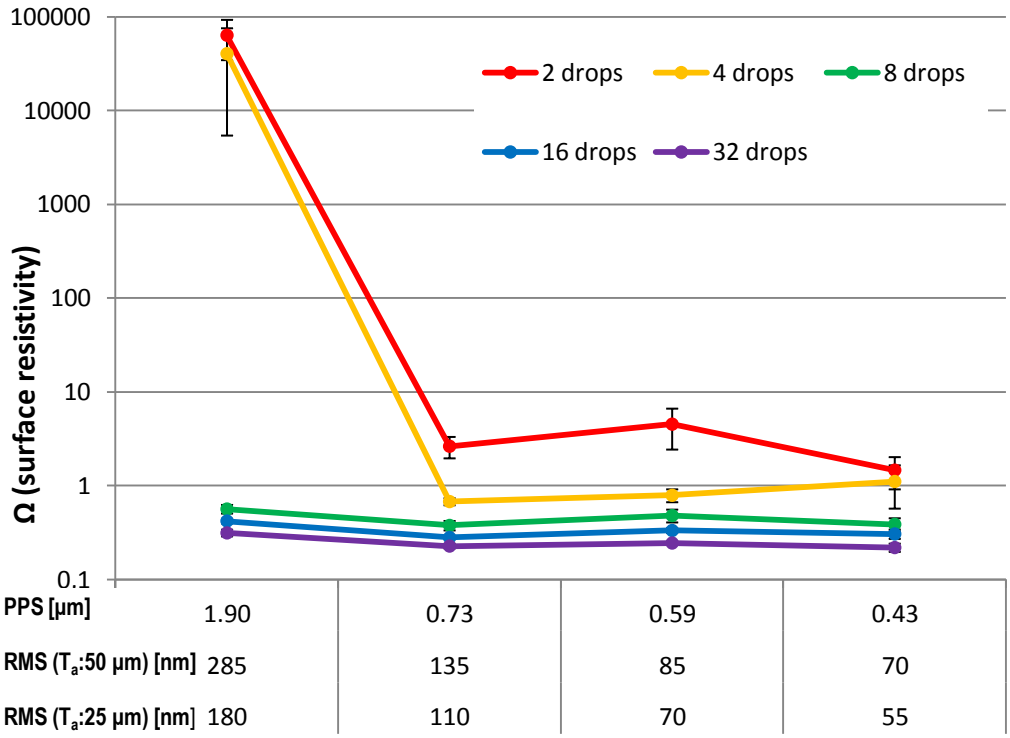

Figure 23. Surface resistivity for printed silver lines as function of surface roughness of a multilayer coated paper with a kaolin based top-coating. The different roughness levels were achieved by different calendering parameters. The line widths are expressed as inkjetted drops. The measured average line widths, used for calculation of the surface resistivity, are listed in Publication VI, Table 2 and full roughness analysis in Publication VI, Figure 2.

Printing of thin lines on a rough surface results in poor conductivity (high surface resistivity), as can be seen for the uncalendered (PPS 1.90µm) multilayer coated substrate. This can be explained by a single defect (peak or valley in the surface under the printed track) weakening the connecting pathway or potentially even causing discontinuities, while in a thick line a minor defect does not necessarily lead to a discontinuity or even significantly impact the conductivity. A rough surface also leads to a more uneven silver layer thickness. A slightly lower surface resistivity could be achieved for the wider lines, since the drop spacing was 20µm and the spreading of one droplet is ca. 40-50µm, meaning the droplets in the printed lines are partly overlapping, leading to an increased thickness. A direct relationship between the conductivity and the surface roughness cannot be seen in these results. The main impact of the low roughness is the minimized risk for defects in narrow printed lines. In devices consisting of several

functional layers high roughness or just a peak in the surface may increase the risk for short circuits.

5.4. Dimensional stability

Poor dimensional stability of a substrate may cause cracks and disconnects in printed tracks, since dimensional changes may occur with an exposure to varying environmental conditions. This is a challenging phenomenon to control for fiber-based materials, since humidity and temperature variations have a strong impact on fiber dimensions and the bonds between them *(153-155)*. Transferring materials onto the substrate, by use of coating or printing methods involves use of solvents combined with harsh drying methods, all having a strong influence on the dimensional stability of the fiber network. From the end product point of view, maintaining functionality in varying weather and temperature conditions is important.

5.4.1. Impact on surface topography

Dimensional stability was analyzed by exposing substrates to humidity cycling. As reference substrates to the multilayer curtain coated (MLCC) paper, commercially available standard copy paper, double coated fine paper and high quality photo paper were tested. Silver lines (20mm by ~100µm, non-sintered) were inkjet printed onto the substrates at 23°C and a relative humidity of 30%. The substrates with the printed lines were stored for 24 hours in 90% relative humidity at 23°C, then dried in a 100°C oven for 30 minutes where after again stored in 90% relative humidity at 23°C for 24 hours. Finally, the substrates were stored at room conditions of 30% relative humidity and 23°C for two days (Figure 24). The printed lines were scanned after each stage with a high resolution (6400dpi) scanner and the line lengths were measured using image analysis to determine the expansion/shrinkage in the x/y-plane. The measurement accuracy is ± 1 pixel equaling ± 4µm or 0.02%.

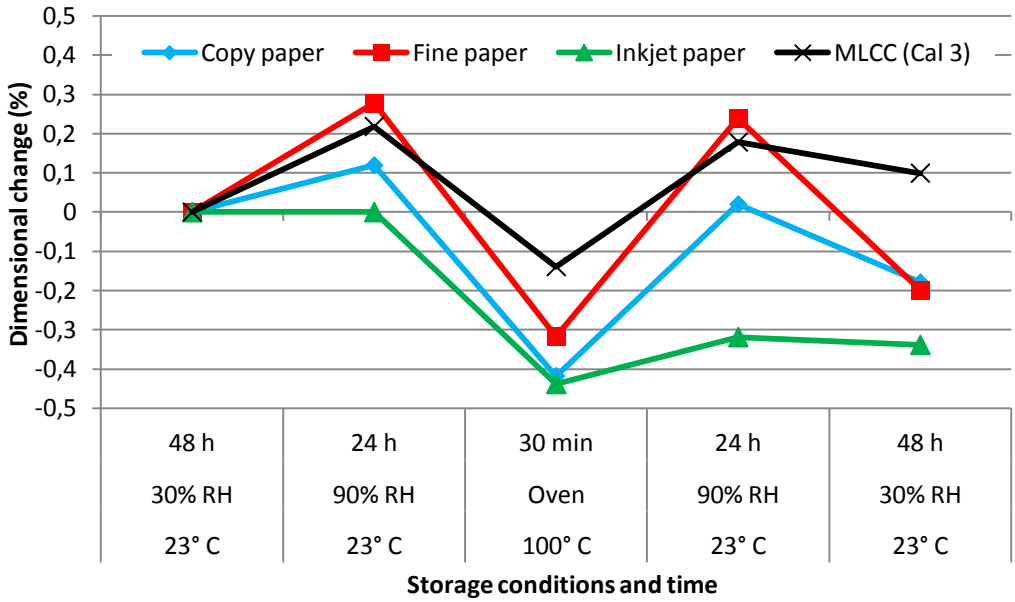

Figure 24. Dimensional stability (line length) as function of humidity and temperature cycling for the different papers. The measurements were made after indicated time periods at each condition.

Exposing the substrates to the first increased humidity level led to 0.1-0.3% expansion of all the substrates except for the inkjet paper which has a polymer film coating. Subsequent drying in oven shrank all the substrates by 0.35-0.6%, with the smallest shrinkage observed for the MLCC paper and the highest for the double coated fine paper. The polymer coated inkjet paper did not fully withstand the high temperature which resulted in permanent cracks in the polymer film. The second humidity level increase resulted in approximately the same dimensional changes as the first one, with the exception of the damaged inkjet paper. Overall, the dimensional changes were the largest for the fine paper and the copy paper. Compared to similar measurements of nanocellulose based sheets conducted by Torvinen et al. (*54*), the dimensional changes observed here were in the same range. The multilayer coated substrate with its strong barrier layer, which strengthens the structure, showed the smallest dimensional changes. Since the MLCC paper had the multilayer coating only on one side, this asymmetry led to curl of the paper. The curl can be reduced or eliminated by coating the backside of the paper, which would also reduce penetration of humidity into the base paper, and thereby improve the dimensional stability.

The changes in surface roughness of the double coated fine paper and MLCC caused by their exposure to high humidity were measured both by AFM and PPS. PPS allowed for fast measuring as a function of "drying" (90% RH → 50% RH @ 23°C) after the samples had been brought into equilibrium at high humidity. The PPS surface roughness increased slightly during the first 15 minutes (MLCC: 0.53→0.60µm and Fine paper:

0.87→1.05µm) after the samples were removed from the high humidity conditions [Publication VI, Figure 5]. This is potentially due to contraction of the fibers, which causes shrinkage of the basepaper fiber network. The initial surface roughness increase was observed for both the fine paper and the MLCC, but after the 15 minutes no change in roughness was detected for either one. Changes in surface roughness as a function of length scale were further studied by AFM (Figure 25). Since obtaining an AFM image takes approximately one hour, the samples were stored for one hour at room conditions (25% RH and 23°C) before starting the measurement, in order to avoid possible roughness change during the image acquisition.

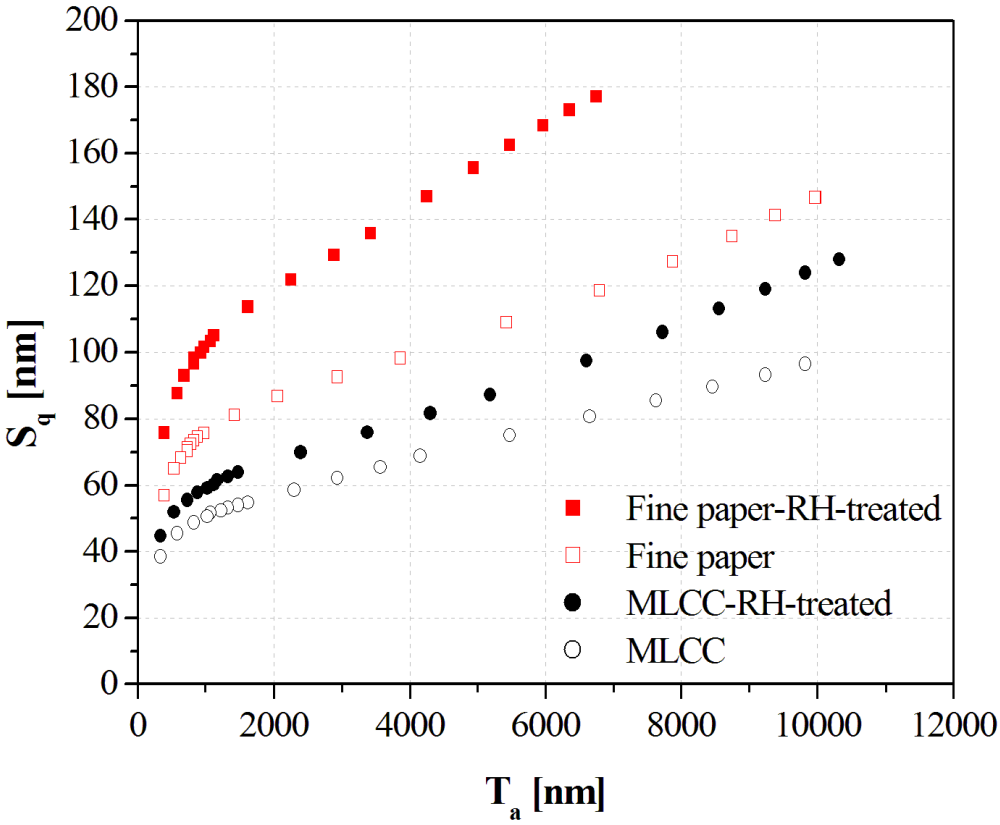

Figure 25. Root mean square roughness (S_q) as function of correlation length (T_a), for multilayer curtain coated paper (MLCC) and double coated fine paper before and after humidity treatment (24h in 23°C and 90% RH).

As can be seen in Figure 25, the increase in roughness is obvious on every length scale for the fine paper whereas it is significantly smaller for the multilayer curtain coated paper. For the fine paper the changes in surface roughness increase at longer length

scales. This suggests that the increase is a result of fiber swelling, since the roughness at longer length scales is determined by the base paper fibers *(156-158)*. Despite fiber swelling, which caused curl of the multilayer coated substrate, the mechanically strong barrier layer ensured that only minimal topographical changes on the coated side occurred.

5.4.2. Impact on electrical properties and functionality

The influence of humidity on conductivity was investigated by exposing printed silver tracks, with different line widths (2-32 inkjet printed 10pl drops, drop spacing 20µm), to humidity cycling. Surface resistivity was measured for the lines as they were printed and sintered (25% relative humidity) and again after 24 hour exposure to 90% relative humidity. As shown in figure 26, the conductivity of the narrow printed tracks on the double coated fine paper, which showed the largest dimensional and surface roughness changes when exposed to high humidity (Figure 24 and 25), decreased considerably. The surface resistivity increased by 4 orders of magnitude for line widths printed with 4 and 8 drops. The impact on conductivity of the wider lines, printed with 16 and 32 drops, was negligible. On the multilayer coated paper, only a minimal impact on conductivity of the thinner lines (2 and 4 drops) could be observed after the humidity treatment. No changes could be seen for the wider lines (8-32 drops). It is obvious that poor dimensional stability and roughening caused by humidity changes in the environment are detrimental to the functioning of narrow printed conductive tracks. In addition to the roughness increase and expansion of the substrate, oxidation of the silver particles might also play a role in slightly reducing the conductivity. Similar reduction in conductivity as function of treatment in high humidity conditions was also reported for printed tracks on different label papers by Wood et al. (*159*).

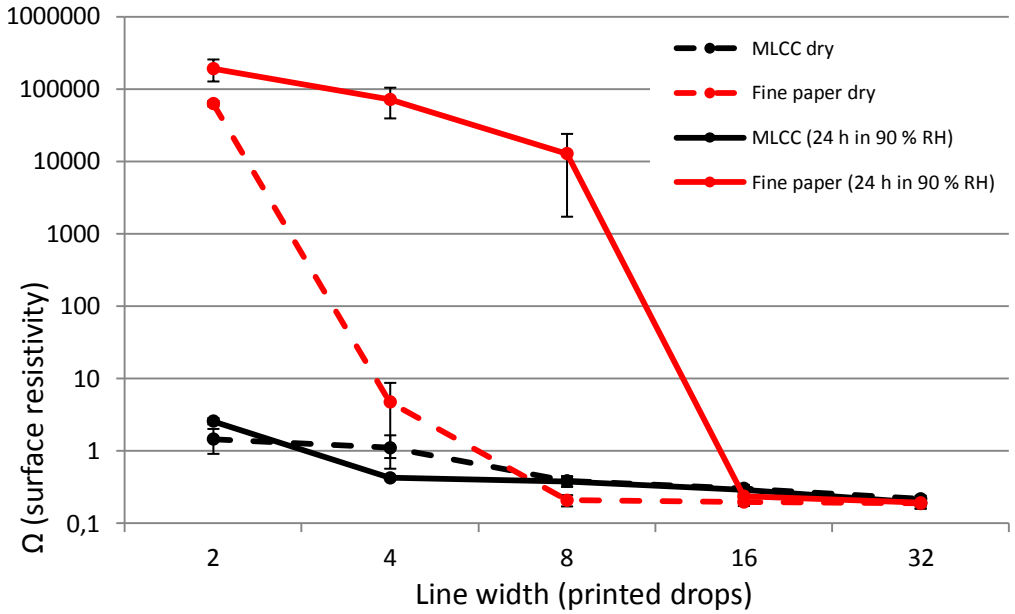

Figure 26. Surface resistivity for different width silver lines on multilayer curtain coated (MLCC) paper and fine paper before and after humidity treatment.

5.5. Proof-of-concept devices

To demonstrate the usability of the multilayer coated paper developed in the current work, different functional devices were manufactured as proofs-of-concept. A low-voltage organic transistor, which has previously been demonstrated on plastic substrate (*160*), consists of four layers printed on top of each other and can be considered a challenging device to manufacture through solution processing. It was therefore chosen as the primary target when developing the multilayer coating structure. The second demonstrator is an electrochromic pixel, which has previously been manufactured also on PE-coated paper by Acreo (*91*). The last demonstrators manufactured on paper in this work, oxygen sensor, hydrogen sulphide sensor and an ion-selective electrode, have previously been created by printing onto plastic substrates *(161-163)*. The proof-of-concept devices were designed and tested in cooperation with the Åbo Akademi Department of Physics, Laboratory of Physical Chemistry and Laboratory of Analytical Chemistry (*19*).

5.5.1. Transistors

As a proof-of-concept, transistors were printed on the paper substrate and their performance was measured. The transistor type used here is a so-called hygroscopic insulator field effect transistor (HIFET), a type of ion-modulated OFET. Figure 27 shows the top gate transistor schematic, the printed transistor, and the current-voltage characteristics for the printed transistor *(160,164)*. The formation of a diffuse electric double layer, thanks to the ion motion in the polyanionic dielectric at normal room humidity, results in high capacitance and enables the low-voltage operation. The HIFET has also been shown to be rather insensitive to the thickness of the dielectric and to the surface roughness of the substrate. Therefore, ion-modulated transistors are excellent candidates for rough substrates and large scale manufacturing for all-printed OFETs operating below 2V. Transistors were first printed in a batch process on the multilayer coated paper substrate. The transistors consisted of inkjet-printed (drop spacing 25µm) silver source and drain electrodes, P3HT as semiconductor, poly(4-vinylphenol) (PVP) as insulator and poly(3,4-ethylenedioxythiophene):poly(styrenesulfonate) (PEDOT:PSS) as gate electrode. The semiconductor and insulator layers were spin-coated and the gate was drop-cast. Figure 27 shows the output characteristics of such a batch process manufactured transistor. Compared to transistors manufactured on a plastic substrate, the transistor shows lower current throughput, which might be due to poor semiconductor coverage or impurities of the paper degrading the charge transport (*61*). An advantage is the off-state at 0V, which is useful when building logic circuits (*165,166*).

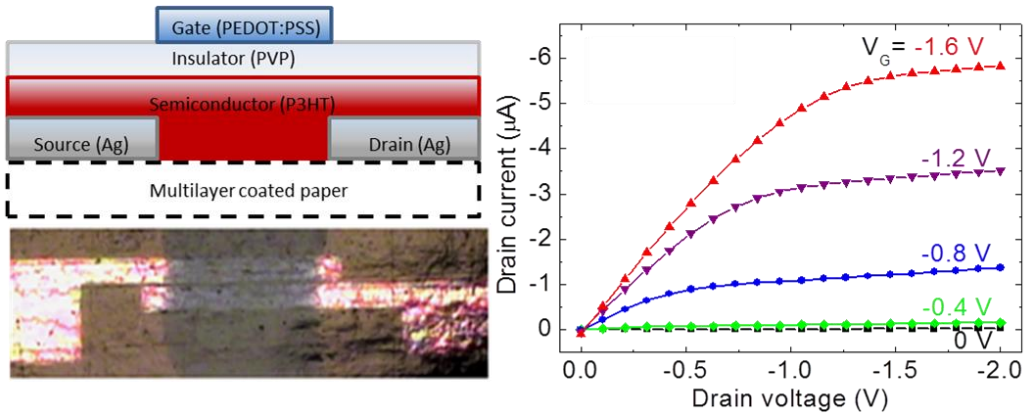

Figure 27. Output characteristics for the batch manufactured transistor. The schematic and the optical images show the structure, inkjet printed silver electrodes with spincoated P3HT (purple) and transparent insulator (PVP). The gate electrode (blue) is drop-casted PEDOT:PSS.

Transistors were also printed with the roll-to-roll hybrid printer (Figure 5) on the multilayer coated substrate. As a compromise to ensure adequate printability of both the silver electrodes and the semiconductor (Section 5.3.1.), a substrate with a 3g/m^2 kaolin top-coating was used. The source and drain silver electrodes were printed using flexography. The electrode width was ca. 350µm, channel length ca. 300µm and channel width 12mm. The semiconductor (P3HT dissolved in (1:1:2) xylene:chlorobenzene:ortho-dichlorobenzene) was inkjet-printed. The insulator (PVP) was coated using the reverse gravure technique. The gate electrode (PEDOT:PSS) was printed with inkjet. The surface tension of the water based PEDOT:PSS was lowered by addition of surfactant (Triton X-100, 0.1 volume-%) in order to ensure adequate wettability. Figure 28 shows the gate electrode in blue (c), printed on top of the transparent insulator layer. Underneath is the purple semiconductor (b) printed on top of the silver electrodes (a).

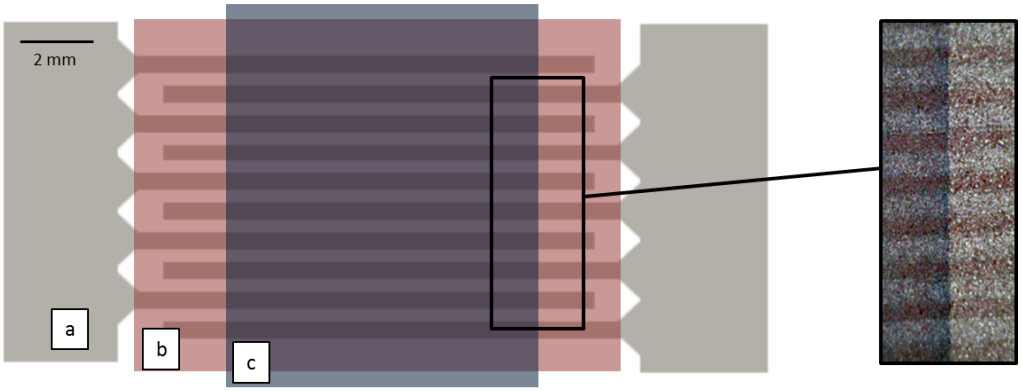

Figure 28. Schematic (left) and optical (right) images showing the structure of the roll-to-roll printed transistor. The interdigitated silver electrodes (a) (channel length ~300µm) are flexography printed. The purple semiconductor (b) (P3HT) is inkjet printed. A transparent insulator (PVP) is reverse gravure coated on top of the semiconductor. The gate electrode (c) (PEDOT:PSS) is inkjet-printed on top of the insulator.

The output characteristics are shown in Figures 29. While the roll-to-roll printed transistor functions, there is still a clear difference to those produced with the batch processing. One reason for this is the smaller design and narrower line widths enabled by the batch processing.

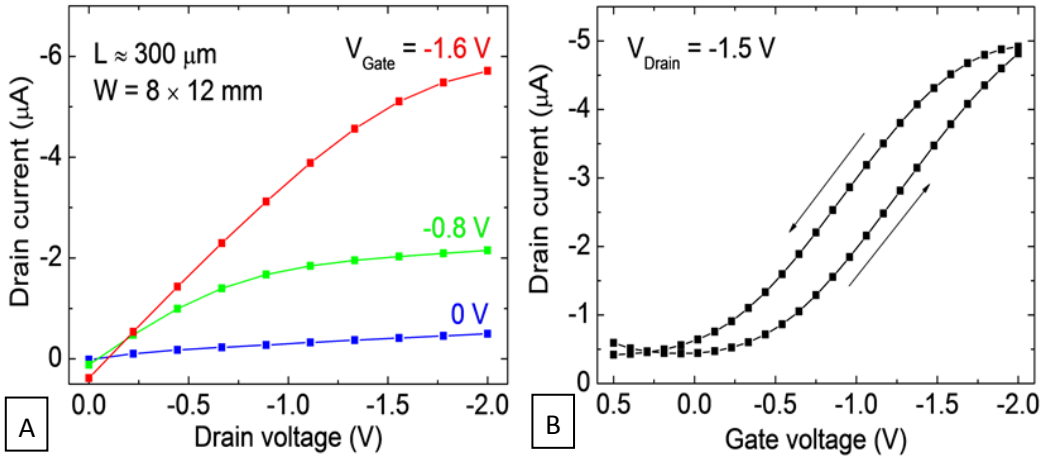

Figure 29. Output (A) and transfer (B) characteristics of the roll-to-roll printed transistor on the multilayer curtain coated paper.

5.5.2. Electrochromic pixel

To further demonstrate further the applicability of the multilayer coated paper as a printed electronics substrate, electrochromic (EC) pixels were fabricated onto it. By flexography printing PEDOT:PSS electrodes and coating the electrolyte (Glyceline, Scionix, UK), low voltage (1.5V) driven EC pixels could be demonstrated (Figure 30). While PEDOT:PSS is dark blue in its reduced state, it becomes (almost) transparent upon oxidation.

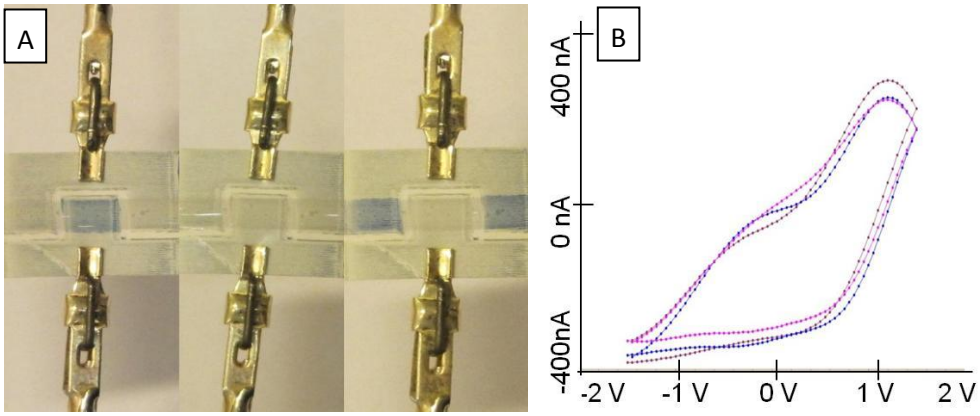

Figure 30. A: A printed EC pixel at three different biases – In the middle an un-switched pixel is shown and to the left and right the pixel at -1.5V and +1.5V, respectively is shown. B: A voltamogram when switching the pixel. The asymmetry in the electrode areas makes this curve also unsymmetrical.

Comparing EC pixels fabricated onto ordinary coated fine paper to ones fabricated on the multilayer coated paper, less spreading and penetration of the electrolyte occurred on the multilayer coated, leading to more stable operation on the latter. Also the flexography printed PEDOT:PSS wets more uniformly and is more conducting on the multilayer coated paper than on ordinary coated fine paper or board (*167*). This type of a pixel can be used as a "display" for simple applications, e.g. for printed indicators. In a more elaborate approach, the EC pixels can be combined with transistors to make matrix addressed, pixelated displays (*91,168*).

5.5.3. Oxygen sensor

Oxygen is a key feature of respiration in most organisms, and the main reason for food spoilage, since oxygen allows for the growth of aerobic micro-organisms. An oxygen sensor can be made of methylene blue combined with photocatalytic titanium dioxide. The methylene blue works as a redox dye, being either blue or white in color. Irreversibility of this indicator can be achieved by using UVA-light activated nanoparticle titanium dioxide *(161,169)*. The irreversible nature is important, if the sensor is to be used for example in modified atmosphere food packages. A minor leakage might let oxygen inside the package, but the microbe metabolism inside the package will consume the oxygen and fill it with carbon dioxide. Here, ethanol was used as the ink solvent, and the viscosity was adjusted to ca. 300mPas, which was optimal for flexographic printing. Printing was carried out on various substrates, Mylar plastic film, latex coated paper and multilayer coated substrates with different porous top-coatings. As shown in the inserted images in Figure 31, the print quality was strongly dependent on the substrate. While a high porosity clearly improved the print quality it also impaired the density decrease by the UVA-activation, since the methylene blue penetrated into the pores where the UVA-light could not reach it. As a good compromise turned out to be the multilayer coated paper with a low top-coating porosity. The ink adhesion to the Mylar and the latex coated paper was poor.

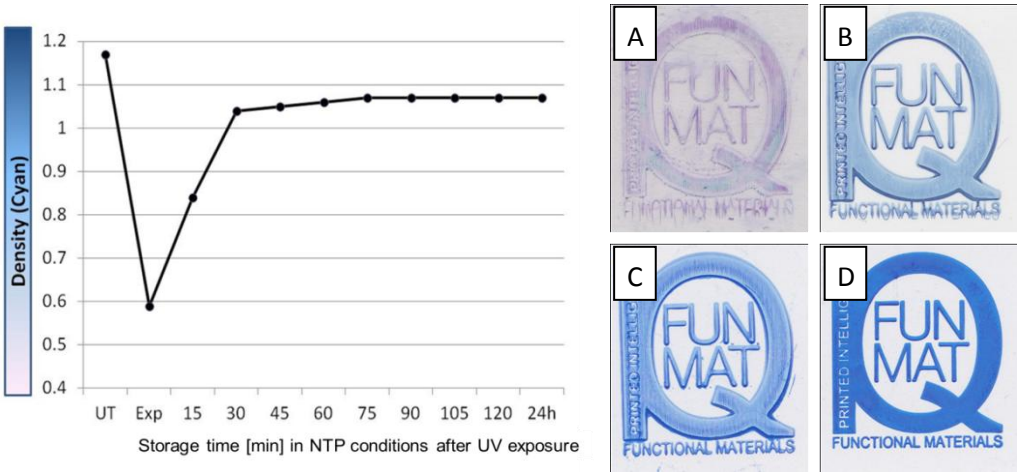

Figure 31. Drop in optical density (cyan) as a function of UV exposure (activation) followed by density recovery as a function of storage time in oxygen containing atmosphere (normal temperature and pressure, NTP). The flexographic print quality was strongly dependent on the substrate properties, especially porosity. A: Mylar, B: Latex coating, C: Low porosity multilayer coating, D: High porosity multilayer coating.

5.5.4. Hydrogen sulfide sensor

Manufacturing of sensors for hydrogen sulfide detection was demonstrated in a roll-to-roll process. As counterpart to the oxygen detection in the previous section, anaerobic organisms generate hydrogen sulfide as a waste product of their metabolism. The sensor consists of two silver electrodes printed with flexography. The same interdigitated finger structure as for the transistor (with a finger width of 350µm and gap of 300µm) (Figure 28, electrodes (a)) was used. Copper chloride and polyaniline ($CuCl_2$/PANI) was applied by spray coating on top of the silver electrodes. In the presence of trace amounts (5-10ppm) of hydrogen sulfide, the increase in the conductivity and color change of the sensing film (polyaniline/copper chloride) can be explained by the formation of copper sulfide with the subsequent protonation of polyaniline (*15*,*163*). Figure 32 shows the change in resistance measured as a function of the exposure to hydrogen sulfide.

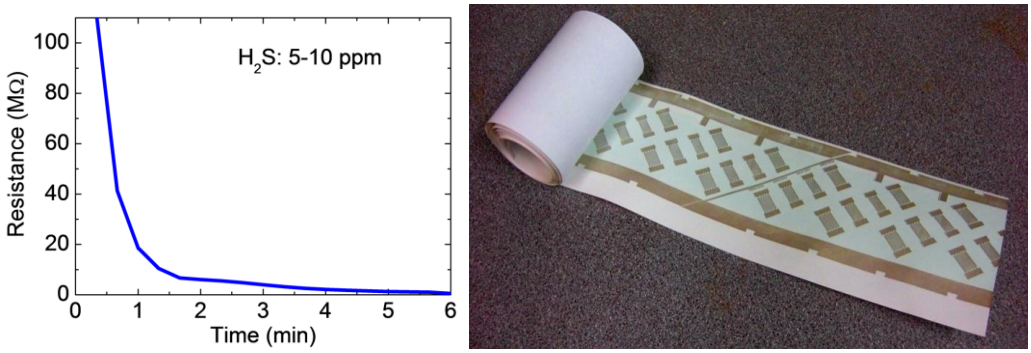

Figure 32. The resistance of the sensor as a function of the exposure time to hydrogen sulfide is shown to the left. To the right, the roll-to-roll printed sensors, flexography printed silver electrodes with spray coated $CuCl_2$/PANI on top (light blue).

5.5.5. Ion-selective electrodes

The last sensor application demonstrated on the multilayer coated paper was an ion-selective electrode (*170*). In earlier work ion-selective electrodes and reference electrodes have been produced by screen printing on a plastic substrate *(127,162)*. The electrodes consist of flexography printed carbon as electronic conductor and flexography printed UV-curable lacquer as an insulating layer (Figure 33). The ion-selective membranes dissolved in tetrahydrofuran were added by drop casting. The slowly evaporating tetrahydrofuran sets high demands on the barrier properties of the substrate. Since ion-selective electrodes are used to determine ion activities in aqueous solutions at wide range of pH, barrier properties against water at different pH were evaluated and found to last for at least one hour against a 1M KCl solution. The requirement of the barrier properties of the substrate were therefore higher compared to the other demonstrated devices. The multilayer coated substrate used for the ion-selective electrodes had a barrier structure consisting of two $10 g/m^2$ platy kaolin/ethylene latex layers with one $10 g/m^2$ polyolefin latex layer in between, as coated layer by layer with the reverse gravure technique. To ensure adequate printability, a $5 g/m^2$ kaolin layer was used as top-coating.

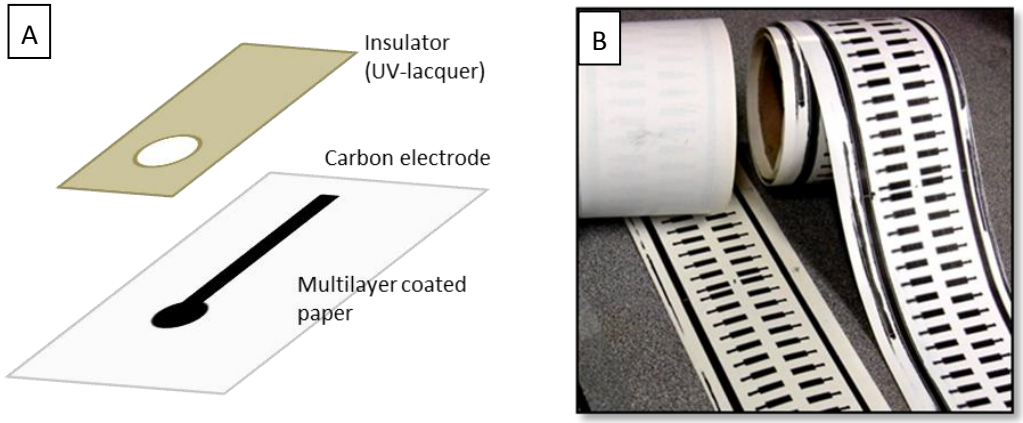

Figure 33. A: Schematic setup for an ion-selective electrode. B: Roll-to-roll printed (flexography) electrodes on multilayer coated paper. A pair of electrodes is needed for measurement: one electrode acts as a reference electrode while an ion-selective membrane is applied by drop casting on the other.

A potassium-selective membrane containing valinomycin as ionophore was deposited on one printed carbon electrode and a reference-electrode membrane containing tetrabutylammonium tetrabutylborate as equitransferent salt was deposited on the adjacent printed carbon electrode (*171*). This resulted in an all-solid-state K^+ selective electrode and a reference electrode adjacent to each other on the paper substrate. The potentiometric response of the sensor to K^+ ions at concentrations from 10^{-6} to 10^{-1}M at a constant ionic background of 0.1M NaCl is shown in Figure 34. The sensor responds to K^+ ions in a selective manner, which is regarded as a proof-of-concept. As can be seen in Figure 33 (top) the sensor shows sub-Nernstian behaviour (slope <59mV/decade) when the potential is recorded after 5 min in each solution. This is related to potential drift illustrated in Figure 34 (bottom). If the potential value is taken immediately after changing the KCl concentration the response will be close to Nernstian.

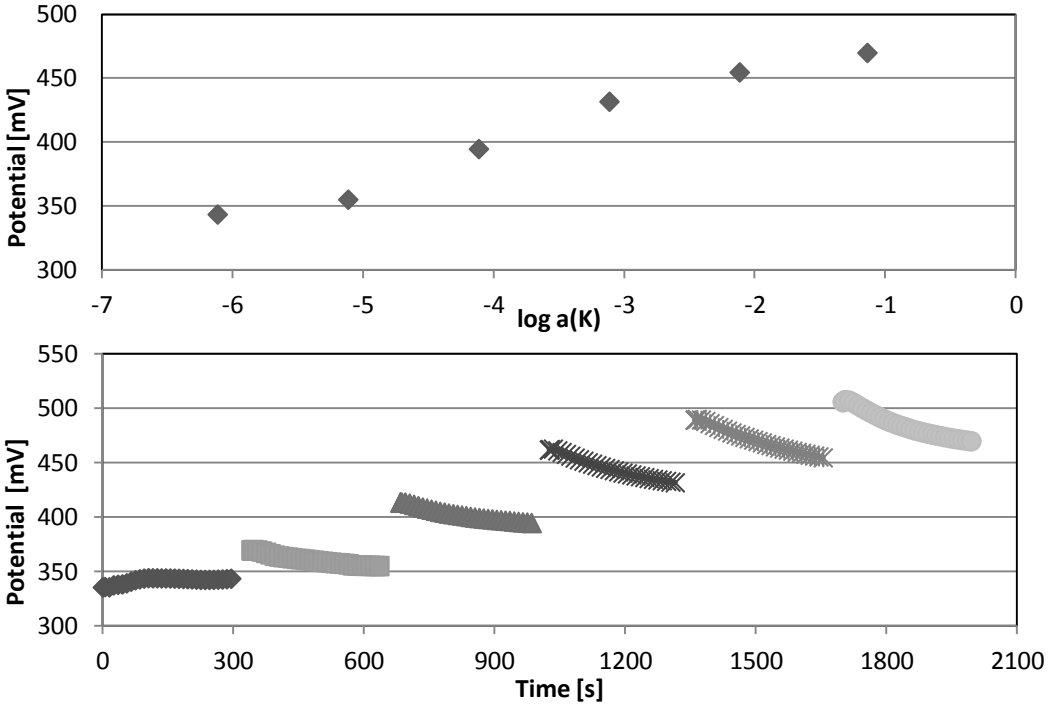

Figure 34. Potentiometric response of the all-solid-state sensor to potassium ions. Calibration plot (top) and potential vs. time curves (bottom) are shown for KCl concentrations from 10^{-6} to 10^{-1}M in a background electrolyte of 0.1M NaCl.

6. Concluding remarks

Manufacturing electronic features by printing and coating requires detailed understanding of the ink - application method - substrate compatibility. These all may be tuned and optimized separately, but the main focus in this work has been set on the substrate. Paper as substrate allows for wide tunability, by choice of coating structure and surface properties, but is also challenging especially regarding requirements for barrier properties and dimensional stability. Furthermore the devices, whether they are electronic or in other ways functional, must be designed keeping in mind the robust manufacturing conditions and methods. The understanding of the interactions between functional materials formulated and applied on paper as inks, however makes it possible to create a paper-based substrate that can be used to manufacture printed electronics-based devices and sensors on paper. The multitude of functional materials and their complex interactions make it challenging to draw general conclusions in this topic area. The results become partially specific to the device chosen and the materials needed in its manufacturing.

Based on the results, it is clear that for inks based on dissolved or small size functional materials, a barrier layer to limit the material penetration deep into the paper, is essential and ensures the functionality of the printed material in a device. When manufacturing functional devices on paper, the required active barrier life time depends on the used ink solvents and their volatility. The targeted end-use application, e.g. in sensoring of liquids, can also determine what kind of the barrier properties are needed. High aspect ratio mineral pigments, which create tortuous pathways and physical barriers within the barrier layer limit the penetration of solvents used in functional inks.

The surface pore volume and pore size can be optimized for a given printing process and ink through a choice of pigment type and coating layer thickness. However, when manufacturing multilayer functional devices, such as transistors, which consist of several printed layers, compromises have to be made. E.g., while a thick and porous top-coating is preferable for printing of source and drain electrodes with a silver particle ink, a thinner and less absorbing surface is required to form a functional semiconducting layer.

With the multilayer coating structure concept developed in this work, it was possible to meet the above listed criteria and requirements, and thereby make the fiber based paper substrate suitable for printed functionality. The possibility of printing functional devices, such as transistors, sensors and pixels in a roll-to-roll process on paper is demonstrated. All the demonstrated devices are manufactured on top of the multilayer coated substrate whereby the porosity of the fiber based basepaper structure is not utilized. Standalone electronic devices require some kind of power source, and in the case where a printed battery or capacitor is to be integrated, also the use of basepaper porosity as electrolyte carrier could potentially be utilized.

For industrial production of paper for printed electronics, curtain coating is a suitable coating technique allowing extremely thin top-coatings to be applied simultaneously with a closed and sealed barrier layer. However, industrial production of functional devices or sensors is still quite limited. One reason for the currently relatively limited use of paper for printed electronics is the dusting issue. Paper is generally not accepted in cleanrooms where most of the printed electronics production today is carried out. The lack of commercial products has also been a limiting factor, but the situation is expected to change along with the market increase for functional packages. Various chemical and biomedical sensors are also expected to reach the market, however from a paper manufacturing point of view, volumes will not be comparable with traditional paper grade production.

References

1. Tobjörk, D.; Österbacka, R. Paper Electronics. *Adv. Mater.* 2011, *23*, 1935-1961.

2. Przybysz, P. E-paper-potential competitor and printing papers. *Forestry Wood Technol.* 2006, *59*, 210-213.

3. Robinson, N.; Berggren, M. Printing organic electronics on flexible substrates. In *Handbook of Conducting Polymers, Conjugated Polymers: Processing Applications*, 3rd ed.; Francis, T., Ed.; New York, 2007; pp 4-1-4-26.

4. Trnovec, B.; Stanel, M.; Hahn, U.; Huebler, A.; Kempa, H.; Sangl, R. Coated paper for printed electronics. *Professional Papermaking* 2009, 48-51.

5. Dragoman, M.; Flahaut, E.; Dragoman, D.; Ahmad, M.; Plana, R. Writing simple RF electronic devices on paper with carbon nanotube ink. *Nanotechnology* 2009, *20*, 375203.

6. Lamprecht, B.; Thunauer, R.; Ostermann, M.; Jakopic, G.; Leising, G. Organic photodiodes on newspaper. *Phys. Status Solidi A* 2005, *202*, 50-52.

7. Shah, J.; Brown Jr, R. Towards electronic paper displays made from microbial cellulose. *Appl. Microbiol. Biotechnil.* 2005, *66*, 352-355.

8. Braam, K.; Volkman, S.; Subramanian, V. Characterization and optimization of a printed, primary silver–zinc battery. *Journal of Power Sources* 2012, *199*, 367-372.

9. Hilder, M.; Winther-Jensen, N.; Clark, N. Paper-based, printed zinc–air battery. *Journal of Power Sources* 2009, *194*, 1135-1141.

10. Siegel, A.; Phillips, S.; Wiley, B.; Whitesides, G. Thin, lightweight, foldable thermochromic displays on paper. *Lab Chip* 2009, *9*, 2775-2781.

11. Kim, Y.; Moon, D.; Han, J. Organic TFT array on a paper substrate. *IEEE Electron Device Lett.* 2004, *25*, 702-704.

12. Andersson, P.; Forchheimer, R.; Tehrani, P.; Berggren, M. Printable all-organic electrochromic active-matrix displays. *Adv. Funct. Mater* 2007, *17*, 3074-3082.

13. Huebler, A.; Trnovec, B.; Zillger, T.; Ali, M.; Wetzold, N.; Mingebach, M.; Wagenpfahl, A.; Deibel, C.; Dyakonov, V. Printed Paper Photovoltaic Cells. *Adv. Energy Mater.* 2011, *1* (6), 1018-1022.

14. Barr, M.; Rowehl, J.; Lunt, R.; Xu, J.; Wang, A.; Boyce, C.; Im Sung, G.; Bulovic, V.; Gleason, K. Direct Monolithic Integration of Organic Photovoltaic Circuits on Unmodified Paper. *Adv. Mater.* 2011, *23*, 3500-3505.

15. Sarfraz, J.; Tobjörk, D.; Österbacka, R.; Lindén, M. Low-Cost Hydrogen Sulfide Gas Sensor on Paper Substrates: Fabrication and Demonstration. *IEEE Sensors Journal* 2012, *12* (6), 1973-1978.

16. Olkkonen, J.; Lehtinen, K.; Erho, T. Flexographically Printed Fluidic Structures in Paper. *Anal. Chem.* 2010, *82*, 10246-10250.

17. Martinez, A.; Phillips, S.; Whitesides, G.; Carrilho, E. Diagnostics for the Developing World: Microfluidic Paper-Based Analytical Devices. *Anal. Chem.* 2010, *82*, 3-10.

18. Pelton, R. Bioactive Paper Provides a Low-Cost Platform for Diagnostics. *Anal. Chem* 2009, *28*, 925-942.

19. Bollström, R.; Tobjörk, D.; Dolietis, P.; Remonen, T.; Wikman, C.-J.; Viljanen, S.; Sarfraz, J.; Salminen, P.; Lindén, M.; Wilen, C.-E.; Bobacka, J.; Österbacka, R.; Toivakka, M. Roll-to-roll printed electronics on paper. *Proceedings of Tappi PaperCon*, New Orleans, 2012; pp 627-639.

20. Sundholm, J. *Papermaking Science and Technology 5, Mechanical Pulping;* Fapet Oy: Jyväskylä, 1999.

21. Gullichsen, J.; Fogelholm, C.-J. *Papermaking Science and Technology 6A, Chemical Pulping;* Fapet Oy: Jyväskylä, 1999.

22. Jokio, M. *Papermaking Science and Technology 10, Papermaking Part 3, Finishing;* Fapet Oy: Jyväskylä, 1999.

23. Lehtinen, E. *Papermaking Science and Technology 11, Pigment Coating and Surface Sizing of Paper;* Fapet Oy: Jyväskylä, 1999.

24. Paulapuro, H. *Papermaking Science and Technology 18, Paper and Board Grades;* Fapet Oy: Jyväskylä, 1999.

25. Bacon, W. Now they're printing transistors on paper. *Popular Sci.* 1968, 124-125.

26. Linhjell, D.; Lundgaard, L.; Gäfvert, U. Dielectric Response of Mineral Oil Impregnated Cellulose. *IEEE Trans. Diel. Electr. Insul.* 2007, *14*, 156-169.

27. Jang, J.; Ryu, S. Physical property and electrical conductivity of electroless Ag-plated carbon fiber-reinforced paper. *J. Mater. Process. Technol.* 2006, *180*, 66-73.

28. Bibikov, S.; Gorshenev, V.; Sharafiev, R.; Kuznetsov, A. Electrophysical properties of electroconducting papers and cardboards treated with colloid-graphite solutions. *Mater. Chem. Phys.* 2008, *108*, 39-44.

29. Johnston, J.; Moraeus, J.; Borrman, T. Conducting polymers on paper fibres. *Synth. Met.* 2005, *153*, 65-68.

30. Ding, C.; Qian, X.; Yu, G.; An, X. Dopant effect and characterization of polypyrrole-cellulose composites prepared by in situ polymerization process. *Cellulose* 2010, *17* (6), 1067-1077.

31. Ding, C.; Qian, X.; Shen, J.; An, X. Preparation and characterization of conductive paper via in-situ polymerization of pyrrole. *BioRes.* 2010, *5* (1), 303-315.

32. Sasso, C.; Zeno, E.; Petit-Conil, M.; Chaussy, D.; Naceur Belgacem, M.; Tapin-Lingua, S.; Beneventi, D. Highly Conducting Polypyrrole/Cellulose Nanocomposite Films with Enhanced Mechanical Properties. *Macromol. Mater. Eng.* 2010, *295*, 934-941.

33. Nyström, G.; Razag, A.; Strömme, M.; Nyholm, L.; Mihranyan, A. Ultrafast All-Polymer Paper-Based Batteries. *Nano Lett.* 2009, *9*, 3635-3639.

34. Mihranyan, A.; Nyholm, L.; Garcia Bennet, A.; Strömme, M. A Novel High Specific Surface Area Conducting Paper Material Composed of Polypyrrole and Cladophora Cellulose. *J Phys Chem B* 2008, *112*, 12249-12255.

35. Agarwal, M.; Lvov, Y.; Varahramyan, K. Conductive wood microfibres for smart paper through layer-by-layer nanocoating. *Nanotechnology* 2006, *17* (21), 5319.

36. Wistrand, I.; Lingström, R.; Wågberg, L. Preparation of electrically conducting cellulose fibres utilizing polyelectrolyte multilayers of poly(3,4-ethylenedioxythiophene):poly(styrene sulphonate) and poly(allyl amine). *Eur. Polym. J.* 2007, *43*, 4075-4091.

37. Montibon, E.; Lestelius, M.; Järnström, L. Electroconductive Paper Prepared by Coating with Blends of Poly(3,4-ethylenedioxythiophene)/Poly(4-styrenesulfonate) and Organic Solvents. *J. Appl. Pol. Sci.* 2010, *117*, 3524-3532.

38. Yang, X.; Forouzan, O.; Brown, T.; Shevkoplyas, S. Integrated separation of blood plasma from whole blood for microfluidic paper-based analytical devices. *Lab on a Chip* 2012, *12* (2), 274-280.

39. Li, X.; Ballerini, D.; Shen, W. A perspective on paper-based microfluidics: Current status and future trends. *Biomicrofluidics* 2012, *6*, 011301.

40. Martinez, A.; Phillips Scott, T.; Butte Manish, J.; Whitesides, G. Patterned paper as a platform for inexpensive, low-volume, portable bioassays. *Angew Chem Int Ed* 2007, *46* (8), 1318-1320.

41. Martinez, A.; Phillips, S.; Whitesides, G. Three-dimensional microfluidic devices fabricated in layered paper and tape. *Proc Natl Acad Sci* 2008, *105* (50), 1906-19611.

42. Martinez, A.; Phillips, S.; Whitesides, G.; Carrilho, E. Diagnostics for the developing world: microfluidic paper-based analytical devices. *Anal Chem* 2009, *82* (1), 3-10.

43. Ballerini, D.; Li, X.; Shen, W. Patterned paper and alternative materials as substrates for low-cost microfluidic diagnostics. *Microfluid Nanofluid* 2012, *13*, 769-787.

44. Gerstner, P.; Paltakari, J.; Gane, P. A method for the measurement of thermal contact diffusivity of paper coating structures. *Nord. Pulp Paper Res J.* 2008, *23* (4), 354-362.

45. Gerstner, P.; Paltakari, J.; Gane, P. Measurement and modelling of heat transfer in paper coating structures. *J. Maters. Sci.* 2009, *44* (2), 483-491.

46. Chang, C.; Hilden, G.; Lyne, B.; Veverka, P. Multi-layer coated copy paper for improved printing and performance. WO2000040424 A1, July 13, 2000.

47. Tobjörk, D.; Aarnio, H.; Pulkkinen, P.; Bollström, R.; Määttänen, A.; Ihalainen, P.; Mäkelä, T.; Peltonen, J.; Toivakka, M.; Tenhu, R.; Österbacka, R. IR-sintering of ink-jet printed metal-nanoparticles on paper. *Thin Solid Films* 2012, *520* (7), 2949-2955.

48. Kattumenu, R.; Rebros, M.; Joyce, M.; Fleming, P.; Neelgund, G. Effect of Substrate Properties on Conductive Traces Printed with Silver-Based Flexographic Ink. *Nord. Pulp Pap Res. J.* 2009, *24*, 101-106.

49. Ihalainen, P.; Määttänen, A.; Järnström, J.; Tobjörk, D.; Österbacka, R.; Peltonen, J. Influence of Surface Properties of Coated Papers on Printed Electronics. *Ind. Eng. Chem. Res.* 2012, *51,* 6025-6036.

50. Denneulin, A.; Blayo, A.; Bras, J.; Neuman, C. PEDOT:PSS coating on specialty papers: Process optimization and effects of surface properties on electrical performances. *Prog. Org. Coat.* 2008, *63,* 87-91.

51. Zhou, J.; Fukawa, T.; Shirai, H.; Kimura, M. Anisotropic Motion of Electroactive Papers Coated with PEDOT/PSS. *Macromol. Mater. Eng.* 2010, *295,* 671-675.

52. Mäkelä, T.; Jussila, S.; Vilkman, M.; Kosonen, H.; Korhonen, R. Roll-to-roll method for producing polyaniline patterns on paper. *Synthetic Metals* 2003, 135-136.

53. Chinga-Carrasco, G.; Tobjörk, D.; Österbacka, R. Inkjet-printed silver nanoparticles on nano-engineered cellulose films for electrically conducting structures and organic transistors: concept and challenges. *J Nanopart Res* 2012, *14,* 1-10.

54. Torvinen, K.; Sievänen, J.; Hjelt, T.; Hellén, E. Smooth and flexible filler-nanocellulose composite structure for printed electronics applications. *Cellolose* 2012, *19* (3), 821-829.

55. Irimia-Vladu, M.; Glowacki, E.; Voss, G.; Bauer, S.; Serdar Sariciftci, N. Green and biodegradable electronics. *Materials Today* 2012, *15* (7-8).

56. Ong, B.; Wu, Y.; Liu, P.; Gardner, S. High-performance semiconducting polythiophenes for organic thin-film transistors. *J. Am. Chem. Soc.* 2004, *126,* 3378-3379.

57. McCulloch, I.; Heeney, M.; Bailey, C.; Genevicius, K.; MacDonald, I.; Shkunov, M.; Sparrowe, D.; Tierney, S.; Wagner, R.; Zhang, W.; Chabinyc, M.; Kline, R.; McGehee, M.; Toney, M. Liquid-crystalline semiconducting polymers with high charge-carrier mobility. *Nat. Mater.* 2006, *5,* 328-333.

58. Sirringhaus, H.; Brown, P.; Friend, R.; Nielsen, M.; Bechgaard, K.; Langeveld-Voss, B.; Spiering, A.; Janssen, R.; Meijer, E.; Herwig, P.; de Leeuw, D. Two-dimensional charge transport in self-organized, high-mobility conjugated polymers. *Nature* 1999, *401,* 685-688.

59. Whitesides, G. Whitesides Group Publications. HYPERLINK "http://gmwgroup.harvard.edu/pubs/index.php?b=2010&t=2019" http://gmwgroup.harvard.edu/pubs/index.php?b=2010&t=2019 (accessed Jan 7, 2013).

60. Mäkelä, T. *Towards printed electronic devices, PhD Thesis;* Åbo Akademi University: Turku, 2008.

61. Tobjörk, D. *Printed Low-Voltage Organic Transistors on Plastic and Paper, PhD Thesis;* Åbo Akademi University: Turku, 2012.

62. Angelo, P. *Inkjet-Printed Light-Emitting Devices: Applying Inkjet Microfabrication to Multilayer Electronics, PhD Thesis;* University of Toronto: Toronto, 2012.

63. Lopez Cabezas, A. *Nanofibrillar Materials for Organic and Printable Electronics, PhD Thesis;* KTH Royal Institute of Technology: Stockholm, 2013.

64. Razag, A. *Development of Cellulose-Based, Nanostructured, Conductive Paper for Biomolecular Extraction and Energy Storage Applications, PhD Thesis;* Uppsala Universitet: Uppsala, 2011.

65. Öhlund, T. *Coated Surfaces for Inkjet-Printed Conductors, Lic. Thesis;* Mid Sweden University: Sundsvall, 2012.

66. Thiele, C.; Das, R. *Brand Enhancement by Electronics in Packaging 2012-2022;* IDTechEx, 2012.

67. Laakso, S. Smart packages has business oppportunities. *Paperi ja Puu,* 2012, 28-33 and 66-67.

68. Security labelling – a counter-offensive on fraud and loss, 2012. HYPERLINK "http://www.upmraflatac.com/europe/eng/images/51_93685.pdf" http://www.upmraflatac.com/europe/eng/images/51_93685.pdf .

69. Intelligent Wireless Power. HYPERLINK "http://fultoninnovation.com/" http://fultoninnovation.com/ (accessed Dec 21, 2012).

70. Touchcode. HYPERLINK "http://www.touchcode.de/" http://www.touchcode.de/ (accessed Jan 4, 2013).

71. Harrop, P. NanoWerk News. HYPERLINK "http://www.nanowerk.com/news/newsid=24351.php" \l "ixzz2FfosjvuY " http://www.nanowerk.com/news/newsid=24351.php#ixzz2FfosjvuY (accessed Dec 21, 2012).

72. Nyström, G.; Razag, A.; Strömme, M.; Nyholm, L.; Mihranian, A. Ultrafast All-Polymer Paper-Based Batteries. *Nano Lett.* 2009, *9,* 3635-3639.

73. Pushparaj, V.; Shaijumon, M.; Kumar, A.; Murugesan, S.; Ci, L.; Vajtai, R.; Linhardt, R.; Nalamasu, O.; Ajayan, P. Flexible energy storage devices based on nanocomposite paper. *Proc. Nat. Acad. Sci.* 2007, *104,* 13574-13577.

74. Hu, L.; Choi, J.; Yang, Y.; Jeong, S.; La Mantia, F.; Cui, L.-F.; Cui, Y. Highly conductive paper for energy-storage devices. *Proc. Natl. Acad. Sci.* 2009, *106,* 21490-21494.

75. Enfucell Soft Battery. HYPERLINK "http://www.enfucell.com/softbattery-products" http://www.enfucell.com/softbattery-products (accessed Dec 2, 2012).

76. Power Paper Products. HYPERLINK "http://www.powerpaper.cn/indexbda1.html?categoryId=43879" http://www.powerpaper.cn/indexbda1.html?categoryId=43879 (accessed Dec 2, 2012).

77. Blue Spark Technologies Batteries. HYPERLINK "http://www.bluesparktechnologies.com/index.php/products-and-services/battery-products/ultra-thin-series" http://www.bluesparktechnologies.com/index.php/products-and-services/battery-products/ultra-thin-series (accessed Dec 18, 2012).

78. Lew, A.; Suter, J.; Le, B. Integrated power source. US 5644207, April 16, 1996.

79. Krebs, F.; Jorgensen, M.; Norrman, K.; Hagemann, O.; Alstrup, J.; Nielsen, T.; Fyenbo, J.; Larsen, K.; Kristensen, J. A Complete Process for Production of Flexible Large Area Polymer Solar Cells Entirely Using Screen Printing - First Public Demonstration. *Sol. Energy Mater. Sol. Cells* 2009, *93,* 422-441.

80. Aarnio, H. *Photoexcitation dynamics in organic solar cell donor/acceptor systems, PhD Thesis;* Åbo Akademi University: Turku, 2012.

81. Sirringhaus, H. Device Physics of Solution-Processed Organic Field-Effect Transistors. *Adv. Mater.* 2005, *17,* 2411-2424.

82. Sirringhaus, H. Reliability of Organic Field-Effect Transistors. *Adv. Mater.* 2009, *21,* 3859-3873.

83. Gelink, G.; Heremans, P.; Nomoto, K.; Anthopoulos, T. Organic Transistors in Optical Displays and Microelectronic Applications. *Adv. Mater.* 2010, *22,* 3778-3798.

84. Guo, Y.; Yu, G.; Liu, Y. Functional Organic Field-Effect Transistors. *Adv. Mater.* 2010, *22,* 4427-4447.

85. Härting, M.; Zhang, J.; Gamota, D.; Britton, D. Fully printed silicon field effect transistors. *Appl. Phys. Lett.* 2009, *94,* 193509.

86. Mannerbro, R.; Ranlöf, M.; Robinson, N.; Forcheimer, R. Inkjet printed electrochemical organic electronics. *Synth. Met.* 2008, *158,* 556-560.

87. Yun, S.; Jang, S.-D.; Yun, G.-Y.; Kim, J.-H.; Kim, J. Paper transistor made with covalently bonded multiwalled carbon. *Appl. Phys. Lett.* 2009, *95,* 104102.

88. Scott, J.; Bozano, L. Nonvolatile memory elements based on organic materials. *Adv. Mater.* 2007, *19,* 1452-1463.

89. Ling, Q.-D.; Liaw, D.-J.; Zhu, C.; Chan, D.; Kang, E.-T.; Neoh, K.-G. Polymer electronic memories: materials, devices and mechanisms. *Prog. Polym. Sci.* 2008, *33,* 917-978.

90. Voit, W.; Zapka, W.; Dyreklev, P.; Hagel, O.-J.; Hägerström, A.; Sandström, P. Inkjet Printing of Non-Volatile Rewritable Memory Arrays. *NIP 21 and Digital Fabrication,* Baltimore, 2005.

91. Andersson, D.; Nilsson, P.; Svensson, O.; Chen, M.; Malmström, A.; Remonen, T.; Kugler, T.; Berggren, M. Active matrix displays based on all-organic electrochemical smart pixels printed on paper. *Advanced Materials* 2002, *14,* 1460.

92. Siegel, A.; Phillips, S.; Wiley, B.; Whitesides, G. Thin, lightweight, foldable thermochromic displays on paper. *Lab Chip* 2009, *9,* 2775-2781.

93. Kim, D.; Steckl, A. Electrowetting on paper for electronic paper display. *ACS Appl. Mater. Interfaces 2* 2010, *11,* 3318-3323.

94. Hayes, R.; Feenstra, B. Video-speed electronic paper based on electrowetting. *Nature* 2003, *425,* 383-385.

95. Sirringhaus, H.; Tessler, N.; Friend, R. Integrated Optoelectronic Devices Based on Conjugated Polymers. *Science* 1998, *280*, 1741-1744.

96. Matyba, P.; Yamaguchi, H.; Eda, G.; Chhowalla, M.; Edman, L.; Robinson, N. Graphene and Mobile Ions: The Key to All-Plastic, Solution-Processed Light-Emitting Devices. *ACS Nano* 2010, *4*, 637-642.

97. Haatainen, T. *Stamp fabrication by step and stamp nanoimprinting, PhD Thesis;* VTT Technical Research Centre of Finland: Espoo, 2011.

98. Rolin, C.; Vasseur, K.; Genoe, J.; Heremans, P. Growth of pentacene thin films by in-line organic vapor phase deposition. *Org. Electron.* 2010, *11*, 100-108.

99. Pykönen, M. *Influence of Plasma Modification on Surface Properties and Offset Printability of Coated Paper, PhD Thesis;* Åbo Akademi University: Turku, 2010.

100. Kipphan, H. *Handbook of Print Media;* Springer: Heidelberg, 2001.

101. Nordström, J.-E. *Studies on Waterless Offset, PhD Thesis;* Åbo Akademi University: Turku, 2003.

102. Pudas, M.; Halonen, N.; Granat, P.; Vähäkangas, J. Gravure printing of conductive particulate polymer inks on. *Prog. Org. Coat.* 2005, *54*, 310-316.

103. Jung, M.; Kim, J.; Noh, J.; Lim, N.; Lim, C.; Lee, G.; Kim, J.; Kang, H.; Jung, K.; Leonard, A.; Tour, J.; Cho, G. All-Printed and Roll-to-Roll-Printable 13.56-MHz-Operated 1-bit RF Tag on Plastic Foils. *IEEE Trans. Electron. Devices* 2010, *57*, 571-580.

104. Ding, J.; Vornbrock, C.; Ting, C.; Subramanian, V. Patternable polymer bulk heterojunction photovoltaic cells on plastic by rotogravure printing. *Sol. Energy Mater. Sol. Cells* 2009, *93*, 459-464.

105. Kopola, P.; Tuomikoski, M.; Suhonen, R.; Maaninen, A. Gravure printed organic light emitting diodes for lighting applications. *Thin Solid Films* 2009, *517* (19), 5757-5762.

106. Deganello, D.; Cherry, J.; Gethin, D.; Claypole, T. Patterning of micro-scale conductive networks using reel-to-reel Flexographic Printing. *Thin Solid Films* 2010, *518*, 6113-6116.

107. Yan, H.; Chen, Z.; Zheng, Y.; Newman, C.; Quinn, J.; Dötz, F.; Kastle, M.; Facchetti, A. A high-mobility electron-transporting polymer for printed transistors. *Nature* 2009, *457*, 679-686.

108. Shin, D.-Y.; Lee, Y.; Kim, C. Performance characterization of screen printed radio frequency identification antennas with silver nanopaste. *Thin Solid Films* 2009, *517* (21), 6112-6118.

109. Beer, W. The Application of Printing Technologies for Pyrotechnic Delays. *EUROPYRO 2011, 37th International Pyrotechnics Seminar*, Reims, 2011.

110. Sekitani, T.; Noguchi, Y.; Zschiechang, U.; Klauk, H.; Someya, T. Organic transistors manufactured using inkjet technology with subfemtoliter accuracy. *Proc. Natl. Acad. Sci. USA* 2008, *105*, 4976-4980.

111. Tekin, E.; Smith, J.; Schubert, U. Inkjet Printing as a Deposition and Patterning Tool for Polymers and Inorganic Particles. *Soft Matter* 2008, *4*, 703-713.

112. Yang, L.; Rida, A.; Vyas, R.; Tentzeris, M. RFID Tag and RF Structures on a Paper Substrate Using Inkjet-Printing Technology. *IEEE Trans. Microw. Theory Tech.* 2007, *55*, 2894-2901.

113. Yang, L.; Zhang, R.; Staiculescu, D.; Wong, C.; Tentzeris, M. A Novel Conformal RFID-Enabled Module Utilizing Inkjet-Printed Antennas and Carbon Nanotubes for Gas-Detection Applications. *IEEE Antennas Prop. Lett.* 2009, *8*, 653-656.

114. Nutbeem, C.; Husband, J.; Preston, J. The role of pigments in controlling coating structure. *PITA Coating Conference*, Bradford, 2005; pp 97-102.

115. Gane, P. Absorption Properties of Coatings: A selected Overview of Absorption Criteria Derived from Recent Pore Network Modelling. *Journal of Dispersion Science and Technology* 2004, *25* (4), 389-408.

116. Preston, J.; Elton, N.; Legrix, A.; Nutbeem, C.; Husband, J. The role of pore density in the setting of offset printing ink on coated paper. *TAPPI JOURNAL* 2002, *1* (3), 3-5.

117. Schoelkopf, J.; Gane, P.; Ridgway, C.; Spielmann, D.; Matthews, G. Imbition behaviour of offset inks Part 1: Gravimetric determination of oil imbition rate into pigmented coating structures. *TAPPI JOURNAL* 2003, *2* (6), 9-13.

118. Webb, T.; Gate, L. Apparatus & method for measuring the average aspect ratio of non-spherical particles in a suspension. PCT/GB94/00090,WO/16308.

119. Owens, D.; Wendt, R. Estimation of the surface free energy of polymers. *J. Appl. Polym. Sci.* 1969, *13*, 1741-1747.

120. Kaelbe, D. Dispersion-polar surface tension properties of organic solid. *J. Adhes.* 1970, *2*, 66-81.

121. Fowkes, F. Attractive Forces at Interfaces. *Ind. Eng. Chem.* 1964, *56,* 40-52.

122. Standard test Methods for Water Vapor Transmission of Material, E 96/E96M-10, 2010.

123. Haya, G.; Southee, D.; Evans, P.; Harrison, D.; Simpson, G.; Ramsey, B. Examination of silver-grafite lithographically printed resistive strain sensors. *Sensors and Actuatiors A* 2007, *135*, 534-546.

124. O'Toolea, M.; Shepherd, R.; Wallace, G.; Diamond, D. Inkjet printed LED based pH chemical sensor for gas sensing. *Analytica Chimica Acta* 2009, *652*, 308-314.

125. Martinez, N.; Messina, G.; Bertolina, F.; Salinas, E.; Raba, J. Screen-printed enzymatic biosensor modified with carbon nanotube for the methimazole determination in pharmaceuticals formulations. *Sensors and Actuators B* 2008, *133*, 256-262.

126. Nilson, D.; Kugler, T.; Svensson, P.; Berggren, M. An all-organic sensor transistor based on a novel electrochemical transducer concept printed electrochemical sensors printed on paper. *Sensors and Actuators B* 2002, *86,* 193-197.

127. Anastasova, S.; Radu, A.; Matzeu, G.; Zuliani, C.; Diamond, D.; Mattinen, U.; Bobacka, J. Disposable solid-contact ion-selective electrodes for environmental monitoring of lead with ppb limit-of-detection. *Electrochim Acta* 2012, *73* (1), 93-97.

128. Saarinen, J. J.; Ihalainen, P.; Määttänen, A.; Bollström, R.; Peltonen, J. Printed sensor and electric field assisted wetting on a natural fiber based substrate. *Nordic Pulp and Paper Research Journal* 2011, *25*, 133-141.

129. Water absorptiveness of sized (non-bibulous) paper, paperboard, and corrugated fiberboard (Cobb test), 2009.

130. Standard Test Method for Rate of Grease Penetration of Flexible Barrier Materials, Designation: F 119 – 82, 2008.

131. Azzam, R. Direct relation between Fresnel's interface reflection coefficients for the parallel and perpendicular polarizations. *J. Opt. Soc. Am.* 1979, *69*, 1007-1016.

132. Bakker, J.; Bryntse, G.; Arwin, H. Determination of refractive index of printed and unprinted paper using spectroscopic ellipsometry. *Thin Solid Films* 2004, *361*, 455-456.

133. Brune, M.; Haller, K. Das FOGRA-kontaktanteilmessgerät zur Glättmessung an Papieren. *Wochenblatt fur Papierfabrikation* 1968, 731-736.

134. Wanske, M.; Klein, R.; Grossmann, H. Assessing the surface structure of printing papers under pressure. *TAGA 58th Annual technical Conference, Professional papermaking*, Vancouver, 2006.

135. Niskanen, I.; Räty, J.; Peionen, K.-E.; Koivula, H.; Toivakka, M. Assesment of the complex refractive index of an optically very dense solid layer: Case study offset magenta ink. *Chemical Physics Letters 442*, 515-517.

136. Colvin, R. Environmentally friendly barrier coating moves to packaging. *Mod. Plastics* 2003, *33* (13), 29.

137. Schuman, T.; Wikström, M.; Rigdahl, M. Dispersion coating with carboxylated and cross-linked styrene–butadiene lattices 2. Effects of substrate and polymer characteristics on the properties of coated paperboard. *Prog. Org. Coat.* 2004, *51* (3), 228.

138. Schuman, T.; Karlsson, A.; Larsson, J.; Wikström, M.; Rigdahl, M. Characteristics of pigment-filled polymer coatings on paperboard. *Prog. Org. Coat.* 2005, *54* (4), 360.

139. Andersson, C.; Ernström, M.; Järnström, L. Barrier properties and heat sealability/failure mechanisms of dispersion-coated paperboard. *Packag. Technol. Sci.* 2002, *15*, 209.

140. Lape, N.; Yang, C.; Cussler, E. Flake-filled Reactive Membranes. *Journal of Membrane Science* 2002, *209* (1), 271-282.

141. Moggridge, G.; Lape, N.; Yang, C.; Cussler, E. Barrier Films using Flakes and Reactive Additives. *Progress in Organic Coatings* 2003, *46* (4), 231-240.

142. Dury-Brun, C.; Jury, V.; Guillard, V.; Desobry, S.; Voilley, A.; Chalier, P. Water Barrier Properties of Treated Papers and Application to Sponge Cake Storage. *Food Research International* 2006, *39* (9), 1002-1011.

143. Zou, Y.; Hsieh, J.; Mehnert, E.; Kokoszka, J. The Effect of Pigments and Latices on the Properties of Coated Paper. *Colloids and Surfaces A: Physiochemical and Engineering Aspects* 2007, *294* (1-3), 40-45.

144. Perera, D. Effect of pigmentation on organic coating characteristics. *Prog.Org. Coat.* 2004, *50,* 247-262.

145. del Rio, G.; Rudin, A. Latex particle size and CPVC. *Prog. Org. Coat.* 1995, *28,* 259-270.

146. Preston, J.; Nutbeem, C.; Chapman, R. Impact of Pigment Blend and Binder Level on the Structure and Printability of Coated Papers. *Tappi PaperCon*, Cincinnati, 2011.

147. Gribble, C.; Matthews, G.; Laudone, G.; Turner, A.; Ridgway, C.; Schoelkopf, J.; Gane, P. Porometry, porosimetry, image analysis and void network modelling in the study of the pore-level properties of filters. *Chem. Eng. Sci.* 2011, *66,* 3701-3709.

148. Ridgway, C.; Gane, P.; Schoelkopf, J. Effect of Capillary Element Aspect Ratio on the Dynamic Imbibition within Porous Networks. *J. Colloid Interface Sci.* 2002, *252,* 373-382.

149. Ridgway, C.; Gane, P. Controlling the Absorption Dynamic of Water-Based Ink into Porous Pigmented Coating Structures to Enhance Print Performance. *Nord. Pulp Pap. Res. J.* 2002, *17,* 119-129.

150. Olsson, R.; van Stam, J.; Lestelius, M. Effects on Ink Setting in Flexographic Printing: Coating Polarity and Dot Gain. *Nord. pulp Pap. Res. J.* 2006, *21,* 569.

151. Cruz, M.; Joyce, M.; Fleming, P.; Rebros, M.; Pekarovicova, A. Surface Topography Contribution to RFID Tag Efficiency Related To Conductivity. *TAPPI Coating and Graphics Arts Conference*, Miami, 2007.

152. Rebros, M.; Hrehorova, E.; Bazuin, B.; Joyce, M.; Fleming, P.; Pekarovicova, A. Rotogravure Printed UHF RFID Antenna Directly on Packaging Materials. *Technical Assosiation of the Graphic Arts (TAGA)*, San Francisco, 2008.

153. Uesaka, T. Dimensional stability of paper. Upgrading paper performance in end use. *Journal of Pulp and Paper Science* 1991, *17,* 39-46.

154. Schulgasser, K. Moisture and thermal expansion of wood, particleboard and paper. *Paperi ja Puu* 1988, *70,* 534-539.

155. Green, C. Dimensional Properties of Paper Structures. *Ind. Eng. Chem. Res. Dev.* 1981, *20*, 151-158.

156. Järnström, J.; Sinervo, L.; Toivakka, M.; Peltonen, J. Topography and gloss of precipitated calcium carbonate coating layers on a model substrate. *Tappi Journal* 2006, *6*, 23-31.

157. Järnström, J.; Ihalainen, P.; Backfolk, K.; Peltonen, J. Roughness of pigment coatings and its influence on gloss. *Applied Surf. Sci* 2008, *254*, 5741-5749.

158. Wang, S.; Ihalainen, P.; Järnström, J.; Peltonen, J. The effect of base paper and coating method on the surface roughness of pigment coatings. *J. Disp. Sci. and Tech.* 2009, *30*, 961-968.

159. Wood, L.; Joyce, T.; Fleming, P.; Joyce, M. *Paper Substrates and Inks for Printed Electronics;* Pira Ink on Paper Symposium: Atlanta, 2005.

160. Tobjörk, D.; Kaihovirta, N.; Mäkelä, T.; Pettersson, F.; Österbacka, R. All-printed low-voltage organic transistors. *Org. Electron.* 2008, *9*, 931-935.

161. Mills, A.; Hazafy, D. A solvent-based ink for oxygen. *Analyst* 2008, *133*, 213-218.

162. Cicmil, D.; Anastasova, S.; Kavangh, A.; Diamond, D.; Mattinen, U.; Bobacka, J.; Lewenstam, A.; Radu, A. Ionic Liquid-Based, Liquid-Junction-Free Reference Electrode. *Electroanalysis* 2011, *23*, 1881-1890.

163. Smolander, M.; Hurme, E.; Koivisto, M.; Kivinen, S. Indicator. PCT/FI2004/000166, WO 2004/102185 A1, May 16, 2003.

164. Sandberg, H.; Bäcklund, T.; Österbacka, R.; Stubb, H. A high performance all-polymer transistor utilizing a hygroscopic insulator. *Adv. Mater.* 2004, *16*, 1112-1115.

165. Tobjörk, D.; Bollström, R.; Dolietis, P.; Määttänen, A.; Ihalainen, P.; Mäkelä, T.; Peltonen, J.; Toivakka, M.; Österbacka, R. Printed low-voltage transistors on plastic and paper. *Proceedings of European Coating Symposium*, Turku, 2011; pp 62-65.

166. Bollström, R.; Tobjörk, D.; Määttänen, A.; Ihalainen, P.; Peltonen, J.; Österbacka, R.; Toivakka, M. Towards Paper Electronics - Printing Transistors on Paper in a Roll-To-Roll Process. *Proceedings of the NIP 27 and Digital Fabrication*, Minneapolis, 2011; pp 636-639.

167. Valtakari, D.; Bollström, R.; Tuominen, M.; Teisala, H.; Aromaa, M.; Toivakka, M.; Kuusipalo, J.; Mäkelä, M.; Uozumi, J.; Saarinen, J. J. Flexographic printing of PEDOT:PSS on coated papers for printed functionality. *Journal of Print Media and Technology Research* 2013, *2* (1), 7-14.

168. Kaihovirta, N.; Wikman, C.; Mäkelä, T.; Wilén, C.; Österbacka, R. Self-Supported Ion-Conductive Membrane-Based Transistors. *Advanced Materials* 2009, *21*, 2520-2523.

169. Lee, S.-K.; Mills, A.; Lepre, A. An intelligence ink for oxygen. *Chem. Commun.* 2004, 1912-1913.

170. Viljanen, S. *Undersökning av jonselektiva elektroder tryckta på papper som substrat, M. Sc. Thesis;* Åbo Akademi University: Turku, 2012.

171. Mattinen, U.; Bobacka, J.; Lewenstam, A. Solid-contact reference electrode based on lipophilic salts. *Electroanalysis* 2009, *21*, 1955-1969.

Publications

Åbo Akademis förlag | ISBN 978-952-12-2934-3